BIOFUNCTIONAL LUBRICANT-INFUSED SURFACES FOR MEDICAL IMPLANTS

BIOFUNCTIONAL LUBRICANT-INFUSED SURFACES FOR MEDICAL IMPLANTS

By MARYAM BADV, B.A.Sc., M.A.Sc.

A Thesis
Submitted to the School of Graduate Studies
in Partial Fulfillment of the Requirements for the Degree
Doctor of Philosophy

McMaster University DOCTOR OF PHILOSOPHY (2019)
Hamilton, Ontario, Canada

TITLE: BIOFUNCTIONAL LUBRICANT-INFUSED SURFACES FOR MEDICAL IMPLANTS

AUTHOR: Maryam Badv
B.A.Sc. (University of Tehran)
M.A.Sc. (McMaster University)

SUPERVISOR: Dr. T. F. Didar

PAGES: xv, 130

Lay Abstract

The work presented in this research aims to create biofunctional lubricant-infused platforms for medical implants. Promoting tissue integration and preventing clot formation and non-specific adhesion of biospecies are two of the main challenges that researchers aim to overcome when designing interfaces for permanent blood-contacting implants. However, limited success has been made in developing functional coatings that integrate both these features on one platform. The work in this thesis describes novel, straightforward and effective surface coating strategies for developing biofunctional lubricant-infused interfaces that attenuate clot formation, prevent non-specific adhesion and promote targeted binding of cells.

Abstract

Device-associated clot formation and poor targeted cell-adhesion are ongoing problems in permanent blood-contacting medical implants. The recent concept of lubricant-infused surfaces has shown promising results in preventing non-specific adhesion and attenuating clot formation on biomaterials. However, the existing surface models do not express biofunctional features, a crucial requirement when designing surface coatings for permanent medical implants such as vascular grafts, stents and mechanical heart valves. The main objective of this thesis is to design and develop novel biofunctional lubricant-infused surface coatings that would simultaneously prevent device-associated thrombosis and actively promote surface biointeractions.

Three main approaches to incorporate biofunctionality into lubricant-infused surfaces are presented in this thesis: (1) Developing biofunctional lubricant-infused surface coatings by creating self-assembled monolayers using fluoro and aminosilane molecules. (2) Creating non-fluorosilanized biofunctional lubricant-infused ePTFE vascular grafts by exploiting the innate chemical properties of the ePTFE grafts and biofunctionalizing the surfaces using silanized bio-inks. (3) Creating fluorinated biofunctional lubricant-infused PET grafts with "built-in" functional groups using oxygen plasma treatment. Using these three modification procedures, for the first time, we were able to generate lubricant-infused surfaces, that expressed biofunctional and targeted-binding features. In the first modification technique, by tuning the ratio between the fluorosilane and aminosilane molecules, we were able to incorporate functional groups on the surfaces without compromising the lubricant-infused repellency properties of the modified substrates. In the second modification technique, we created non-fluorosilanized biofunctional lubricant-infused ePTFE grafts by eliminating the need to chemically modifying the surface with silane molecules. Our designed surfaces were further biofunctionalized using our developed silanized bio-inks. Lastly, in order to created fluorinated biofunctional lubricant-infused PET grafts, we developed the third modification process, where fluorinated PET surfaces were hydroxyl-terminated using oxygen plasma treatment, and biofunctionalized using silanized bio-inks.

The designed surfaces using the three proposed modification procedures had excellent repellency properties by attenuating plasma and blood clot formation, thrombin generation and preventing non-targeted adhesion of proteins and cells. In addition, our developed surfaces were biofunctional and were able to actively promote targeted binding of endothelial cells.

With the new surface coatings created in this thesis, lubricant-infused surfaces with excellent repellency properties and biofunctional features can be achieved and applied to blood-contacting medical devices where preventing non-specific adhesion and promoting targeted binding are of immense importance.

Acknowledgment

First and foremost, I would like to thank my supervisor and mentor Dr. Tohid Didar for his constant support and guidance. Thank you for letting me explore different topics and trusting me whenever I would come to you with new ideas. You always used to say that one of your jobs as a supervisor is to make sure that your students love the research that they do and you did so by supporting me and giving me the freedom to explore, experience and pursue the research that I found most interesting. I cannot express my appreciation for having you as my mentor and it is truly an honor to be your first PhD graduate.

I would like to extend my sincere thanks to my committee members, Dr. Jeffrey Weitz and Dr. Carlos Filipe. For their support and insightful feedback that allowed me to broaden my perspective and better understand my research. Thank you for always making my committee meetings fun and productive.

I am very grateful to have been part of DidarLab, working along side my amazing, smart and fun labmates. To all current and past members, thank you for your support and for making my experience memorable.

Above all, I would like to thank my dear family. Mom, words cannot describe how much I love you and how grateful I am to have you by my side. This journey would have never come to an end if it wasn't for your constant support, light, positivity, unconditional love and endless sacrifices. I know we are miles away, but I always feel you by my side and cherish you. Dad, you are the reason why I chose this path and decided to become an engineer. Your work ethics, passion, persistence and love for your family are things that I always admire and learn from. Thank you for everything you have done for us. My two brothers, Hadi and Mohsen, you know you have a special place in my heart that no one can take. You two have always been my rock. Thank you for always having my back and empowering me, and for always letting me be the driver! I love you two and will always be your "Chalim"!

Lastly, I would like to thank my husband, Sajjad. For his love, friendship, unconditional support and kindness. Thank you for always making me look at the bright side and for patiently answering all my research related questions. Non of this would have been possible without having you by my side. Thank you for everything.

This thesis is dedicated to my dear friend, Nahid Dadashpour, whose smiles, generosity and uplifting spirit has touched countless hearts.

Table of Contents

List of Figures

Chapter 1

Chapter 2

Chapter 3

Chapter 4

Chapter 5

List of Tables

List of Abbreviations

APTES	aminopropyltriethoxysilane
ATRP	atom transfer radical polymerization
BLIPS	biofunctional lubricant infused ePTFE surface
BLIS	biofunctional lubricant infused surface
BSA	bovine serum albumin
CFU-EC	colony forming unit-endothelial cells
CTI	corn-trypsin inhibitor
CVD	chemical vapour deposition
EC	endothelial cells
ECFC	endothelial colony forming cells
ECM	extracellular matrix
EDC	N-(3-Dimethylaminopropyl)-N′-ethylcarbodiimide
EPC	endothelial progenitor cell
ePTFE	expanded polytetrafluoroethylene
FBLIS	fluorinated biofunctional lubricant-infused surface
LIS	lubricant infused surface
LPD	liquid phase deposition
MES	2-(N-Morpholino)ethanesulfonic acid
MPC	2-methacryloyloxyethyl phosphorylcholine
MS	mass spectrometry
NHS	N-Hydroxysuccinimide
NO	nitric oxide
PBS	phosphate Buffered Saline
PC	phosphorylcholine
PCU	Polycarbonate-urethane
PDMS	polydimethylsiloxane
PEG	poly (ethylene glycol)
PEO	polyethylene oxide
PET	polyethylene terephthalate
PFD	perfluorodecalin
PFPE	perfluoropolyether
PFPP	perfluoroperhydrophenanthrene
PMEA	poly-2-methoxyethyl acrylate
PMMA	poly (methyl methacrylate)

PTFE	polytetrafluoroethylene
PVC	polyvinyl chloride
QSI	quorum sensing inhibitor
RFP-HUVEC	red fluorescent protein expressing human umbilical vein endothelial cell
rTM	recombinant human thrombomodulin
SAM	self-assembled monolayer
SBMA	sulfobetaine methacrylate
SEM	scanning electron microscopy
SLIPS	slippery lubricant infused porous surfaces
SMC	smooth muscle cell
TaARI	Thrombosis & Atherosclerosis Research Institute
TBST	Tris-buffered saline tween
TM	thrombomodulin
TPFS	tridecafluoro-1,1,2,2-tetrahydrooctyl trichlorosilane
VEGF	vascular endothelial growth factor
vWF	von Willebrand factor
XPS	X-ray photoelectron spectroscopy

Chapter 1 *Introduction and literature review*

1.1. Overview

Blood-contacting medical devices such as catheters, vascular grafts and mechanical heart valves are widely used for vascular access, drug delivery, revascularization and repair of defective heart valves. However, all such devices trigger physiological responses that cause complications such as device-associated thrombosis and ultimately result in device failure. Thrombus formation on medical devices occurs through a series of complex and integrated pathways including, protein adhesion, platelet adhesion and activation and thrombin generation [1]. The immediate adhesion and adsorption of plasma proteins such as fibrinogen is known to be the initiating event, triggering the activation of the coagulation cascade and resulting in thrombin generation (***Figure 1.1***) [2], [3].

Since foreign synthetic surfaces are innately thrombogenic, prophylactic treatments with anticoagulant agents such as heparin and warfarin are required in order to prevent the complications caused by synthetic blood-contacting devices [4]–[6]. However, the administration of these reagents can result in life-threatening side effects such as bleeding and thromboembolism [6]–[9]. In a comprehensive study conducted on patients who underwent mechanical heart valve replacement between 1988 and 2005, thromboembolic and bleeding were the two leading causes of valve-associated complications [10]. In addition to thrombogenicity, synthetic surfaces suffer from poor biofunctionality and the inability to promote tissue integration. This is critical for permanent medical implants such as vascular grafts and mechanical heart valves, since improving tissue integration and cell infiltration at the site of implantation has shown to reduce the risk of post-operative device failure and rejection [11].

To combat the many issues caused by synthetic blood-contacting interfaces, extensive research has been devoted to developing new surface coatings that would enhance the hemocompatibility and biofunctionality (in case of permanent implants such as stents and vascular grafts) of these surfaces and avert the need for systemic anticoagulant administration.

1.2. Introduction

Cardiovascular disease is the global leading cause of mortality and morbidity, causing about 17 million deaths every year, nearly one third of all deaths worldwide. More than 50% of the deaths caused by cardiovascular complications are caused by ischemic

cardiovascular diseases such as peripheral and coronary artery diseases [12], [13]. In often cases where vessel occlusion has progressed, surgical intervention is inevitable and this has led to performing more than 1 million coronary revascularization surgeries in the US alone, making this procedure one of the most common medical interventions provided by the US healthcare system [14]. As a result of this prevalence, it has been predicted that the annual global financial burden of cardiovascular disease will exceed USD 1 trillion by 2030 [15]. The surgical treatment of occluded arteries often requires bypass surgery, where, as the standard of care, autologous blood vessels such as the saphenous veins, mammary or radial arteries are harvested from the patient's body and grafted at the desired site [16], [17]. However, more than 30% of the patients do not have available or appropriate vessels [17], [18], due to prior vascular complications such as pre-existing vascular diseases or past surgeries [19]–[21]. This insufficiency of viable autologous vessels has led to the development and utilization of synthetic graft alternatives.

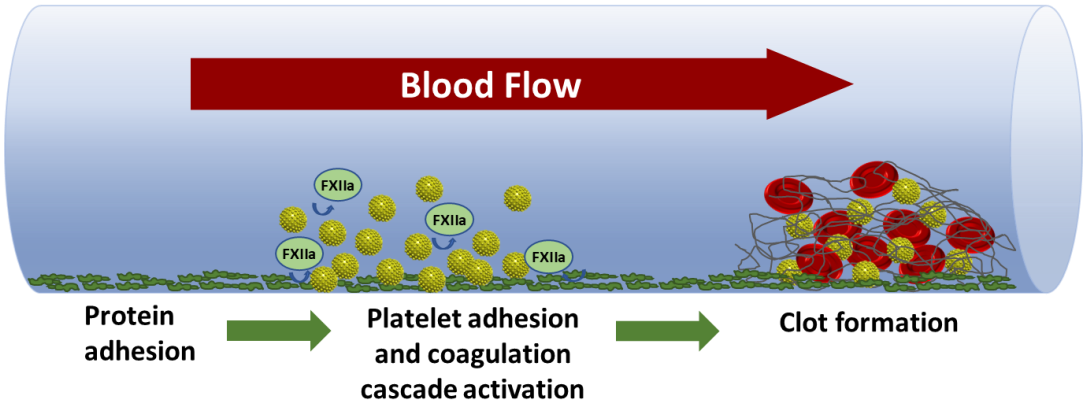

Figure 1.1 Schematic representation of the pathways involved in device-associated clot formation. Unlike a healthy endothelium that has innate anti-thrombogenic properties, once synthetic surfaces such as the inner surface of vascular grafts come in contact with blood, they actively induce thrombus formation through a series of complex and integrated pathways. Protein adhesion on the surface induces platelet adhesion and the activation of the contact pathway of the coagulation cascade, by activating factor (F) XII and ultimately resulting in device-associated clot formation.

Synthetic vascular grafts made of stable polymers such as expanded polytetrafluoroethylene (ePTFE, Teflon) or polyethylene terephthalate (PET, Dacron) suffer from low patency rates and have low patient outcomes compared to autologous vessels [16], [17], [20], [22]. This is mainly due to the thrombogenicity of the synthetic graft surfaces which leads to clot formation and graft occlusion. In addition, thrombus formation on vascular grafts prevents the complete and rapid coverage of the surface by endothelial cells (ECs) and ultimately thwarts the formation of a healthy endothelium [18]. This is troublesome since a healthy endothelium itself has innate anti-thrombogenic

properties by effectively decreasing platelet and protein adhesion and actively preventing clot formation [23], [24]. Moreover, forming a healthy and confluent endothelial layer is critical to facilitate and accelerate the integration of the permanent prostheses into the nearby tissue [16], [20] and to prevent intimal hyperplasia which may be caused by smooth muscle cell proliferation [20].

To date, several surface modification techniques have been purposed to improve the biocompatibility and biofunctionality of blood-contacting medical devices. These modification strategies mainly involve coating the surfaces with bioinert polymers [25]–[28] or antithrombotic agents [29]–[34]. In addition, EC specific antibodies [35]–[38] and vascular endothelial growth factors [39], [40] have been explored and applied to vascular graft or stent surfaces to improve their EC-specific capturing features. Although extensive research has been devoted to this area, creating a suitable and stable surface coating that integrates both biofunctionality and hemocompatibility still remains a challenge (***Table 1.1***) [40].

1.3. Surface coating strategies

1.3.1. Bioinert polymeric coatings

1.3.1.1. Poly (ethylene glycol) (PEG) coatings

PEG (also know as polyethylene oxide (PEO)) is one of the most common synthetic polymers used for coating blood-contacting medical interfaces [25], [41]. Methods used for PEG surface modification range from physical adsorption [42], graft polymerization [43] and chemical and covalent coupling [44], [45]. Covalent grafting of PEG is the preferred method since this modification procedure creates more stabile coatings for long-term applications [46]. The neutrally charged, hydrophilic PEG polymer brushes have the ability to bind to water molecules and form a hydration layer on the surface and as a result, effectively resist nonspecific adhesion of proteins and cells [25], [41]. However, studies have shown that the biocompatibility and repellency properties of the PEG coated surfaces highly depend on the chain length and surface density of the grafted PEG polymer [41], [47].

Kim *et al.* found that by increasing the grafting density and chain length of PEO in a polyurethane/polystyrene interpenetrating polymer network, a biocompatible interface is formed that decreases fibrinogen and platelet adhesion *in vitro* [47]. Similar results were found in a study where the adsorption of fibronectin in serum decreased by increasing the PEG chain density up to 0.12 PEG chains/nm^2, and then slightly increased on surfaces with 0.29 PEG chains/nm^2 [41]. PEG coatings have also been applied on ePTFE and PET surfaces in order to improve their surface biocompatibility and thrombogenicity properties and similar to the previous studies, these studies have demonstrated that the PEG surface

density and molecular weight affect the hemocompatibility of the coated surfaces [45], [48], [49]. ePTFE surfaces modified with 3% weight/volume PEG-600 Da had the best biocompatibility properties compared to 1% and 5% PEG modified surfaces and increasing the PEG surface density to more than 3% had an adverse effect on preventing platelet adhesion [49]. Likewise, PET surfaces coated with PEG-6000 Da were more blood-repellent and had significantly lower platelet adhesion compared with non-treated PET substrates and PET surfaces treated with PEG-200,1000 or 10,000 Da [45]. The inconsistency seen in the optimal PEG chain length and surface density required to obtain an ideal biocompatible surface coating could be mainly attributed to the differences present in the experimental conditions, grafting methods, incubation times and physical and chemical properties of the underlying coated surfaces.

Although short-term *in vitro* results obtained from PEG coated surfaces have shown some success in preventing nonspecific adhesion, *in vivo* and clinical outcomes have not been promising with this coating technique [48], [50]. One of the main issues seen with PEG coated surfaces in long-term *in vivo* experiments is the degradation and depletion of PEG chains caused by oxidation. The superoxide anions released by cells present in an *in vivo* environment can easily attack the ether linkage present on the PEG chain and generate a peroxide bond. The peroxide bond can then decompose and as a result reduce the chain length and surface density of the PEG layer overtime [51], [52]. These findings suggest that PEG coated surfaces are mainly suitable for short-term, single-use blood-contacting medical applications [28].

1.3.1.2. Zwitterionic polymers

As an alternative to PEG coating strategies, other novel bioinert polymers have been developed and investigated for medical applications [53]. Among these, zwitterionic structures, mainly those that contain, carboxybetaine [54] , phosphorylcholine [28] and sulfobetaine [55] have shown promising results in creating antifouling and hemocompatible surfaces. Zwitterionic polymers are neutrally charged polymers that have equal numbers of anionic and cationic groups on their polymer chains and this unique characteristic makes them highly hydrophilic and resistant to non-specific adhesion [56], [57].

The development of zwitterionic materials was bioinspired by the natural, bio-inert properties of the external surface of cell membranes that are rich in phospholipids containing zwitterion head groups [58], which gives them the innate antifouling and thrombogenic properties [59]. Among the zwitterion structures developed for blood-contacting applications, phosphorylcholine (PC)-bearing polymers have been the most promising candidates [60]. Although the results obtained from the first generation of PC-bearing polymers used for biomedical applications were promising, the low yield and purity

of the synthetized polymers were not satisfactory [28]; hence, scientists aimed to synthetize a new class of PC polymers using methacrylate monomers called 2-methacryloyloxyethyl phosphorylcholine (MPC) and were able to optimize and simplify the synthesis conditions and obtain sufficient amounts of MPC with high purity [61]. This achievement led to considerable progress in developing various MPC polymers for blood-contacting applications [62]–[65].

Table 1.1 Different surface modification techniques for enhancing hemocompatibility and endothelial cell adhesion on blood-contacting biomaterials

Surface coating/substrate	**Modification technique**	**Cell marker**	**Outcomes**	**Limitations**
Heparin/heparin-mimicking multilayers / Polyvinylidene difluoride membrane [23]	Layer-by-layer assembly	NA	Reduced platelet adhesion and activation Prolonged clotting times Improved EC adhesion	Non-specific adhesion to Heparin [66] Leaching, degradation, depletion and instability of the coating [6], [54] Not EC specific
Anti-CD34 antibody immobilization / ePTFE grafts [36]	Covalent attachment through peptide linkages	Anti-CD34 antibody	Rapid endothelialization *in vivo* 95% coverage with ECs after 28 days	Hemocompatibility was not investigated Grafts Stimulated intimal hyperplasia
Heparin and fibronectin films/ titanium surfaces [67]	Electrostatic interaction and co-immobilization technique	NA	Lower hemolysis rate Prolonged blood coagulation time Reduced platelet adhesion and activation More EC adhesion and proliferation	Non-specific adhesion to the coating [66] Leaching, degradation, depletion of the coating [6] Thrombogenicity of fibronectin [68] Not EC specific
Poly(1,8-octanediol-co-citrate)-Heparin coating/ePTFE grafts [34]	Chemical immobilization through carboxyl functional groups	NA	Maintained bioactivity *in vitro* Inhibited blood clot formation and platelet adhesion Supported EC adhesion	Non-specific adhesion to Heparin [66] Not specific to ECs Non-specific adhesion of SMCs Coating degradation
Heparin/Collagen Multilayer functionalized with anti-CD133 antibody/ePTFE grafts [40]	Layer-by-layer assembly	Anti-CD133 antibody	Prolonged blood coagulation time Reduced platelet adhesion ECs adhered "well" to the ePTFE coated surface *in vitro* Rapid endothelialization *in vivo*	Non-specific adhesion to heparin [66] Thrombogenicity of collagen [69] Instability of the coating [54] Low expression of CD133 on ECs circulating in the blood stream [70]
Anti-CD34 antibody functionalized heparin-collagen multilayer/316L stainless steel	Layer-by-layer assembly	Anti-CD34 antibody	Good hemocompatibility Promoted cell attachment and growth	Non-specific adhesion to heparin [66] Thrombogenicity of collagen [69]

stents [71]			Rapid endothelialization *in vivo*	Instability and degradation of the coating [54]
Co-immobilization of Heparin and Cell-Adhesive Peptides /polyurethane grafts [72]	Chemical immobilization technique	Cell-adhesive peptide	Slightly reduced adhesion of platelets Decreased fibrinogen adsorption Enhanced EC attachment	Non-specific adhesion of fibroblasts, and smooth muscle cells (SMCs) to the peptides [72] Non-specific adhesion to heparin [66] Leaching of the heparin coating [6] Not EC specific
Heparin release from PCL/chitosan grafts [73]	Ionic bonding between heparin and chitosan fiber	NA	Reduced platelet adhesion Prolonged coagulation time Promoted EC growth	Non-specific adhesion to heparin [66] Leaching of the heparin coating [6] Not EC specific
Chitosan-Heparin coating / 316L stainless steel stents [74]	Layer-by-Layer assembly	NA	Improved hemocompatibility Improved EC adhesion promote re-endothelialization *in vivo*	Non-specific adhesion to heparin [66] Leaching of the heparin coating [6] Instability of the coating [54] Not EC specific
PEG and anti-CD34 antibody immobilization / titanium surfaces [75]	Covalent immobilization	Anti-CD34 antibody	Reduced platelet adhesion Improved EC adhesion	Degradation and depletion of PEG chains caused by oxidation [51] Not suitable for long-term applications [28]
Heparin, fibronectin and VEGF / titanium surfaces [68]	Layer-by-Layer deposition	VEGF	Prolonged clotting time Reduced platelet adhesion and activation Promoted EC adhesion and proliferation	Non-specific adhesion to heparin [66] Thrombogenicity of fibronectin [68] Instability of the coating [54] Risk of tumor development caused by VEGF release [76]
VEGF immobilization / poly(L-lactide-co-ε-caprolactone) elastomer [77]	Multistep chemical immobilization	VEGF	Improved EC adhesion and the formation of an endothelial layer	Hemocompatibility has not been investigated Risk of tumor development caused by VEGF release [76]
Heparin immobilization on plasma treated surface / Polycarbonate-urethane (PCU) grafts [78]	Chemical modification	NA	Antithrombogenic properties Higher patency rates *in vivo* Formation of a more confluent endothelial layer	Non-specific adhesion to heparin [66] Leaching of the heparin coating [6] Not EC specific

The amount of protein adhering to blood-contacting devices depends on the free-water fraction of the surface and less protein adsorbs to surfaces with a higher free-water fraction [79]. MPC polymers have extremely high levels of free-water fraction and the PC groups

present on the polymer chains effectively reduce the protein adsorption force at the interface [60]. Chen *et al.*, observed that coating ePTFE surfaces with MPC through physical absorption, significantly reduced platelet adhesion and neointimal hyperplasia *in vivo* and all implanted femoral arteriovenous grafts modified with MPC were patent at 4 weeks compared with control grafts [80].

While the results obtained from these experiments were promising, the stability of the coating for long-term applications is questionable, since the MPC layer is not covalently attached to the surface and could be removed by physiological shear stresses. In order to overcome this limitation, Chevallier *et al.*, optimized the modification strategy and investigated the biological performance of a dichloro derivative, PC-grafted ePTFE surface by covalently attaching PC polymers to the substrate using radio-frequency glow discharge ammonia plasma treatment [81]. The blood compatibility of the PC-grafted ePTFE surface was investigated by conducting *in vitro* tests such as thromboelastography, platelet adhesion and neutrophil adsorption. The results obtained from the *in vitro* experiments showed that the PC-modified ePTFE grafts significantly decreases thrombin generation, platelet and neutrophil adhesion compared with control ePTFE grafts [81].

Among the new generation of MPC zwitterionic polymers, poly(sulfobetaine methacrylate) (polySBMA) has become a popular candidate, mainly because of the low cost and simplicity in synthesising this polymer and its ability to create a strong hydration layer on the coated surface [55], [82]. Vascular catheters coated with a non-leaching polySBMA surface using a graft from redox polymerization process, effectively reduced platelet activation, protein and cells adhesion and prevented clot formation both *in vitro* and *in vivo* [83]. These polymers have also been grafted on hydrogen plasma treated PTFE membranes using atom transfer radical polymerization (ATRP) where the C-F groups present on the PTFE surface were used as initiators for the ATRP reaction [84]. Coating the PTFE surface with the polySBMA polymer significantly decreased the hydrophilicity of the PTFE substrate and the coated surfaces were highly protein (human fibrinogen) repellent compared with control samples. Studies have shown that the film thickness and grafting density of the polySBMA-grafted surfaces can affect the blood and plasma protein repellency properties [85]; thus, using a controlled polymerization technique such as ATRP for grafting this polymer could be highly beneficial since the molecular weight distribution, molar mass ratios and the architecture of the grafted polymer could precisely be controlled using this technique [86].

1.3.2. Plasma surface modification techniques

The hydrophobicity of both ePTFE and PET vascular grafts, prevents EC adhesion and growth and promotes platelet activation and clot formation [19]. To make these surfaces

more hydrophilic, plasma modification techniques are one of the methods used that allow the surfaces to bond with different atmospheric gases and as a result decrease the hydrophobicity of the substrates [21], [87], [88]. In addition, plasma treatment also increases the capacity of the synthetic vascular grafts for biomolecule immobilization by creating appropriate chemical functional groups such as hydroxyl or carboxyl groups on their surfaces [89]. Moreover, studies have shown that plasma modification, is an effective way to modify and functionalize biomaterials, such as ePTFE, without altering their surface bulk properties [89]. Depending on the plasma energy and type of gas used, plasma radiation only affects the surface of the substrate to a shallow depth, leaving the bulk properties of the substrate intact [90].

Dekker *et al.* investigated the affect of nitrogen plasma treatment of ePTFE surfaces on EC spreading and adhesion [87]. Depending on the plasma treatment time, the hydrophilicity and wettability of the treated surfaces changed, with surfaces that were exposed to higher plasma times being more hydrophilic and having lower water contact angles. In addition, plasma treating ePTFE surfaces increased cell spreading and adhesion after 6 hours of incubation and they had significantly larger number of ECs adhered to their surfaces compared to unmodified ePTFE substrates [87]. The affect of ammonia plasma treatment of PET and PTFE surfaces on EC adhesion has also been investigated [91]. Both PET and ePTFE surfaces significantly increased cell adhesion (1.3-fold and 5.5-fold respectively) compared to unmodified surfaces after 1 day and 7 days of incubation and cell numbers continued to grow on all surfaces, except for untreated PTFE substrates which was conversely reduced by 41% [91]. Despite the improved EC adhesion on these surfaces, further studies need to be conducted in order to investigate their hemocompatibility properties and their ability to prevent blood protein and platelet adhesion as well.

A number of studies from Laroche's lab have focused on using ammonia plasma treatment as an initial step in multistep functionalization procedures of PTFE surfaces [81], [92], [93]. In these studies, ammonia plasma treatment was first used in order to create amino functional groups on the PTFE surface and subsequently the amino groups were utilized to covalently attach various biomolecules such as fibronectin [93], vascular endothelial growth factor (VEGF) [92] and also the zwitterionic phosphorylcholine polymer [81]. The main purpose of these studies was to assess the blood compatibility [81], biological activity [93], and endothelialization [92] of the modified PTFE surfaces compared with unmodified substrates. In addition to ammonia, argon plasma treatment has also been used to covalently attach specific bioactive molecules, such as collagen IV and prostaglandin E1 on ePTFE and PET surfaces in order to enhance their hemocompatibility, without significantly modifying the graft structure [94]. As a result of these coatings, fibrinogen adsorption and

platelet adhesion were significantly reduced and the adhesion of the bioactive molecules on these surfaces significantly improved the biocompatibility of the vascular grafts.

1.3.3. Antithrombotic agents

1.3.3.1. Heparin

Using anticoagulant agents alone or in combination with other bioactive and bioinert molecules has widely been investigated for creating antithrombotic blood-contacting surfaces [54]. Among these, heparin is the most widely anticoagulant agent used for creating hemocompatible surfaces that inhibit platelet adhesion and thrombin generation (***Table 1.1***) [21], [95]. As an anticoagulant, heparin binds to antithrombin and acts as a catalyst, accelerating the antithrombin-mediated inhibition of clotting proteases such as thrombin and factor X [96]. Several immobilization techniques such as covalent attachment [29], [34], [72], physical adsorption [97], [98], electrostatic attachment via the negatively charged sulfate groups of heparin [99] and layer-by-layer deposition [23], [74] have been used to graft heparin on biomaterials. The efficiency of the heparin coated layer in preventing non-specific adhesion and preventing thrombin generation depends on several factors such as the quality and stability of the heparin coating and whether the heparin molecule remains biologically active after the modification process [89]. Physical adsorption of heparin is one of the techniques used to coat the surfaces of biomaterials; however, this modification procedure results in creating unstable heparin coatings that deplete overtime [100]. For examples, ePTFE grafts coated with silyl-heparin though physical adsorption have shown to lose 98% of heparin activity after 7 days of implantation *in vivo* and due to the poor retention of the heparin coating on the ePTFE surface, the patency rates were not significantly different in heparin-coated grafts compared with control ePTFE surfaces [100].

In order to circumvent this limitation, covalent immobilization of heparin is the preferred method for creating heparin-coated surfaces. The covalent immobilization strategy used to attach the heparin molecule on the surface plays an important role in the biological activity of the immobilized heparin molecule. One heparin molecule has multiple carboxylic acid groups present on its surface. The free carboxyl groups could create multiple covalent linkages with other functional groups such as amino or hydroxyl groups present on the biomaterial and as a result robustly immobilize the heparin molecule on the surface. Although multiple covalent linkages could better stabilize the heparin molecule on the surface, this nonspecific immobilization and linkage inhibits the free movement of heparin molecules and ultimately hinders the natural configuration and biological activity of the heparin layer [54]**.**

In order to better understand this matter, Gore *et al.*, investigated how the heparin immobilization technique affects the hemocompatibility and protein resistant properties of the coated surface in human whole blood [96]. End-point attachment of heparin was compared with other covalent attachment techniques, such as heparin immobilization using carbodiimide crosslinking chemistry which results in nonspecific linkage of the heparin molecule. End-point immobilization of heparin creates one single covalent bond at the end of the heparin chain and retains the natural configuration and biological activity of the heparin molecule. The results obtained from this study revealed the relationship between the immobilization strategy and heparin antithrombotic activity where the surfaces coated using the end-point attachment technique had significantly better antithrombotic properties and reduced platelet adhesion, activation and clot formation compared with other modification techniques [96]. The effectiveness of end-point immobilization of heparin in creating blood-compatible surfaces has been reported by several other studies as well [78], [101]–[103]. Begovac *et al.*, investigated the thromboresistance of end-point immobilized heparin coated Gore-Tex® ePTFE vascular grafts *in vivo* [102]. Both short-term (1 week) and long-term (12 weeks) experiments showed significantly higher patency rates ($P < 0.05$) and greater thrombus-free luminal surfaces in heparin-coated ePTFE grafts compared with unmodified control ePTFE surfaces and no significant difference was seen in heparin bioactivity after 12 weeks of implantation [102].

Introducing a hydrophilic spacer between the heparin molecule and the biomaterial surface has shown to be an effective way to create biofunctional, bioactive and hemocompatible heparin coatings and to protect the heparin molecule from denaturation [104]. PEG is one of the most common hydrophilic spacers used for heparin immobilization [72], [105], [106]. Pan *et al.* investigated the blood compatibility and EC adhesion of titanium surfaces modified with heparin-PEG [106]. Titanium surfaces were initially oxygen plasma treated and subsequently modified with heparin-PEG using the carbodiimide coupling chemistry. The resulting heparin-PEG modified surfaces significantly decreased plasma fibrinogen and platelet adhesion and prolonged the activated partial thromboplastin time compared with control surfaces. In addition, the negatively charged, heparin-PEG surfaces were cell compatible and showed better EC adhesion and spreading compared with unmodified surfaces [106]. Similar to the PEG coating techniques discussed earlier, the chain length of the PEG spacer has shown to be an important factor that could affect the bioactivity level and the antithrombotic properties of the heparin molecule [107], [108]. By increasing the PEG chain density, the bioactivity of heparin increases and PEG with the molecular weight of 1000 Da has shown to provide the optimum heparin dynamic motion required to prevent platelet adhesion and clot formation on coated surfaces [72].

In recent studies, co-immobilizing heparin with other biomolecules has been one of the most popular methods used for generating hemocompatible interfaces (***Table 1.1***), [67], [68], [73], [109], [110]. For example, aminosilanized titanium surfaces were biofunctionalized with heparin and fibronectin (Hep/Fn), which is one of the extracellular matrix (ECM) proteins, and their blood compatibility and endothelialization was studied [67]. Blood experiments showed that co-immobilization of Hep/Fn prolonged the blood clotting time, decreased fibrinogen adhesion and platelet activation and aggregation compared with unmodified titanium substrates. In addition, the EC seeding and fibronectin bioactivity experiments showed more cell attachment and proliferation on biofunctionalized surfaces compared with control surfaces [67]. Intimal hyperplasia caused by smooth muscle cell proliferation and migration is one of the major reasons for restenosis after cardiovascular intervention [20]. Cai *et al.*, explored the Hep/Fn complex further and investigated the inhibitory effect of this coating on smooth muscle cell proliferation [111]. The obtained results from this study revealed that Hep/Fn immobilization on titanium surfaces inhibits smooth muscle cell proliferation up to 5 days compared with control samples.

In addition to fibronectin, collagen is another ECM protein that has been used to create ECM inspired heparin surface coatings [109], [112]. In a recent study, ePTFE films were biofunctionalized with a Hep/collagen complex that included an EC adhesive peptide and the anticoagulant and EC adhesion properties were investigated [109]. After modifying the ePTFE films with the Hep/collagen multilayer, less platelet adhesion and aggregation was observed, and the blood clotting time significantly increased compared with unmodified surfaces. In addition, the presences of the EC adhesive peptide positively influenced EC adhesion and proliferation, something that was not observed in control ePTFE films.

Collagen and fibronectin are two of the most important proteins present in the ECM which have shown to promote cell adhesion and improve cell compatibility on biomaterials [34], [68], [113] However, these ECM proteins also promote platelet adhesion and activation and thrombus formation and the excessive use of these highly thrombogenic materials on the surface of blood-contacting implants that have not yet been completely covered with an endothelial layer could be problematic [68], [69]. Therefore, the ultimate antithrombotic, EC-friendly complex developed using ECM proteins must be precisely designed so that it promotes endothelialization without compromising the antithrombotic properties of the coating.

Overall, surface modification of biomaterials with heparin coatings is an established method that is used to create hemocompatible substrates. However, several limitations still challenge this modification technique. Heparin's anticoagulant property is highly

dependent on the attachment of antithrombin to heparin via its active (pentasaccharide) sequence [96]. This could be problematic since the concentration of antithrombin depends on the velocity of blood and might decrease in occluded regions that have a higher blood velocity [114]. Further, heparin-binding affinity is not specific to antithrombin and it can bind to other biomolecules such as growth factors [66]. This nonspecific interaction could decrease the anticoagulant activity and efficiency of the coating. Lastly, heparin coated surfaces are prone to degradation and depletion over time, which could result in the gradual lose of their bioavailability and anticoagulant properties [6], [7].

1.3.3.2. Other anticoagulant agents

In addition to heparin, other anticoagulant agents with different mechanisms of action such as corn-trypsin inhibitor (CTI) [115], [116], direct thrombin inhibitors such as hirudin [117], thrombomodulin (TM) [118] or recombinant human thrombomodulin (rTM) [119] and nitric oxide (NO) releasing coatings [120] have been investigated to create hemocompatible biointerfaces. CTI is a protein, derived from corn kernels that is known to specifically inhibit FXIIa and block the root cause of device-associated coagulation [1]. In order to both inhibit FXIII activation and decrease plasma protein deposition, researchers have co-immobilized CTI with PEG (PEG-CTI) on biomaterials. Surfaces coated with PEG-CTI conjugates have shown to inhibit FXIII autoactivation, reduce fibrinogen adhesion and thrombin generation and prolong plasma clotting times compared with non-coated surfaces [116], [121], [122]. In addition, *in vivo* studies have shown that PEG-CTI modified catheters significantly prolong the time to catheter occlusion by 2.5-fold compared with unmodified catheters and catheters modified with PEG only [115].

Direct thrombin inhibitors such as TM are another class of anticoagulant agents used for coating blood-contacting medical devices. TM is a membrane protein expressed on the surface of ECs which binds to thrombin. The thrombin-thrombomodulin complex supresses coagulation by promoting protein C activation which ultimately results in inhibiting thrombin generation [123]. Several groups have immobilized TM alone [119], [124]–[126] or in combination with other anticoagulant agents such as heparin [127] to create biocompatible surfaces that locally prevent coagulation and thrombin generation. These surfaces have shown promising short-term results in reducing clot formation, thrombin generation, platelet adhesion and activation [124]–[127] and inhibiting neointimal hyperplasia [119]. One of the main disadvantages of the modification techniques used in these studies is the random orientation and inherent reduction in the bioactivity of TM after the immobilization process. This is mainly due to the non-targeted conjugation and immobilization of the protein on the substrate which leaves limited accessibility to the active catalytic site and reduces the anticoagulant properties of the protein [123]. In order

to protect the antithrombin activity of TM, several site-specific, targeted binding strategies have been developed [128]–[130]. For example, Qu *et al.*, reported a novel technique to site-specifically immobilize active TM on ePTFE surfaces by using a molecular engineering and bioorthogonal chemistry approach [129]. In this technique, human TM fragments expressing a signal C-terminal azide moiety were synthetized and immobilized onto the luminal surface of polyurethane coated ePTFE vascular grafts using the Staudinger Ligation reaction chemistry. The TM coated surfaces were stable *in vitro* and significantly reduced platelet adhesion and activation and clot formation *in vivo,* over a 60-minute perfusion period. Despite the promising results obtained from this study, the complex synthesis procedure, low yield and scalability of the reaction limits the implementation of this modification technique in clinical applications.

Nitric oxide (NO) generating and releasing substrates are another class of surface coatings that have been explored for blood-contacting surfaces. NO is a signalling molecule produced and released by ECs, which regulates several biochemical processes in the vascular system [131]. Most importantly, the protective role and anticoagulant properties of the endothelium has mainly been attributed to the presence of NO which has shown to prevent platelet adhesion and activation, clot formation and SMC proliferation [132]. Smith *et al.*, were the first to apply a NO-releasing polyethylenimine coating on PTFE surfaces by incorporating diazeniumdiolate groups ($[N(O)NO]^-$) in polymeric matrices and testing its hemocompatibility [133], [134]. The NO-releasing, polyethylenimine coated PTFE vascular grafts showed potent antiplatelet activity and were significantly less thrombogenic compared with untreated PTFE surfaces when tested *in vivo* [133]. Moreover, several other modification approaches have been developed for obtaining diazeniumdiolate, NO-releasing functional surfaces, however one of the main disadvantages of using diazeniumdiolates as NO donors is that the amount of NO released from these surfaces is limited and it depletes over time. As a result the coated substrates are prone to loosing their anticoagulant properties in long-term applications [135]. Because of these limitations, new surface coating techniques, which contain catalytic agents that convert endogenous NO donors such as S-nitrosoglutathione, S-nitrosocysteine and S-nitrosoalbumin to NO and thereby generate a sustained source of NO have been explored [136]–[139]. These surface coatings have shown to reduce restenosis, collagen-induced platelet activation and enhance human umbilical vein EC (HUVEC) adhesion.

1.3.4. Surface coating with EC specific growth factors and antibodies

The endothelium consists of a monolayer of ECs that lines and covers the interior lumen of vessels and is in direct contact with blood. It is well understood that the endothelial layer plays a crucial role in regulating inflammation and clot formation [76]; therefore, the

establishment of a healthy and confluent endothelial layer on newly implanted vascular grafts, stents and heart valves is crucial in order to prevent occlusion and thrombin generation and to retain the patency of the blood-contacting medical device [21], [76]. To address this requirement, in the past few years, several research groups have investigated *in vitro* EC seeding on synthetic vascular grafts (***Figure 1.2***), [140]–[142]. Although these studies have shown the effectiveness of this technique in improving the patency and performance of the grafts, the implementation of this technique in clinical applications is still impractical. *In vitro* EC seeding requires harvesting of autologous ECs, culturing and expanding them *ex vivo* and further, seeding the cells on the luminal surface of vascular grafts prior to implantation (***Figure 1.2***) [143]. This process is costly and time consuming and requires extensive culture times (up to 8 weeks) [71] and there is a high possibility of contamination and infection of the coating during the process [76], [143]. In addition, the stability of the pre-seeded endothelial monolayer during and after implantation remains a concern [76]. Due to these drawbacks, researchers have explored alternative options such as promoting *in situ/in vivo* endothelialization on vascular grafts. *In situ* endothelialization techniques aim to reconstruct a functional endothelial layer after vascular grafts are implanted *in vivo* [76]. These techniques mainly consist of immobilizing EC specific biomarkers and cell adhesive molecules on biomaterial prior to implantation.

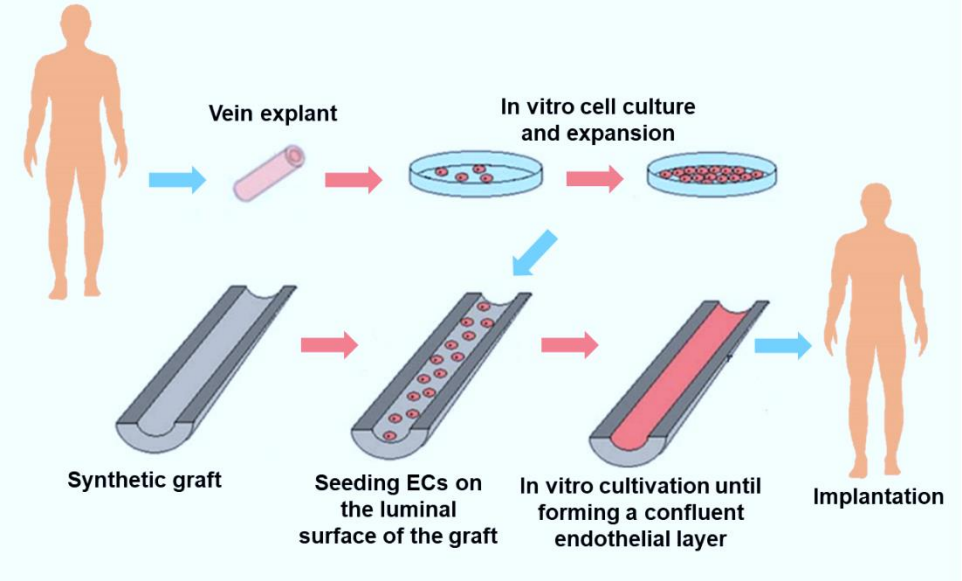

Figure 1.2 Schematic representation of *in vitro* EC seeding on synthetic vascular grafts. ECs are extracted from the patient's vein and expanded *in vitro*. Once the cells are ready, they are seeded on the luminal surface of the synthetic vascular grafts and cultured until a confluent and functional endothelial layer is achieved. The EC seeded vascular graft is then implanted in the patient's body. Adapted from Avci-Adali *et al.* [144].

1.3.4.1. Vascular endothelial growth factor (VEGF) coated surfaces

VEGF is well know for its key role in vascular development, angiogenesis and stimulating the proliferation, differentiation and migration of ECs [145], [146]. Surface immobilization of VEGF, alone or in combination with other biomolecules has shown to promote EC adhesion, proliferation, migration and growth *in vitro* (***Table 1.1***), [39], [77], [147]. In a recent study, Randall J. *et al.*, investigated the ability of VEGF/heparin coated surfaces to capture ECs under flow conditions [39], using a microfluidic device and under a series of shear stresses ranging from low to physiological shear stresses. The growth factor remained biologically active after the immobilization process and selectively captured ECs and not other cell types such as human dermal or mouse fibroblast. In addition, these surfaces were able to capture ECs from complex biological solutions such as whole blood under high flow rates [39]. In another approach, instead of coating the surface of the biomaterial with free VEGF, Xu *et al.*, incorporated VEGF-loaded poly-lactic-co-glycolic acid microparticles on anti-CD34 antibody coated surfaces and investigated the effect of VEGF release on endothelialization and hemocompatibility [148]. Although the sustained release of VEGF decreased platelet activation, and significantly improved endothelial progenitor cell (EPC) adhesion and proliferation, when compared with non-coated surfaces, a burst release and high dose of this growth factor may lead to developing immature capillaries and tumors [149]; therefore its safe usage for promoting *in vivo* endothelialization of biomaterials should be closely investigated.

Despite the promising results obtained from *in vitro* experiments using VEGF immobilization, *in vivo* experiments have revealed that VEGF coated surfaces are not specific to capturing endothelial cells and these surfaces could also promote non-specific adhesion of other cell types. *In vivo* studies performed using ePTFE vascular grafts coated with a VEGF/ECM [150] or fibrin/VEGF [151] complex have shown that, in addition to increasing EC capture, these surface coatings also promote SMC adhesion and growth and as a result increase myointimal hyperplasia and decrease the patency rates of the vascular grafts overtime [150], [151].

1.3.4.2. Promoting endothelialization by immobilizing endothelial cell targeting antibodies

EPCs are mononuclear cells that are mainly accumulated in the bone marrow and can be found in low concentrations in the peripheral blood stream. After entering the blood stream, EPCs have the ability to differentiate into mature ECs and attain EC specific markers and antigens. [70], [76]. Peripheral blood contains at least two types of “early” and “late” EPC populations, which are fundamentally different. Early EPCs also called colony forming unit-endothelial cells (CFU-ECs) have low proliferative capabilities and express

hematopoietic and monocytic features in addition to endothelial cell characteristics. In contrast to early EPCs, late EPCs or endothelial colony forming cells (ECFCs) have high proliferative capacity, express endothelial cell specific markers and phenotype but have no hematopoietic or monocytic characteristics [76], [143]. In general, EPCs present in the bone marrow express CD34, VEGFR-2 and CD133 surfaces markers. However, EPCs circulating in the blood stream, loose CD133 expression and begin to express more endothelial cell specific markers such as VE-cadherin (CD144) and von Willebrand factor (vWF) in addition to CD34 and VEGFR-2 (***Figure 1.3***) [70]. Lately, immobilizing monoclonal antibodies against these endothelial specific surface markers have been explored as an effective technique for capturing circulating ECs and promoting endothelialization on the surface of vascular implants.

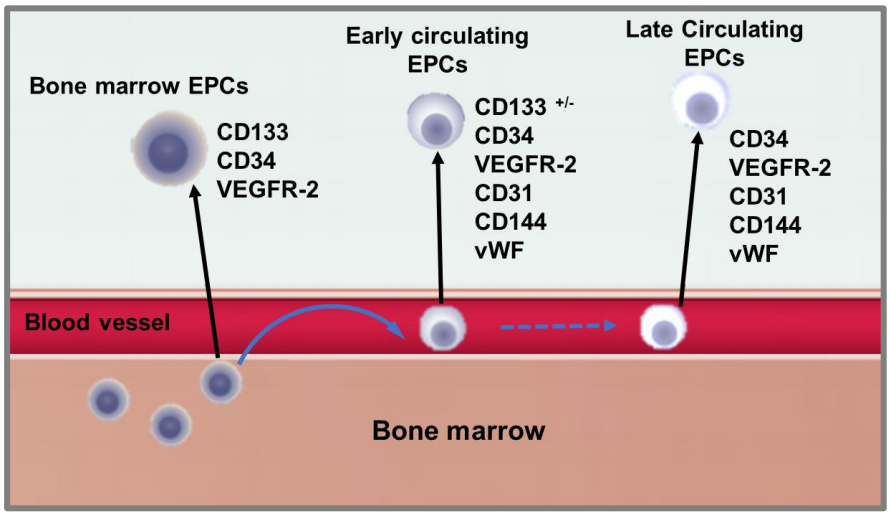

Figure 1.3 Schematic representation of the expression of different markers during the differentiation and migration of EPCs from the bone marrow into the blood stream. Adapted from Hristov *et al.* [70], and De La Puente *et al.* [152].

Anti-CD34 antibody is one of the most popular endothelial cell capturing markers used in designing vascular stents [71], [75], [153]–[158]. The Genous™ stents, designed by Orbus Medical Technologies (Hong Kong), where the surface of the 316L stainless steel stents are covalently modified with a polysaccharide layer and functionalized with monoclonal anti-human CD34 antibodies [76] are the first commercially available EPC capturing stents [143]. The results obtained from the first clinical study conducted on these stents, investigating the short-term safety and feasibility of these surfaces revealed that the bioengineered, EPC capturing stents are safe and promote rapid endothelialization and no stent thrombosis was seen 30 days or 6 months post implantation [159]. The use the EPC capturing stents during primary percutaneous coronary intervention in patients suffering from acute myocardial infarction has also shown to be safe and feasible, with low rates of

major adverse cardiac events 30 days (4.2%) or 6 months (5.8%) after the surgery [160]. Lastly, the clinical results obtained from the 12-month follow-up of the e-Healthy Endothelial Accelerated Lining Inhibits Neointimal Growth (e-HEALING) worldwide registry revealed that coronary stenting with the Genous™ bioengineered stents results in promising clinical outcomes, with low stent thrombosis and repeat revascularisation incidences [161].

Lin *et al.*, integrated anti-CD34 antibody with antithrombogenic agents and designed a heparin-collagen/anti-CD34 antibody functionalized multilayer to investigate *in situ* endothelialization and hemocompatibility of intravascular stents [71]. In addition to good hemocompatibility, the *in vitro* results obtained from the cell studies showed the targeting features of anti-CD34 antibody functionalized surfaces towards ECs and not SMCs, something that was not observed in heparin/collagen functionalized surfaces with no anti-CD34 antibody immobilization. In addition, ECs adhered to anti-CD34 antibody functionalized surfaces had better viability and metabolic activity compared to ECs present to non-antibody functionalized surfaces. Lastly, results obtained from *in vivo* experiments revealed that in contrast to unfunctionalized and surfaces functionalized with heparin-collagen only, heparin-collagen/antiCD34 antibody functionalized surfaces significantly inhibited neointimal hyperplasia [71]. In a similar approach, Chen *et al.*, incorporated PEG into the coating and studied the biocompatibility and endothelialization of PEG/anti-CD34 antibody functionalized titanium surfaces [75]. In this technique, 3-(2-amino-ethylamino) propyltrimethoxysilane was used as the base coupling agent for grafting PEG polymer chains and further, anti-CD34 antibodies were immobilized on the PEG functionalized surfaces using carbodiimide crosslinker chemistry. The results obtained from *in vitro* experiments confirmed the superior performance of PEG/anti-CD34 antibody functionalized surfaces compared to control samples. These surfaces significantly decrease platelet adhesion, promoted targeted ECs adhesion and inhibited SMC adhesion [75].

In contrast to vascular stents, anti-CD34 antibody immobilization on synthetic vascular grafts has not yet been fully investigated. In the limited studies performed on ePTFE substrates, anti-CD34 antibody immobilization has shown to inhibit platelet adhesion [38] and stimulate endothelialization [36], [38] in short-term applications; however, the long-term efficacy of these grafts and their capability to promote *in vivo* endothelialization and hemocompatibility is not yet fully understood.

Although EPCs loose the expression of CD133 as they differentiate and enter the peripheral blood stream (***Figure 1.3***) [143], a few studies have investigated anti-CD133 antibody immobilization for capturing ECs as well [40], [162]–[164]. Stents coated with anti-CD133 antibody have shown to improve endothelialization *in vitro* [162], [163]*;* however, long-

term *in vivo* experiments showed an increase of non-specific adhesion of other cell types and no significant difference in endothelial recovery [162], [163] or neointima formation [163] was seen when comparing the results with uncoated surfaces. Lu *et al.*, coated ePTFE synthetic grafts with a heparin/collagen multilayer functionalized with anti-CD133 antibody, using a layer-by-layer technique and investigated *in vivo* endothelialization and blood compatibility of the coated surfaces in a pig common carotid artery transplantation model [40]. No difference was seen in the *in vitro* blood compatibility and platelet adhesion results when comparing the heparin/collagen coated surfaces in the presence or absence of anti-CD133 antibody. The results obtained from the SEM imaging and histopathological staining of the explanted grafts indicated that the anti-CD133 coated grafts were able to promote endothelial cell adhesion after seven days. In contrast, heparin/collagen modified surfaces showed incomplete endothelialization and more platelet deposition on their surfaces [40].

Mature and circulating ECs highly express VEGFR-2, also know as kinase insert domain receptor (KDR) [70]; hence, immobilizing antibodies against this receptor on the surface of biomaterials is another technique used to promote EC adhesion and growth [165]–[167]. However, these surfaces seem to be less effective in promoting EC spreading, adhesion and differentiation when compared with VEGF coated substrates [168], [169]. To study this phenomenon, Matsuda *et al.* investigated the capture of EPCs on surfaces coated with either VEGF or anti-VEGF receptors [168]. These biomarkers were covalently attached to hydroxyl terminated poly (ethylene- co-vinyl alcohol) surfaces and EC adhesion and differentiation was studied. VEGF coated surfaces significantly increased cell differentiation after 2 weeks and the number of cells expressing VEGF receptors were significantly higher on these surfaces compared with anti-VEGFR coated surfaces, making them a better candidate for EC capture.

1.4. Lubricant-Infused Surfaces

1.4.1. Design principals

Recently, lubricant-infused surfaces (LIS) have gained extensive attention as a unique and promising approach for solving the ongoing problem of non-specific adhesion in medical and non-medical applications (***Figure 1. 4***). Inspired by the repellent and non-sticky liquid-infused surfaces which are widely present in nature [170]–[173] , scientists have began integrating liquids into their surface engineering designs and investigating the unique repellency properties of these new types of substrates [174]–[178]. The thin, lubricant layer, integrated within the solid substrate creates a mobile liquid interface with new surface behaviours that could repel organic, aqueous [179] and complex biological liquids [174], [178] and prevent cell adhesion and biofilm formation [174], [180].

The solid underlying substrate and the immobilized liquid layer are the two main components present in the lubricant-infused system that interact and work together to create a stable yet dynamic liquid interface. Most importantly, the underlying flat or porous/rough solid substrate needs to have a high chemical affinity for the infiltrating lubricant layer and a relatively low affinity for the contaminating liquid. This can be achieved by either exploiting the innate chemical properties of the solid surface ***Figure 1. 4*****a**) [175], [179] or by chemically modifying the surface with an appropriate functional monolayer that is compatible with the desired lubricant (***Figure 1. 4b*** *and* ***c***) [176], [178]. Once the appropriate conditions are met, the solid substrate is able to "lock-in" the liquid layer through a combination of van der Waal and capillary forces and as a result create a stable, highly repellent and homogenous lubricant-infused interface. In other terms, the chemical affinity and physical properties of the underlying substrate most meet the requirements to create a platform in which it is more energetically favourable for the lubricant layer than for the contaminating liquid to infiltrate and wet the solid substrate [181].

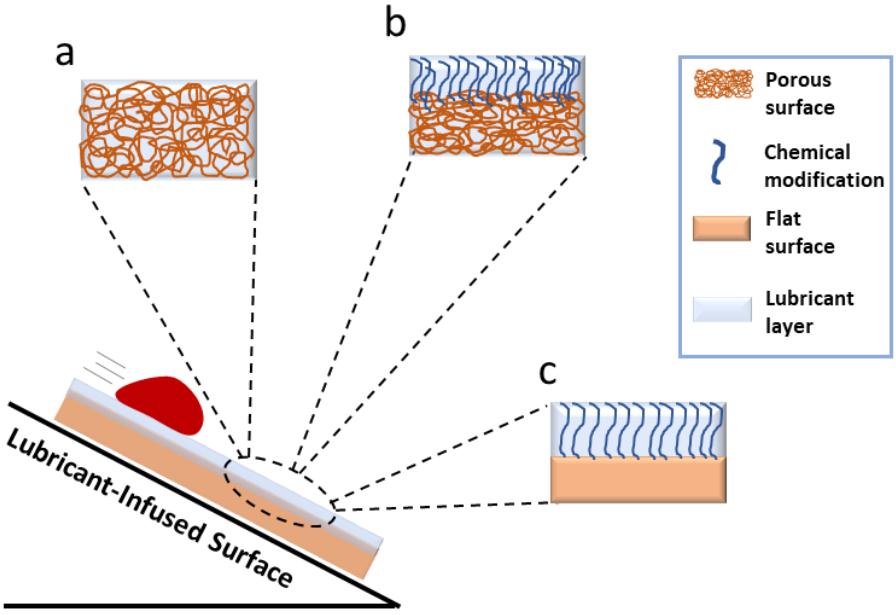

Figure 1. 4 Schematic representation of Lubricant-Infused Surfaces prepared using different modification procedures. (a) A lubricant-infused layer can be generated using a porous surface with appropriate surface chemical properties that will interact with the desired lubricant layer (*e.g.* ePTFE surfaces saturated with perfluorocarbon-based lubricants). Lubricant-infused surfaces can be generated by chemically modifying porous **(b)** or flat **(c)** substrates with appropriate chemical molecules to create substrates that possess appropriate chemical properties for stabilizing the lubricant layer.

1.4.2. Platforms and modification techniques

LIS have shown to be compatible with numerous solid substrates used in medical applications such as glass [182], [183], stainless steel [174], [184], gold [185], aluminum [186], [187], polyether amide [178], ePTFE [174], [175], [179], PET, polycarbonate, poly (methyl methacrylate) (PMMA) [174] and polydimethylsiloxane (PDMS) [188]. The first reported slippery lubricant infused porous surfaces (SLIPS), inspired by *Nepenthes* pitcher plants were created using epoxy-resin-based nanostructured substrates and ePTFE nanofibrous membranes and infiltrated with perfluorinated lubricants [179]. The porous epoxy-resin-based substrates did not posses a surface chemistry matching the chemical nature of the perfluorinated lubricants; therefore, they were chemically modified using a fluorosilane monolayer prior to adding the lubricant layer. In contrast to the epoxy surfaces, ePTFE membranes which are made from a synthetic fluorocarbon-based polymer [54] did not need further chemical modification steps, since they were porous and had the appropriate surface chemical composition for interacting with the perfluorinated lubricant layer [179]. SLIPS created using both these surfaces had low contact angle hysteresis (< 2.5 °), were able to repel various aqueous and organic liquids and complex solutions such as blood and were able to function under high pressures. In a different study, Chen *et al.*, investigated the bacterial repellency properties of lubricant-infused ePTFE substrates and their ability to prevent medical device associated infection [175]. ePTFE-SLIPS were highly resistant to biofilm formation and exhibited a 99% reduction in *S. aureus* adhesion *in vitro*.

When the innate surface chemical properties of the underlying substrate are not suitable for generating a stable LIS, this limitation can be resolved by chemically modifying the substrate with compatible functional groups such as organosilanes. Silanization has become one of the most popular and straightforward modification techniques used to enhance the surface chemical properties of the substrate and can be easily preformed using different surface modification techniques such as liquid phase deposition (LPD) [174], [178] or chemical vapour deposition (CVD) [176], [178]. In our recent study (*Chapter 2*), we used the two CVD and LPD modification techniques and developed slippery lubricant-infused coronary catheters by creating self-assembled monolayers (SAMs) of tridecafluoro-1,1,2,2-tetrahydrooctyl trichlorosilane (TPFS) and investigated the antithrombotic properties of the modified catheters (***Figure 1.5g***) [178]. Although LPD is a well know technique used for producing SAMs of silanes [189], the results obtained from our study suggest that CVD is a more efficient and effective method for creating LIS and rendering medical grade polymeric catheters less thrombogenic. One of the main drawbacks of the LPD method is that the treated surfaces are directly exposed to the side products produced and released in the liquid phase (*e.g.* hydrochloric acid), which may be harmful and damage the treated

surfaces [189]. This concept was supported when looking at the SEM images obtained from our study, where catheters treated with LPD method exhibited surface roughness along with etching and exposure of inner layers, something that was not seen in the CVD treated samples [178].

In addition to chemical properties, creating porosity and adding roughness on flat surfaces (*e.g.* incorporating micro or nano features) has shown to be an effective technique for stabilizing the lubricant layer and increasing the repellency and omniphobic properties of the LIS (***Figure 1.5c, d, e, f*** and ***h***) [181]. These surface characteristics could be achieved by applying diverse surface modification techniques such as layer-by-layer deposition of particles, organic and synthetic charged polymers [176], [177], [190]–[192], surface wrinkling [185], [193], UV initiated [183] and supramolecular polymerization [194]. LIS generated using these techniques have shown to effectively prevent infection [193], protein [192], [193], bacterial [177], [183] and platelet adhesion [193] and attenuate thrombus formation [185], [190], [193]. When creating porous structures, Kratochvil *et al.,* took an interesting approach and created a dynamic LIS by incorporated antivirulence agents, active against *Pseudomonas aeruginosa* in their multilayer structure and studied the gradual release of these molecules and their ability to attenuate virulence phenotypes through non-biocidal pathways [177]. The quorum sensing inhibitor (QSI) agents loaded in the lubricant-infused layer did not compromise the slippery and repellency properties of the surface and remained biologically active after the modification process, enabling the QSI-loaded LIS to both prevent bacterial adhesion (through the slippery lubricant-infused coating) and reduce the production of key virulence factors in planktonic cultures of this bacterium (***Figure 1.5e***).

1.4.3. Surface Stability

The stability of the lubricant-infused layer is one of the important factors that needs to be taken into consideration when designing LIS for medical applications. The dynamic liquid layer present on the surface of medical implants and instruments need to be stable under physiological shear stresses and flow conditions, withstand the mechanical forces that could be applied to the surface when implanting or inserting/extracting the medical device and also resist evaporation when placed in open environments. In addition, the designed surfaces should be able to survive the standard sterilization procedures used in the hospital settings such as rinsing the medical device with ethylene oxide and/or UV exposure. To investigate the stability of the lubricant layer, Howell *et al*., studied the stability and longevity of different immobilized lubricant layers under various flow conditions, both in closed and open systems [195]. Krytox 103 perfluoropolyether and perfluorodecalin (PFD) were the two types of lubricants tested in the experiments, with the first one being favorable

for industrially relevant applications [196] and the later being a suitable candidate for medical applications [174]. Medical-grade, polyvinyl chloride (PVC) tubing was used as the base substrate and the lubricant loss was investigated on both structured PVC surfaces functionalized with perfluoroalkyl phosphate surfactant and flat substrates that were functionalized with a SAM of TPFS using LPD. Results obtained from these experiments

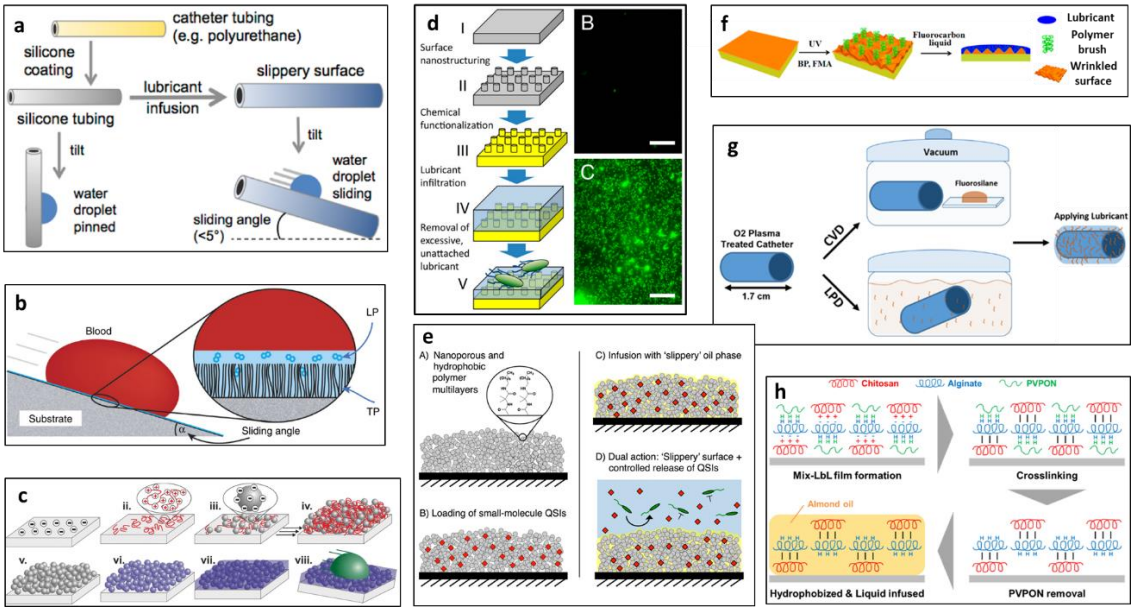

Figure 1.5 Examples of different substrates and modification techniques used to create LIS. (**a)** Flat silicon tubes or polyurethane catheters were chemically coated with a silicon coating and lubricant-infused with a compatible oil such as silicon oil to create slippery LIS. Tubes exhibited low contact angles and antifouling properties. Reproduced from Maccallum *et al.* [197]. **(b)** Slippery lubricant-infused surfaces were created by coating medical devices with a SAM of fluorosilane using LPD and further infiltrating them with a fluorocarbon-based lubricant such as perfluorodecalin. These surfaces were able to prevent device associated thrombosis and biofouling. Reproduced from Leslie *et al.* [174]. **(c)** Nanoporous LIS were created by a layer-by-layer deposition of charged nanoparticles and further functionalizing them with a SAM of fluorosilane. In order to complete the process, a fluorinated lubricant layer is wicked on the porous surface. Reproduced from Sunny *et al.* [192]. **(d)** SLIPS are created by nanopatterning glass substrates and chemically modifying them with a fluorosilane and immobilizing perfluorinated lubricants on their surfaces. These surfaces had excellent bacterial repellency properties. Reproduced from Epstein *et al.* [180]. **(e)** Antifouling SLIPS were produced by creating nanoporous structures and loading them with small antibacterial molecules that would be gradually released from the LIS. Reproduced from Kratochvil *et al.* [177] **(f)** In this study, LIS were generated by creating rough wrinkled surfaces, chemically modifying the surface with a perfluoro polymer brush and ultimately immobilizing a fluorocarbon based lubricant on the surface. These surfaces were able to prevent thrombus formation and infection. Adapted from Yuan *et al.* [193] **(g)** The flat surfaces of medical grade catheters were functionalized with a fluorosilane SAM, using CVD or LPD modification techniques and infiltrated with fluorine-based lubricants in order to create stable LIS. Reproduced from Badv *et al.* [178]. **(h)** Non-fluorinated porous LIS were created on glass substrates using chitosan, alginate and polyvinylpyrrolidone. The porous film was created using layer-by-layer deposition and cross-linking chemistry and further lubricated with almond oil. Reproduced from Manade *et al.* [190].

indicated that both structured and flat LIS-PVC surfaces, treated with either of the lubricant types were highly stable under physiological shears stresses and flow conditions only when placed in a closed environment. However, when these surfaces were exposed to an air/water interface and placed in an open environment, there was a significant increase in the amount of lubricant lost and removed from the surface [195]. In another study, the stability and thrombogenicity of LIS-acrylic surfaces coated with TPFS were tested under physiological shear stresses using human whole blood and the results obtained from this study confirmed that these surfaces remain functional and continue to effectively repel blood and prevent clot formation even after being exposed to a constant shear strain rate (1,000 s^{-1}) for up to 16 hours [174]. Although these results look promising for short-term applications, more investigation should be done in order to study the long-term stability of the LIS under more complex physiological conditions.

Evaporation of the lubricant layer could also be a concern, depending on the type of lubricant applied on the substrate and the conditions used to store the LIS prior to the application. In a study preformed on lubricant-infused ePTFE surfaces, three types of perfluoropolyether (PFPE), perfluoroperhydrophenanthrene (PFPH), and PFD lubricants with different chemical properties and vapour pressures were tested and the stability of the lubricant layer was investigated when surfaces were stored in either PBS or kept in open air conditions [175]. All three lubricants showed high stability rates when immersed in PBS for up to 1 week, however, after only 30 minutes of incubation in air, a significant decrease in surface lubricant was seen in PFD treated samples (the lubricant used in medical applications and the most volatile lubricant), whereas PFPE and PFPH lubricants displayed greater stability with retaining more than 75% of the initial amount of lubricant after 120 minutes [175]. These results suggest that the high evaporation rate of medical-grade lubricants such as PFD could be attenuated by storing these surfaces in a compatible aqueous buffer such as PBS, prior to their use. Moreover, designing a surface with vasculature features, inspired by natural self-replenishing surfaces, has shown to be an effective technique to create self-lubricating systems, capable of retaining the lubricant layer for longer periods of time [198].

1.4.4. Biomedical applications

Due to the extraordinary performance of LIS and their excellent repellency properties, these surfaces have gained extensive attention in biomedical applications where preventing non-specific adhesion is crucial. Device associated infection and clot formation are two of the main concerns and challenges that surface engineers need to address when designing platforms for biomedical purposes. LIS have shown to be a promising candidate to mitigate these issues by effectively preventing the adhesion and proliferation of different cell types

and significantly reducing bacterial biofilm formation and thrombosis [174], [177], [178], [190], [197]. Moreover, these surfaces have shown to outperform conventional surface blocking techniques such as PEGylated or bovine serum albumin (BSA) coated surfaces [180], [182].

Taking into account the design flexibility and surface material compatibility offered by LIS, they can be applied in a variety of medical related applications such as, implants [175], surgical equipment [199], [200], point-of-care diagnostics [185] and medical catheters and tubing [174], [178], [197]. Medical catheters such as urinary and central venous catheters play a significant role in daily medical procedures preformed on patients. The interior walls of these tubes are susceptible to fouling and clot formation once they come in contact with biological fluids such as blood and urine. These complications, impair the performance of the device, delay and interfere with the treatment, and result in further device associated complications such as mild or life-threatening infection [201], [202]. Work done on medical catheters and tubing modified with a lubricant-infused layer, using different modification techniques and various lubricants, have shown that these surfaces are capable of supressing thrombin generation, fibrinogen and platelet adhesion [174], [178] and biofilm formation [164], [188] *in vitro*.

Although to date, most of the studies performed on LIS have focused on *in vitro* investigations, the few initial *in vivo* studies conducted on these surfaces have shown that the promising results obtained from *in vitro* studies can be translated to more complicated biological settings as well. For example, using a porcine femoral arteriovenous shunt model, it has been shown that lubricant-infused PVC cardiopulmonary perfusion tubing can remain patent and prevent blood clot-associated occlusion for up to 8 hours in the absence of systemic heparin anticoagulation (***Figure 1.5b***) [174]. In another study, ePTFE surfaces infiltrated with different fluorocarbon-based lubricants and implanted subcutaneously in a rat model, showed that lubricant-infused implants effectively resist bacterial infection and significantly reduce local inflammatory response, even after being exposed to high levels of *S. aureus*. Further, ePTFE-SLIPS were biocompatible and reduced the thickness of the collagen connective tissue formed around the implant by about 50%, compared with unmodified ePTFE implants [175].

Despite the promising results obtained from the new LIS that are created using different substrates and various modification techniques, these surface models all suffer from one mutual drawback, and that is the lack of biofunctionality and the repulsion and exclusion of all bio-interactions with the surface. This limitation is troublesome for permanent medical implants such as vascular grafts, where tissue integration and endothelial cell capture play a significant role in the performance and patency of the device. In our recent

study, we intended to tackle this limitation by creating a new class of LIS where biofunctionality and targeted binding were incorporated in the lubricant-infused platform, without compromising the repellency and blocking properties of the surface (*Chapter 3*) [182].

Biofunctional lubricant-infused surfaces (BLIS) were generated by creating SAMs of a 3-aminopropyltriethoxysilane (APTES)-TPFS mixture using CVD and further, utilizing the APTES coupling agents for biomarker immobilization. APTES was chosen as the silane coupling agent since this molecule has extensively been used for creating stable, biofunctional interfaces in the past [203], [204]. In our study, we investigated the repellency properties of our designed surfaces by preforming blood and plasma clotting assays and the biofunctionality and targeted-binding features of the surfaces were investigated by immobilizing endothelial cell specific biomarkers (*e.g.* anti-CD34 antibody) on the BLIS and studying targeted endothelial cell-capture from a complex biological system such as human whole blood. The designed BLIS surfaces had excellent blocking properties by preventing clot formation and non-specific adhesion of cells and proteins. In addition, these surfaces were biofunctional and promoted targeted binding of endothelial cells [182].

In a further study (*Chapter 4*), we translated our new developed coating from glass substrates to medical grade vascular grafts and aimed to develop a new class of biofunctional lubricant-infused ePTFE surfaces by eliminating the need for chemically modifying the ePTFE substrate with mixed silanes and exploiting the innate chemical properties of the grafts. In this approach, hydroxyl terminated ePTFE substrates were directly biofunctionalized using APTES-silanized anti-CD34 antibodies and further lubricated with a perfluorocarbon-based lubricant, creating stable, biofunctional lubricant-infused ePTFE substrates. Similar to the previous study, our designed ePTFE substrates were biocompatible and significantly attenuated thrombin generation and blood clot formation and promoted targeted binding of endothelial cells. The results obtained from our studies revealed that promoting targeted-binding and preventing non-specific adhesion on LIS are not mutually exclusive concepts and the new class of lubricant-infused surfaces can retain their repellency and blocking properties in the presence of biofunctional features. These surfaces could open new doors for medical applications, where both preventing non-specific adhesion and promoting targeted binding of cells and biospecies are of immense importance.

1.5. Research Objectives

Based on the demonstrated promise of LIS in preventing non-specific adhesion, the focus and objective of this thesis was to develop and investigate novel LIS modification techniques, that would better suit medical devices and medical related applications. In

particular, the thesis focuses on developing strategies and optimization procedures that would integrate biofunctionality and targeted-binding on lubricant-infused surfaces, without compromising their unparalleled repellency properties. More specifically, the main focus of the thesis was to create biofunctional lubricant-infused surfaces that could be applied to synthetic vascular grafts or permanent medical implants, in order to enhance their biocompatibility and targeted-binding features.

1.6. Thesis Outline

This thesis is written in a "sandwich" format and consists of 6 chapters. ***Chapter 1*** and ***Chapter 6*** enclose relevant introductory and concluding remarks respectively and ***Chapters* 2** to **5** consist of journal articles that are either published, submitted for publication or in preparation for submission.

Chapter 2 focuses on optimizing the surface modification procedure used to create LIS on polymeric substrates. Specifically, medical grade polymeric catheters were modified using CVD or LPD techniques and their surface topography, surface chemical composition, repellency properties and their ability to attenuate clot formation was investigated. Since surface chemical and physical properties are of immense importance when designing LIS, this investigation revealed that the modification technique used to create LIS can affect the surface properties and ultimately the repellency and blocking characteristics of the modified surface.

Chapter 3 describes a novel modification procedure for impregnating lubricant-infused platforms with biofunctional features without negatively impacting their repellency and blocking properties. Although LIS have shown outstanding results in blocking surfaces and preventing unwanted adhesion, they all lack the ability to promote targeted-binding and biofunctionality, which are crucial requirements when designing interfaces for biosensors and permanent medical implants such as vascular grafts. This is the first description of a method to obtain a biofunctional lubricant-infused surface (BLIS) that promotes targeted binding of cells and effectively attenuates clot formation and prevents non-specific adhesion of blood proteins and cells.

Chapter 4 describes the translation of the BLIS from a generic platform such as glass to medical grade ePTFE vascular grafts and focuses on developing a novel (patent filed) and simplified modification technique for creating BLIS using silanized bio-inks. Preserving the surface chemical properties of the base substrate such as ePTFE is critical in order to further infiltrate the surface with perfluorocarbon-based lubricants and to create functional and stable LIS without the need for chemically modifying the surface with appropriate functional groups. In order to do so, a novel method was developed where silanized biomarkers were produced and directly immobilized on ePTFE

substrates. The biofunctional lubricant-infused ePTFE surfaces (BLIPS) were examined for their blood compatibility and ability to capture endothelial cells from human whole blood. This technique streamlines the modification procedure required to create functional BLIPS and results in surfaces with excellent repellency properties and targeted-binding features.

Chapter 5 describes a novel method (patent filed) to coat PET vascular grafts in order to make their surfaces biofunctional and repellent. In this study, the modification techniques used in ***Chapters 2***, ***3*** and ***4*** were integrated, tuned, optimized and applied to PET substrates. Specifically, PET grafts were modified with a fluorosilane layer using CVD, secondary oxygen plasma treated to create hydroxyl functional groups on their surface and lastly, biofunctionalized using silanized bio-inks. Compared to the method described in ***Chapter 3*** for creating BLIS, this new method simplifies the modification procedure where the required functional groups for biomolecule immobilization are generated by applying a secondary plasma treatment on the fluorosilanized surface and therefore, the need to treat the surface with both amino and fluorosilane molecules in eliminated. Similar to BLIPS, the biofunctional lubricant-infused PET surfaces were tested for their hemocompatibility and endothelial cell adhesion properties.

Chapter 2 *An omniphobic lubricant-infused coating produced by chemical vapor deposition of hydrophobic organosilanes attenuates clotting on catheter surfaces*

Preface

This chapter reports a non-invasive and straightforward method for creating LIS on medical grade polymeric catheters using CVD. The reported method is compared to other common modification techniques used to create LIS such as LPD. This study investigates the compatibility of the purposed coating technique by performing different surface characterization techniques. Further, the thrombogenicity of the coated catheters are investigated by performing plasma clotting assays. This study demonstrates that the coating technique used to create LIS could negatively affect the surface properties of the underlying substrate. In addition, this study reveals that catheters coated using the CVD method are highly blood-repellent and significantly attenuate clot formation and platelet adhesion.

Citation:

This research was originally published in *Scientific Reports.* M. Badv, I. H. Jaffer, J. I. Weitz, and T. F. Didar, "An omniphobic lubricant-infused coating produced by chemical vapor deposition of hydrophobic organosilanes attenuates clotting on catheter surfaces," *Sci. Rep.*, vol. 7, no. 1, p. 11639, 2017.

Relative Author Contributions

I prepared the samples, performed all experiments and analyzed the data. The manuscript was drafted by myself and subsequently edited by my academic supervisor Dr. T. F. Didar and Dr. J. I. Weitz. I. H. Jaffer assisted with the plasma clotting experiments. XPS measurements were done at the BioInterface Institute at McMaster University. The SEM images obtained from the plasma clotting assays were acquired at the Canadian Center for Electron Microscopy at McMaster University.

2.1. Abstract

Catheter associated thrombosis is an ongoing problem. Omniphobic coatings based on tethering biocompatible liquid lubricants on self-assembled monolayers of hydrophobic organosilanes attenuate clotting on surfaces. Herein we report an efficient, non-invasive and robust process for coating catheters with an antithrombotic, omniphobic lubricant-infused coating produced using chemical vapor deposition (CVD) of hydrophobic fluorine-based organosilanes. Compared with uncoated catheters, CVD coated catheters significantly attenuated thrombosis via the contact pathway of coagulation. When compared with the commonly used technique of liquid phase deposition (LPD) of fluorine-based organosilanes, the CVD method was more efficient and reproducible, resulted in less disruption of the outer polymeric layer of the catheters and produced greater antithrombotic activity. Therefore, omniphobic coating of catheters using the CVD method is a simple, straightforward and non-invasive procedure. This method has the potential to not only prevent catheter thrombosis, but also to prevent thrombosis on other blood-contacting medical devices.

2.2. Introduction

Blood-contacting medical devices such as catheters, heart valves and vascular grafts are widely used. All such devices are prone to thrombosis, which can lead to thromboembolic complications and device failure [205]. Cancer patients often have central venous catheters implanted for venous access and for parenteral delivery of chemotherapy, antibiotics and nutrition. Catheter thrombosis is common in these patients and can lead to deep-vein thrombosis and pulmonary embolism; complications that often delay treatment, extend hospital stay and increase healthcare costs [206]. Therefore, methods to reduce catheter thrombosis are worthwhile.

Thrombosis on catheters and other blood-contacting medical devices is a multi-step process that starts with adhesion of proteins and cells, and culminates in the formation of a platelet-fibrin mesh [1], [207]. Coagulation on these surfaces is activated via the contact pathway, which is initiated by the adsorption and activation of factor (F) XII [208]. Therefore, attenuation of thrombosis on medical devices requires processes that prevent activation of the contact pathway. Such processes can be active or passive. Active processes designed to limit contact activation include surface coating with heparin [209] which inhibits multiple steps in blood coagulation, or with corn trypsin inhibitor [115], a potent and specific inhibitor of FXIIa. Passive processes to retard contact activation include surface modifications with synthetic or natural polymers and biomolecules [46], [50], [210] such as poly (ethylene oxide) (PEO) [211]–[215] and polyethylene glycol (PEG) [25], [26], [216], poly-sulfobetaine [83], [217], poly-2-methoxyethyl acrylate (PMEA) [218], and

albumin [219]–[224]. More recently, omniphobic lubricant-infused coatings have been developed based on tethering biocompatible, perfluorocarbon lubricants on self-assembled monolayers (SAMs) of hydrophobic organosilanes [174], [179]. Based on fluorous chemistry, fluorous molecules can be physically adsorbed onto fluorous-containing surfaces [225]. The strong intermolecular interaction between the fluorinated lubricant and the fluorosilane layer locks the lubricant liquid onto the surface, thereby creating a highly stable, omniphobic lubricant-infused coating [179]. These surfaces outperform heparin-coated surfaces, as well as a range of hydrophilic coatings [83] developed to resist blood clot formation. Furthermore, lubricant-infused omniphobic coatings have been more effective than PEG or albumin for blocking non-specific adhesion of cells and bacteria [181], [226]. In addition to increasing blood-compatibility, these surfaces are stable and durable when exposed to physiological shear stress *in vitro* [174], [195]. Therefore, lubricant-based omniphobic coating of biomedical devices is a promising method for preventing thrombus formation.

Lubricant-based omniphobic coatings are produced by applying SAMs of hydrophobic organosilane (*e.g.* tridecafluoro-1,1,2,2-tetrahydrooctyl trichlorosilane) onto the surface. Liquid phase deposition (LPD) is the main technique reported in the literature for producing SAMs of fluorine-based silanes in order to obtain lubricant-infused omniphobic coatings [181]. However, the LPD method has several limitations. First, the high volumes of solvent waste produced during the procedure are harmful to the environment, which restricts the industrial viability of the process [227]. Second, self-polymerization of silanes in the solution phase may impair the formation of homogenous silane layers on the surface [228]. Third, and most important, surfaces treated by LPD are exposed to the impurities and side products produced during the treatment process, which may compromise the material and alter the bulk properties of its surface [227]. Such alterations are particularly problematic for materials used for biomedical applications.

To overcome the limitations of LPD, we set out to develop a more robust, simplified and clinically relevant chemical vapor deposition (CVD) method for creating a lubricant-infused omniphobic coating on FDA-approved catheters. The surface properties, chemical composition and antithrombotic activity of catheters coated in this manner were compared with those of uncoated catheters and catheters coated using the LPD method. We show that the CVD method has less of an effect on the surface topography of catheters than the LPD method and endows them with greater antithrombotic activity.

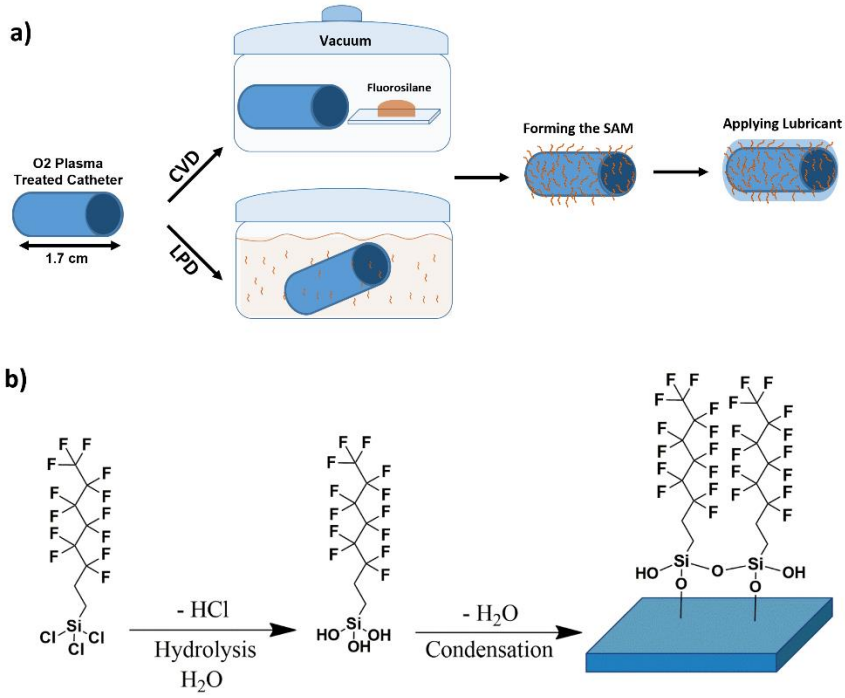

Figure 2.1 Schematic illustration of the treatment process and the purposed reaction. a) Schematic representation of catheters treated with trichloro (1H,1H,2H,2H-perfluorooctyl) silane (TPFS) through chemical vapor deposition (CVD) and liquid phase deposition (LPD). **b)** Chemical structure of TPFS and surface functionalization steps of plasma treated catheters with TPFS.

2.3. Results

2.3.1. Producing omniphobic lubricant-infused catheters

Omniphobic coatings on coronary catheters, composed of a soft polyether amide block on the outer layer were produced using two different chemical modification techniques: 1) The LPD technique, which is the most commonly used method to create omniphobic slippery surfaces[174], and 2) Our developed CVD method, which is a more efficient, non-invasive and robust process for creating anti-thrombogenic coatings on catheters (***Figure 2.1*****a**). Catheter segments were oxygen plasma treated and silanized with trichloro (1H, 1H, 2H, 2H-perfluorooctyl) silane (TPFS) using one of the techniques mentioned above (***Figure 2.1*****b**). In the final step, a biocompatible, FDA approved liquid lubricant such as perfluorodecalin (PFD) or perfluoroperhydrophenanthrene (PFPP) was added to complete the modification process.

2.3.2. Assessment of surface chemical composition

To examine the changes in the chemical composition of the catheters after oxygen plasma treatment and after CVD or LPD surface modification, X-ray photoelectron spectroscopy (XPS) was performed (***Figure 2.2***). Oxygen plasma treated and silanized catheters showed a significant difference in chemical composition compared with controls. As expected, after

oxygen plasma treatment, a high percentage of oxygen (about 50 atom %) was detected on the surface of the catheters, indicating the presence of hydroxyl (OH) groups and consistent with initial activation of the catheter surfaces.

Although fluorine (F) was detected after silanization with both the CVD and LPD method, the fluorine surface concentration was significantly higher with CVD treatment than with LPD treatment (about 45 atom % and 15 atom %, respectively).

Bismuth, the filling used in catheters to render them radiopaque [229], was detected on the surface of catheters subjected to LPD treatment (> 15 atom %). In contrast, bismuth was not detected on the surface of catheters coated using the CVD method. LPD-treated catheters also exhibited chlorine (> 10 atom %) on their surface, which was not present on the surface of CVD-treated catheters.

2.3.3. Contact and sliding angle measurements

To investigate the relative hydrophobicity/hydrophilicity of the control and treated catheters, contact and sliding angle measurements were performed using a 5µL droplet of deionized water. The sliding angle was defined as the minimum tilting angle required for the droplet to start moving along the catheter surface. A sliding angle of 90 degrees was assigned to droplets that failed to slide at angles of 90 degrees or higher. The static contact angle measurements of the control and treated surfaces before adding the lubricant layer are shown in ***Figure 2.3*****a and b**. Control catheters exhibited a relatively high contact angle (θ_{st} = 107 ± 4°) indicative of their hydrophobicity. After CVD treatment and before lubricant addition, the water contact angle increased to 121 ± 2°. After the addition of PFD or PFPP lubricant layers to the CVD treated catheters, the water contact angles were lower (104.7 ± 2° and 104.8 ± 2°, respectively).

In contrast to CVD treated surfaces, LPD surfaces had a lower static contact angle (θ_{st} = 83.6 ± 7°) compared with control surfaces. After adding the lubricants onto these surfaces, the water contact angles remained low. Although the PFPP lubricant increased the contact angle by about 7°, the difference was not significant, and the wettability of the surfaces remained high.

Sliding angle measurements of the treated and control surfaces are shown in ***Figure 2.3*****c**. The 5µL water droplet did not slide on lubricated LPD catheters even with tilting angles higher than 90°, suggesting that these surfaces do not have slippery properties, which is a major characteristic of omniphobic lubricant-infused surfaces. In contrast, with CVD treatment there was a significant increase in liquid repellency compared with the control or LPD catheters as demonstrated by sliding angles as low as 3°. When sliding angle

measurements on control and coated catheters were repeated four months later, the results were similar to those obtained on initial measurement (results not shown).

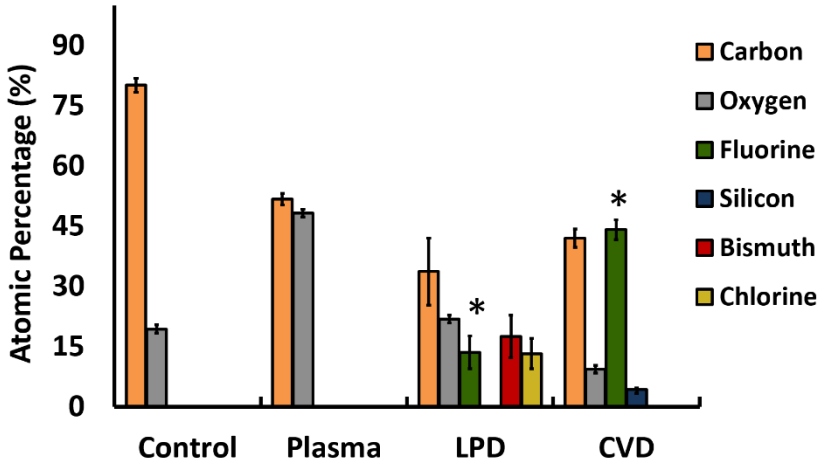

Figure 2.2 The chemical composition (reported as the percentage atomic concentrations) of the catheter surfaces at different stages of surface modification determined by XPS. Following oxygen plasma, an increase in the oxygen surface concentration was observed and catheters contained up to 50 atom % oxygen. Surfaces treated with LPD had a significantly lower amount of fluorine (about 15 atom %), compared with CVD treated catheters (about 45 atom %). In addition, LPD treated samples showed a large surface concentration of bismuth (>15 atom %) which indicates this treatment method has modified the bulk properties of the catheters. In addition to bismuth, LPD treated catheters had up to 15 atom % of chlorine on their surfaces, an impurity that was not seen on CVD treated catheters. Three samples from each group were analyzed and measurements where performed on four spots on each sample. *Significant difference between the fluorine atom percent when comparing the CVD and LPD treated catheters ($P < 0.001$). The results are presented as means ± S.D.

2.3.4. Sliding angle measurements with whole blood

To investigate catheter-blood interactions and the stability of the coatings, sliding angle measurements were performed with whole blood on catheters that had been treated four months earlier. As seen in **supporting videos 1-3**, similar to the results obtained with water, whole blood sliding angles on control and LPD-PFPP treated catheters were greater than 90°. In contrast, CVD-PFPP treated catheters exhibited excellent blood repellency as evidenced by sliding angles less than 3° and immediate sliding of the blood droplet off the catheter surface.

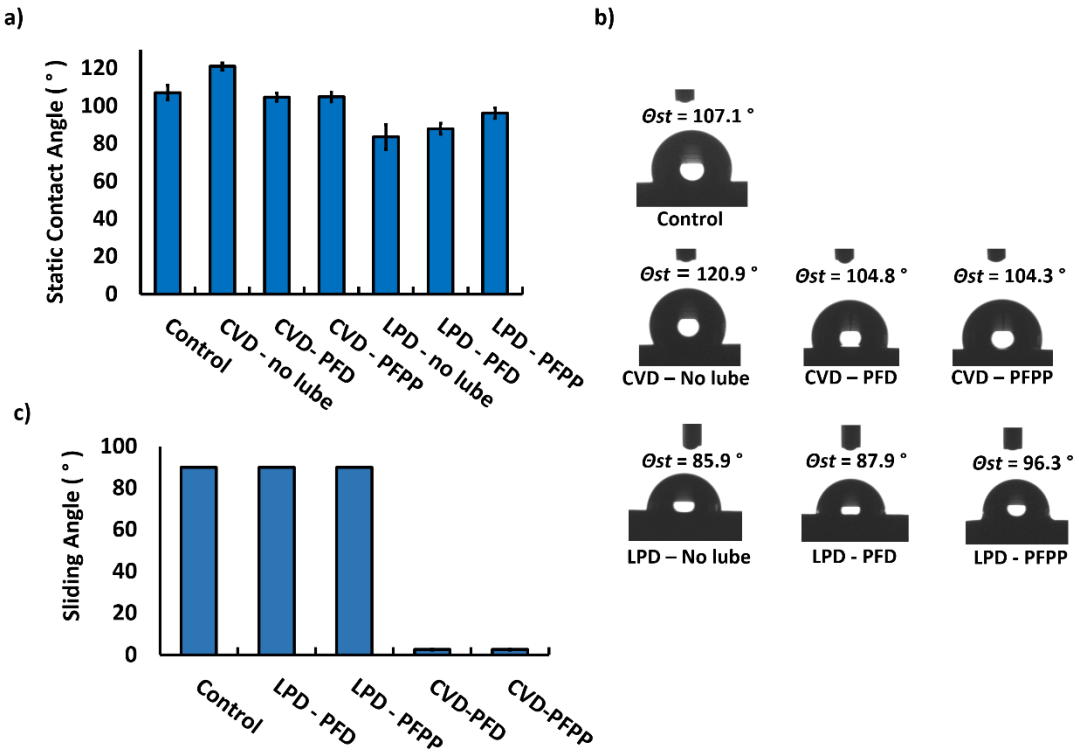

Figure 2.3 The sliding and contact angle measurements of the control and treated catheters. (a) Static contact angle measurement of samples before surface modification (control) and after silanizing the catheters and after adding the lubricant layer. (b) Contact angle images of a 5 µL water droplet on the surface of the catheters before and after adding the fluorinated lubricant coating. (c) Sliding angle results of the surfaces after adding the lubricant layer. The results are presented as means ± S.D.

2.3.5. Effect of catheter modification on plasma clotting times

Clotting assays were performed to compare the antithrombotic activities of the various coatings. After gently flattening the catheter segments with a plastic roller, they were shaped into rings, placed around the inner walls of the wells of a 96-well plate and saturated with 150 µL of PFPP or PFD lubricant for about 1 min. Empty wells and wells with only lubricant were used as controls. Excess lubricant was removed from the wells and 100 µL aliquots of citrated human plasma were added to wells that did or did not contain catheter segments. The clotting assay was performed as explained in the methods section. As seen in Figure 2.4, the average clotting time in wells without a catheter and with no lubricant was 1258 ± 168 s. Empty wells containing PFD or PFPP lubricant had average clotting times of 1239 ± 250 s and 1199 ± 216 s, respectively. Control catheters with no surface modification significantly shortened the clotting time by 2-fold to 577 ± 67 s. Catheters silanized using the CVD method significantly ($P < 0.001$) prolonged the clotting time compared with non-coated catheters to 935 ± 115 s and 1031 ± 123 s, using PFD or PFPP lubricants, respectively. These catheters had the longest clotting times compared with other

experimental groups **(*Figure 2.4*)**. Both LPD-PFD and LPD-PFPP catheters slightly prolonged the clotting time (689 ± 119 s and 636 ± 87 s, respectively) compared with control catheters, but the differences were not statistically significant. When comparing the results with CVD and LPD catheters, clotting times were significantly ($P < 0.002$) longer with the CVD modification method than with the LPD method (***Figure 2.4***).

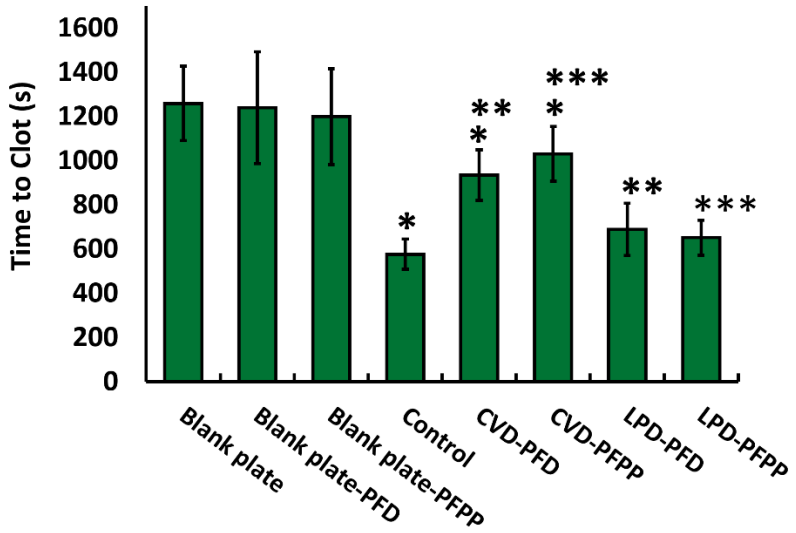

Figure 2.4 Plasma clotting time when in contact with treated and non-treated catheters and when in blank plates. Catheters were rolled and placed in 96-welplates. After incubating the catheters with the citrated plasma at 37 °C for 5–7 minutes, clotting was initiated by adding 100 µL of CaCl2 solution. Absorbance was calculated over time and clotting time was determined at the time to half-max. The bars represent the means of at least nine repeats from each group. *Significant difference between control catheters vs. CVD treated catheters ($P < 0.05$). **, ***Significant difference when comparing the results from the two different treatment types of CVD and LPD ($P < 0.05$). The results are presented as means ± S.D.

2.3.6. Identification of the coagulation pathway activated by modified and unmodified catheters

To identify the coagulation pathway involved in catheter-induced clotting, and to determine the effect of the various coatings on such clotting, results from clotting assays performed in control plasma were compared with those in plasma depleted of FXI or FXII, key components of the contact pathway, or FVII, which is the critical component of the extrinsic or tissue factor pathway of the coagulation cascade. Whereas control and modified catheters shortened the clotting time in control or FVII depleted plasma (***Figure 2.5*b**), they did not do so in plasma depleted of FXII or FXI (***Figure 2.5*a**). This suggests that the procoagulant activity of catheters is dependent on FXII and FXI, but not FVII. Similar to the results in normal plasma, CVD treated catheters shortened the clotting time less than LPD catheters in FVII depleted plasma.

2.3.7. Protein adhesion and clot formation on the catheter surfaces

After coating the catheter surfaces with TPFS using either the CVD or LPD method and after performing the clotting assay in normal plasma, catheter segments were subjected to scanning electron microscopy (SEM) to examine the effect of treatment on the catheter surface topography and to investigate their protein repellency properties. As seen in ***Figure 2.6*****b**, catheters treated with the CVD method had a smooth silane layer on their surface and the surface morphology and roughness were similar to those of control catheters. In contrast, with LPD treatment, there was no evidence of a silane layer and roughness of the surface with etching and exposure of inner layers in some areas was seen under higher magnification.

In addition, as illustrated in ***Figure 2.6*****a and b**, a highly dense protein layer was formed on control and lubricated LPD-treated catheters. In contrast, lubricated CVD-treated catheters exhibited significantly less protein deposition on their surfaces, consistent with the normal clotting assay results.

2.3.8. Protein deposition and platelet adhesion to catheters in whole blood

To assess the stability of the omniphobic slippery coating and the capacity of the coated catheters to resist protein deposition and platelet adhesion, catheter segments that had been treated four months earlier were incubated with whole human blood. Since the PFPP lubricant was superior to PFD lubricant in the clotting assays, CVD and LPD catheters were only lubricated with PFPP in the whole blood experiments. As seen in ***Figure 2.7***, after immersing catheter segments in whole blood for 15 s, clot formation was evident on control and LPD-PFPP treated catheters. In contrast, no clot formation was observed on CVD-PFPP treated catheter segments. To further investigate the catheter-blood interaction, blood treated catheter segments were fixed in 4% formaldehyde and submitted for SEM imaging. As seen in the SEM images presented in ***Figure 2.7***, a highly dense protein layer was formed on both control and LPD-PFPP catheters, whereas CVD-PFPP catheters showed no protein on their surface. Platelet adhesion was also evident on the control and LPD-PFPP treated catheters, but not on CVD-PFPP catheters.

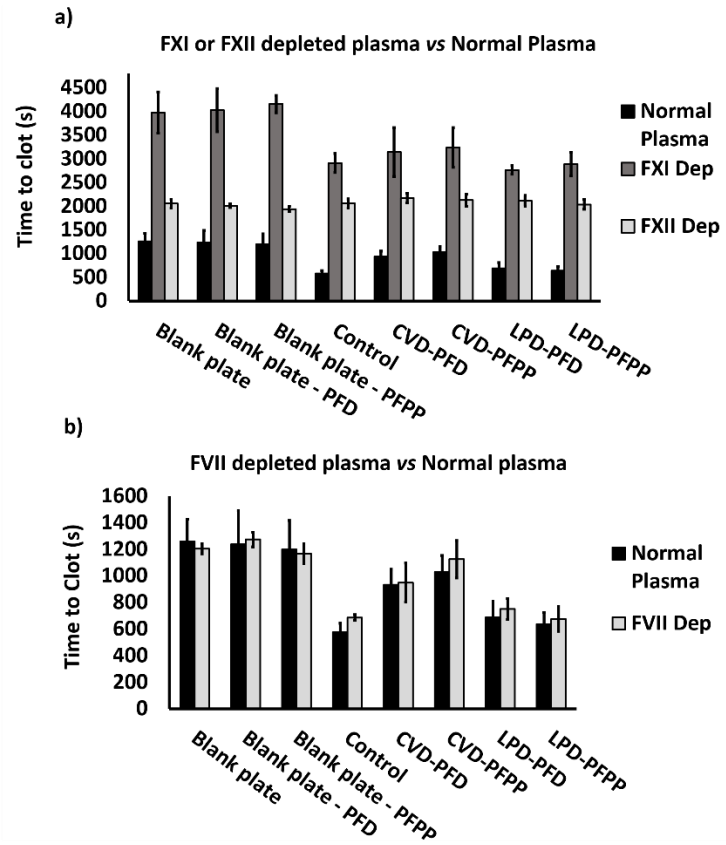

Figure 2.5 Comparison between the clotting times in normal and FVII, FXII or FXI depleted plasma. Similar to whole plasma clotting assay, catheters were rolled and placed in 96-welplates. After incubating the catheters with depleted plasma at 37 °C for 5–7 minutes, clotting was initiated by adding 100 µL of CaCl2 solution. Absorbance was calculated over time and clotting time was determined at the time to half-max. (**a**) Clotting assay in FXI and FXII depleted plasma. Both Control and treated catheters significantly prolong the clotting time in FXI or FXII depleted plasma when comparing the results to normal plasma. (**b**) Clotting assay in FVII depleted plasma. There was no significant difference between the clotting times in FVII depleted plasma when comparing the results to normal plasma. The bars represent the means of at least nine repeats from each group. The results are presented as means ± S.D.

2.4. Discussion and Conclusions

Thrombosis on blood-contacting medical devices is an ongoing problem. Therefore, there remains a need for surface modification techniques that render such devices more biocompatible [1]. Although LPD is a well described method for producing SAMs of fluorine-based silanes [227] and is the most widely used technique for producing omniphobic coatings on biomaterials [174], [181], the results of this work show that the CVD method is more efficient and effective than the LPD method for rendering medical grade polymeric catheters less thrombogenic.

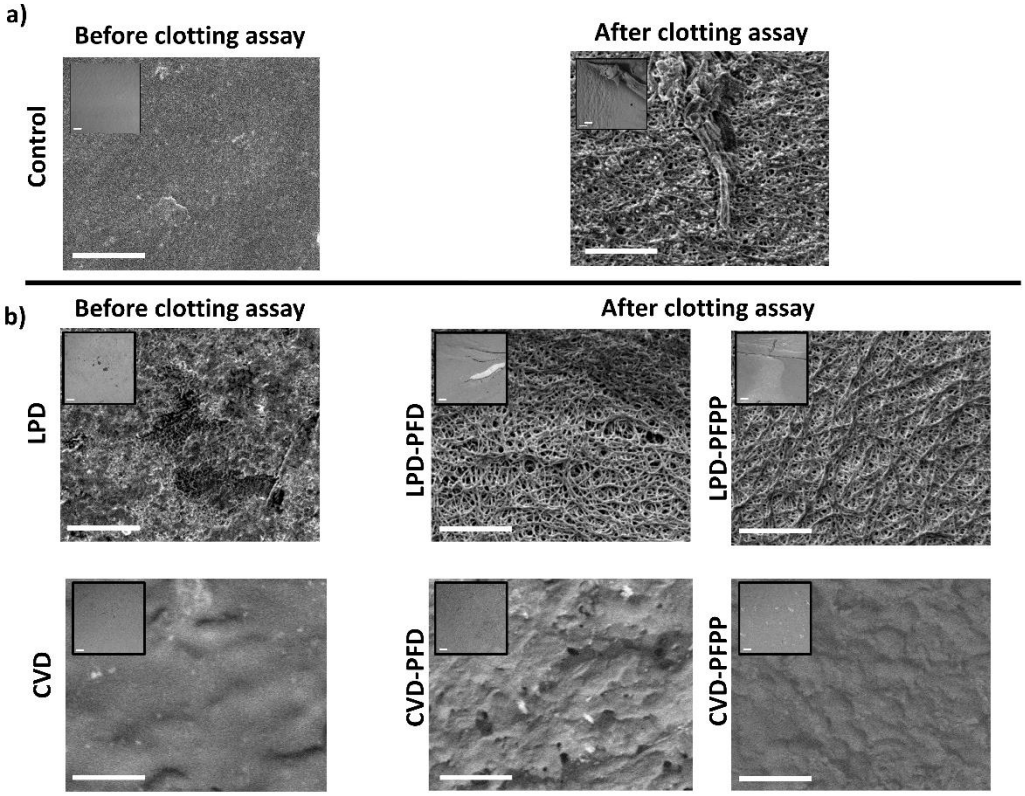

Figure 2.6 Scanning electron microscopy images of catheters before, after silanization, and after plasma clotting assay. Control (**a**), LPD and CVD treated catheters (**b**) before and after the clotting assay are shown. A uniform smooth silane layer is formed on the catheter surfaces after CVD treating them. In contrast, LPD treated catheters have a rough surface compared with the Controls. Both Control (**a**) and LPD treated catheters (**b**) form a dense protein layer on their surfaces, after the clotting assay, something that is not evident in CVD treated catheters (**b**). The magnification bars are 10 μm on the small images and 1 μm on the larger images.

A major drawback of the LPD method is the direct exposure of the treated surfaces to the side products produced and released in the liquid solution [227]. Hydrochloric acid, which is the main side product generated during the hydrolysis step of TPFS (***Figure 2.1*****b**), may damage the polymeric surface of the catheters. Such damage is evident from the XPS and SEM results. With LPD treatment a high atomic concentration of bismuth (> 15 atom %) is evident on the surface of the catheters while with CVD treatment no bismuth was detected. Bismuth is introduced to render the catheters radiopaque so that they can be visualized on x-rays during and after insertion [229]. It is likely that hydrochloric acid produced during the liquid treatment process partially degraded the outer polymeric layer of the catheter, thus exposing the bismuth on the surface. This concept is supported by the SEM images, which reveal surface roughness under higher magnification along with etching and exposure of inner layers in some areas in LPD treated but not in CVD treated catheters (***Figure 2.6*****b**). Although CVD treated catheters were incubated with TPFS for a longer period than LPD catheters (5 h and 1 h, respectively), this did not negatively affect

the surface properties of CVD treated catheters. In addition to bismuth, chlorine (> 10 atom %) was also present on the surfaces of LPD treated catheters; an impurity not seen on CVD treated surfaces. The presence of chlorine on these catheters could be due to the partial hydrolysis of the Si-Cl bonds and the unsuccessful formation of inner covalent bonds between the silane molecules [230], suggesting that the LPD method is not as efficient as the CVD method. After treatment with TPFS, the presence of fluorine (F) is expected as a result of formation of the fluorosilane SAM on the catheter surfaces. Although fluorine was detected on both LPD and CVD treated catheters, the fluorine atom concentration on CVD treated samples was significantly higher than that on LPD treated samples (about 45 atom % and 15 atom %, respectively), indicating that the CVD method is a more efficient technique for producing SAM layers of the organosilane. This is further supported by the lower oxygen content on CVD treated samples compared to LPD treated ones, suggesting that with the CVD method, more of the active OH groups were coated with fluorosilane.

Water repellency was greater with the CVD method than with the LPD method as evidenced by lower sliding angles ($\theta \leq 5°$ and $\theta > 100°$ respectively). The CVD silanization step transformed the hydrophobic surface of the control catheters to a more hydrophobic surface by increasing the static water contact angle from 107 ± 4° to 121 ± 2°, thereby confirming the presence of the hydrophobic silane coating. In contrast, LPD treated surfaces had a lower contact angle (θ_{st} = 83.6 ± 7 °) compared with the control and CVD treated catheters, confirming the fact that the catheter surfaces were not efficiently coated with a hydrophobic silane layer. In addition, the hydrophobic surface properties were disrupted with the LPD method due to the surface degradation caused by the side products produced during the LPD modification step.

Although the static contact angles decreased in the CVD treated catheters after adding the PFD or PFPP lubricant layer, they were highly water and blood repellant. In contrast, sliding angels were significantly higher with the LPD method ($\theta > 90°$), indicating less omniphobicity and lower water and blood repellency (***Figure 2.3*c, supporting videos 1-3**). This could be due to the etching of the catheter surface and the roughness of the outer layer that occurs with the LPD method. In addition, there is less efficient formation of a SAM layer with the LPD method, which may limit the capacity of the lubricant to completely wet and cover the catheter surface. Therefore, LPD treated catheters showed poorer water and blood repellency compared with CVD treated catheters.

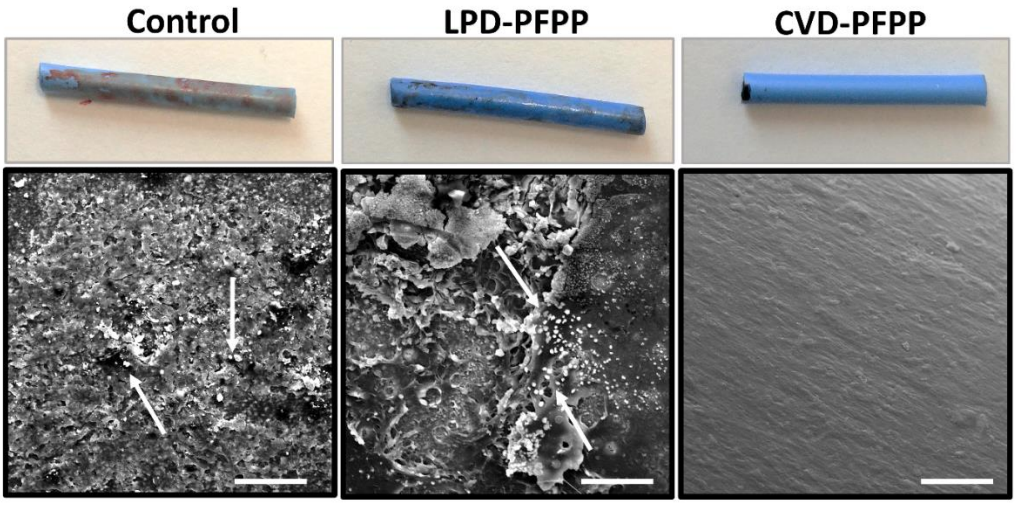

Figure 2.7 SEM images of catheters incubated with whole blood. Silanized catheters were stored at room temperature and four months after the surface modification procedure, the blood-catheter interaction was investigated. Control, CVD-PFPP and LPD-PFPP catheters were submerged in whole blood for 15 s and images were taken afterwards. Further on, they were washed with PBS, fixed in 4% formaldehyde for 20 mins, and submitted for SEM imaging. Blood clots were formed on control and LPD-PFPP treated catheters immediately after being in contact with blood. However, no blood clot formation was seen on CVD-PFPP treated catheters. In addition, platelet adhesion (shown with white arrows) was evident on control and LPD-PFPP treated catheters, while no platelets or protein adhesion was seen on CVD-PFPP treated catheters. The magnification bars are 50 µm.

Both lubricants (PFD or PFPP) increased the antithrombotic activity of CVD treated catheters as evidenced by significantly longer clotting times compared with control or LPD treated catheters. The enhanced antithrombotic activity of catheters coated using the CVD method is due to reduced activation of the contact system because this activity is evident in plasma depleted of FVII, which is essential for the extrinsic pathway of coagulation, but not in plasma depleted of FXI or FXII, key components of the contact system. Thus, the findings from these experiments, suggest that modified catheters, similar to unmodified ones, initiate coagulation through the contact pathway and have minimal effect in activating the tissue factor pathway. In both the normal and FVII depleted plasma assays, clotting times were longest with CVD-PFPP catheter segments. PFPP has shown to be more stable than PFD [175] and has a lower vapor pressure and greater viscosity. Although, immobilized liquid layers modified with PFPP are more durable in open-air environments, this is unlikely to have influenced our results because the lubricated samples were immediately covered with plasma and were maintained in a closed space.

SEM analysis of catheters incubated in plasma or whole blood reveals differences between the CVD and LPD catheters. Due to the omniphobic slippery properties of the CVD treated catheters, no clot formation or platelet adhesion was seen after incubation with whole

blood. In contrast, protein deposition and platelet adhesion were observed on the control and LPD treated catheters.

In summary, we reported a simple and biocompatible method for successful production of omniphobic lubricant-infused polymeric medical catheter coatings using CVD of hydrophobic organosilanes. Catheters modified in this manner are less thrombogenic than uncoated catheters and catheters modified using the LPD method.

2.5. Materials and Methods

2.5.1. Materials

Trichloro (1H,1H,2H,2H-perfluorooctyl) silane (TPFS), perfluoroperhydrophenanthrene (PFPP) and perfluorodecalin (PFD) were purchased from Sigma–Aldrich (Oakville, Canada). Human plasma depleted of FVII, FXI, or FXII was purchased from Affinity Biologicals (Ancaster, Canada). Coronary catheters (Medtronic, Minneapolis, USA) composed of a soft hydrophobic polyether amide block on the outer layer and a thin walled polytetrafluoroethylene (PTFE) tube on the luminal side [231] were generously provided by S. Gracie. Whole blood and pooled citrated plasma was generated from blood samples collected from healthy donors as previously described [3]. All donors provided signed written consent. All procedures were approved by the McMaster University Research Ethics Board.

2.5.2. Oxygen plasma treatment of catheter segments

Prior to silanizing the catheters, they were cut into 1.7 cm segments, a length chosen to enable placement in the wells of 96-well polystyrene plates (Evergreen Scientific). Segments were then vertically fixed on plastic petri dishes, placed in an oxygen plasma cleaner (Harrick Plasma Cleaner, PDC-002, 230V) and exposed to high-pressure oxygen plasma for 2 minutes to functionalize their surfaces and to enable reaction with TPFS.

2.5.3. Preparation of silanized catheters using CVD

After removing the oxygen plasma-treated catheters from the plasma cleaner, they were immediately placed in a desiccator connected to a vacuum pump and two droplets (200 µL) of TPFS were added in a separate petri dish on the side of the catheters. The vacuum pump was turned on and once a pressure of -0.08 MPa was achieved, the exit valve was closed and CVD of the silane onto the catheters was initiated. The silanization reaction was carried out for 5 hours at room temperature. After the CVD step, catheters were removed from the desiccator and placed in an oven at 60 ºC for a minimum of 12 h in order to complete the reaction. After removing the catheters from the oven, CVD-modified catheters were placed under vacuum for 30 mins with an open exit valve to ensure removal of non-bonded silanes from the surface.

2.5.4. Preparation of silanized catheters using LPD

Catheters were oxygen plasma treated as described above and then immediately incubated in a 20 mL glass vial containing TPFS in anhydrous ethanol solution (5% (v/v)). The solution was stirred with a small magnetic stir bar for 1 h at room temperature. LPD-treated catheters were removed from the solution and then washed with 100% anhydrous ethanol followed by deionized water and ultimately with 70% ethanol. Washed catheters were left to dry at room temperature and then placed in the oven at 60ºC overnight. Similar to CVD treated catheters, after removing the LPD treated catheters from the oven, they were placed under vacuum for 30 mins with an open exit valve to ensure removal of non-bonded silanes from the surface.

2.5.5. Applying fluorinated lubricants on silanized catheters

As a final step, and before preforming different measurements, CVD and LPD treated catheters were submerged into fluorinated lubricants in order to complete the surface modification. Two types of fluorinated lubricants were used: perfluoroperhydrophenanthrene (PFPP) and perfluorodecalin (PFD).

2.5.6. X-ray photoelectron spectroscopy (XPS)

XPS was used to assess the surface chemical composition of the catheters before and after each treatment step. For each condition, three catheter segments were subjected to XPS analysis, measurements were taken from four distinct sites on each segment, and means were determined. XPS spectra were recorded using a Physical Electronics (PHI) Quantera II spectrometer equipped with an Al anode source for X-ray generation and a quartz crystal monochromator was used to focus the generated X-rays (BioInterface Institute, McMaster University). The monochromatic Al $K^{-\alpha}$ X-ray (1486.7 eV) source was operated at 50W 15kV with a system base pressure no higher than 1.0×10^{-9} Torr and an operating pressure that did not exceed 2.0×10^{-8} Torr. A pass energy of 280 eV was used to obtain survey spectra and spectra were obtained at 45˚ take off angles using a dual beam charge compensation system for neutralization. The raw data were analyzed using the instrument software and the atom percentages of carbon, oxygen, fluorine, bismuth, silicon and chlorine were calculated.

2.5.7. Contact and sliding angle measurements

Contact and sliding angles of the treated and non-treated catheters were measured using a droplet of deionized water (5µL). Water sessile drop contact angle measurements were performed at room temperature before and after each modification step using a Future Digital Scientific OCA20 goniometer (Garden City, NY), which was calibrated prior to each measurement. Sliding angles were measured using a custom-made goniometer. Immediately prior to testing, silanized samples coated with PFPP or PFD were placed on

the calibrated goniometer. A droplet of deionized water (5µL) was placed on the catheter surface and the sample was gently tilted until the droplet started to move. The sliding angle was defined as the minimum tilting angle required for droplet movement. A sliding angle of 90 degrees was assigned to droplets that failed to slide at angles of 90 degrees or higher. Measurements were made in triplicate on three different catheter segments and means were determined.

2.5.8. Antithrombotic activity of modified catheters

Clotting assays were performed to compare the antithrombotic activities of the various coatings. After flattening the catheter segments with a plastic roller, they were shaped into rings, placed around the inner walls of the wells of a 96-well plate and saturated with 150 µL of PFPP or PFD lubricant for about 1 min. Excess lubricant was removed and 100 µL aliquots of citrated human plasma were added to wells that did or did not contain catheter segments. After incubating the plate for 5-7 minutes at 37°C, clotting was initiated by adding HEPES (100 µL of 20 mM, pH 7.4) containing $CaCl_2$ (1M) to each well, yielding a final $CaCl_2$ concentration of 25 mM [115], [232]. Clot formation was assessed by monitoring absorbance at 405 nm at 10-sec intervals for 60 min in kinetic mode using a SPECTRAmax plate reader (Molecular Devices). Clotting times were defined as the time to reach half-maximal absorbance as calculated by the instrument software from plots of absorbance versus time. The same procedure was repeated in FVII, FXI, or FXII depleted plasma, except that absorbance was monitored over 3 hours to account for the longer clotting times.

2.5.9. Human whole blood experiments

Treated catheters were stored at room temperature and four months later, the stability of their coating was investigated by performing sliding angle measurements and catheter-blood interaction experiments using whole human blood. Sliding angle measurements with blood were performed according to the procedure described above (contact and sliding measurements).

To investigate catheter-blood interactions, control and treated catheters were submerged in whole human blood for 15 s. Catheters were then washed with PBS, fixed in 4% formaldehyde for 20 min and stored at room temperature in PBS until SEM analysis. Using SEM, the extent of clot formation and platelet adhesion on the catheter surfaces was evaluated.

2.5.10. Scanning Electron Microscopy (SEM)

Catheter segments were washed three times, fixed in 4% formaldehyde in PBS for 2 hours, washed with PBS (0.1 M) and sputter-coated with a 4 nm thick platinum coating. SEM

imaging (JSM- 7000F) was performed in secondary electron image (SEI) mode with voltages of 1.0 kV at 10,000x magnification or 2.0 kV at 1000x magnification.

2.5.11. Statistical Analysis

Data are presented as means ± S.D. In the control and depleted plasma clotting assays, each experimental condition was repeated at least nine times. For all other studies, experiments were repeated at least three times. One-way analysis of variance (ANOVA) followed by post hoc analysis using Tukey's test was performed to assess statistical significance. For all comparisons, P values less than 0.05 were considered statistically significant.

Chapter 3 *Lubricant-Infused Surfaces with Built-In Functional Biomolecules Exhibit Simultaneous Repellency and Tunable Cell Adhesion*

Preface

This chapter describes a novel method for incorporating biofunctionality and targeted-binding onto lubricant-infused platforms. For the first time, LIS with the ability to both prevent non-specific adhesion and promote targeted binding of desired antibodies and cells is reported. The designed BLIS had excellent repellency and biofunctionality properties and were able to attenuate clot formation, prevent no-specific adhesion of blood cells and proteins and promote targeted endothelial cell capture and adhesion from whole blood.

Citation:

This research was originally published in *ACS Nano.*
M. Badv, S. M. Imani, J. I. Weitz, and T. F. Didar, "Lubricant-Infused Surfaces with Built-In Functional Biomolecules Exhibit Simultaneous Repellency and Tunable Cell Adhesion," *ACS Nano*, vol. 12, no. 11, pp. 10890–10902, Nov. 2018.

Relative Author Contributions

This work was an equal collaboration between me and S. M. I. I wrote the manuscript with editorial assistant from other authors. S.M.I. and I performed the surface chemical and physical characterization experiments. S.M.I. performed the biofunctionality studies, short-term cell studies on anti-CD34-conjugated samples and MTT assay with my assistance. I performed the human whole blood clotting assay and SEM imaging with S M. I's assistance. I performed the plasma clotting assay experiments and fibrinogen and platelet adhesion studies. Dr. Ran Ni and Dr. Jim Fredenburgh from McMaster's Thrombosis & Atherosclerosis Research Institute (TaARI) are acknowledged for their help in performing the fibrinogen and platelet adhesion experiments. I performed the long-term cell studies and live/ dead cell viability experiments on anti-CD34 and anti-CD144 functionalized substrates with assistance from S.M.I. XPS measurements were done at the BioInterface Institute at McMaster University.

Note to Reader:

A supplementary section containing the additional figures and information referenced in the chapter is included at the end of the chapter.

3.1. Abstract

Lubricant-infused omniphobic surfaces have exhibited outstanding effectiveness in inhibiting nonspecific adhesion and attenuating superimposed clot formation compared with other coated surfaces. However, such surfaces blindly thwart adhesion, which is troublesome for applications that rely on targeted adhesion. Here we introduce a new class of lubricant-infused surfaces that offer tunable bioactivity together with omniphobic properties by integrating biofunctional domains into the lubricant- infused layer. These novel surfaces promote targeted binding of desired species while simultaneously preventing non- specific adhesion. To develop these surfaces, mixed self- assembled monolayers (SAMs) of aminosilanes and fluorosilanes were generated. Aminosilanes were utilized as coupling molecules for immobilizing capture ligands, and nonspecific adhesion of cells and proteins was prevented by infiltrating the fluorosilane molecules with a thin layer of a biocompatible fluorocarbon-based lubricant, thus generating biofunctional lubricant-infused surfaces. This method yields surfaces that (a) exhibit highly tunable binding of anti-CD34 and anti-CD144 antibodies and adhesion of endothelial cells, while repelling nonspecific adhesion of undesirable proteins and cells not only in buffer but also in human plasma or human whole blood, and (b) attenuate blood clot formation. Therefore, this straightforward and simple method creates biofunctional, non-sticky surfaces that can be used to optimize the performance of devices such as biomedical implants, extracorporeal circuits, and biosensors.

3.2. Introduction

The design, development and optimization of engineered interfaces has been the subject of intensive research because of their numerous applications in bioengineering [233]. Synthetic biointerfaces are often utilized in complex biological environments (*e.g.*, whole blood) and thus their optimum performance relies on their capability to prevent non-specific protein and cell adhesion [234], [235]. This non-sticky behavior, however, must often be paired with biofunctional features in order to promote specific and targeted binding of desired biomolecules, thereby enhancing the biocompatibility of the biointerface. Biofunctionality and preventing non-specific adhesion is of significant importance when designing medical implants such as vascular grafts and mechanical heart valves, however limited success has been made in integrating both blood biocompatibility and biofunctionality on these surfaces [40]. When cell targeting is promoted through immobilizing cell specific biomarkers on the surface, the biocompatibility of the device decreases and when improving the antithrombotic activity, cell adhesion and growth is mainly inhibited [67]. Hence, most studies have focused on improving one aspect of blood compatibility or promoting targeted cell binding. Failure to design a targeted biofunctional platform with protein and bacterial repellant properties may result in delayed recovery,

thrombosis, biofilm formation and infection, which can all lead to impaired performance or rejection of the implanted device [37], [75], [155], [236], [237].

Various strategies have been developed to minimize non-specific adhesion of proteins and cells to bioengineered surfaces [233], [238]. Bovine serum albumin (BSA) [75], [153], [236], [239], [240], heparin [29]–[34], zwitterionic polymers [241], [242], and poly-(ethylene glycol) (PEG) [27], [75], [243], [244] are widely used to attenuate non-specific adhesion of cells, proteins, and bacteria. Although surfaces coated with these agents exhibit improved early performance, their durability is limited because of degradation or desorption of the coating over time [234], [235], [245].

More recently, immobilized lubricant layers have been introduced as a highly effective approach to decrease non-specific adhesion [179], [181], [246]–[248]. Such surfaces are created by infiltrating a fluorinated layer with compatible fluorocarbon-based lubricants [174], [179], [185], [188], [249]. Lubricant-infused slippery surfaces exhibit anti-biofouling [175], [180], [249], anti-thrombogenic [174], [178], [193], anti-icing and anti-frosting properties [196] and outperform PEG-coated surfaces for prevention of non-specific binding of bacteria and proteins [181]. The major shortcoming of omniphobic lubricant-infused surfaces is that they blindly thwart adhesion. While highly advantageous when operating in complex fluids such as whole blood, this blind repulsion is troublesome for applications that rely on targeted binding, or applications that benefit from specific adhesion such as implants, prosthesis, and extracorporeal devices. The main challenge in integrating specific bioadhesion into omniphobic liquid-infused surfaces is designing a chemistry that covalently inserts functional biomolecules on the liquid-infused surface, without disturbing the lubricant-infused layer. We designed such chemistry by combining the fluorinated SAMs with silane coupling agents, a method that has widely been used for creating functional platforms for covalent attachment of biomolecules and producing biofunctional interfaces [250]–[253]. Aminosilanes (such as 3-aminopropyltriethoxy-silane, APTES) are among the most commonly used coupling agents [254]–[259] for covalent immobilization of biomolecules [203], [258] and surfaces coated with APTES have shown promising results in creating stable and durable biointerfaces [203], [204], [260]–[262].

Here we report for the first time, the development of biofunctional lubricant-infused surfaces (BLIS). By creating SAMs of organosilanes with mixed ratios of APTES and trichloro (1H,1H,2H,2H-perfluorooctyl) silane (TPFS), using chemical vapor deposition (CVD) or liquid phase deposition (LPD) we achieved simultaneous targeted adhesion and non-specific repellency. We further demonstrate control over the degree of antibody and cell adhesion by varying the ratios between the two APTES and TPFS molecules and show

that our created BLIS with "built-in" capture ligands are capable of tunable target cell adhesion while preventing coagulation and non-specific adhesion with superior performance compared with previously reported bio-interfaces.

3.3. Results and discussion

3.3.1. Design and fabrication of biofunctional lubricant-infused surfaces

Immobilized lubricant layers (on fluorinated SAMs) can be used to create non-sticky biointerfaces that repel micro/nano solids as well as organic and aqueous liquids [175], [181]. Here for the first time we demonstrate that replacing a proportion of the fluorosilanes with different SAMs provides anchors for bioconjugation without compromising the repellency of the surface. The BLIS were produced by LPD or CVD of mixed ratios of APTES and TPFS as explained in the methods section (***Figure 3.1***). APTES provided amine groups for conjugating biomolecules and TPFS served as the substrate for immobilizing a fluorocarbon-based lubricant on the surface. The following three ratios were selected for preparing the SAMs: 95% APTES:5% TPFS, 75% APTES:25% TPFS, and 50% APTES:50% TPFS. Samples treated with 100% APTES or 100% TPFS were used as positive and negative controls, respectively (Figure 1a and b). For protein and cell adhesion experiments, APTES was utilized to immobilize the cell-specific anti-CD34 or anti-CD144 antibodies using carbodiimide crosslinker chemistry and TPFS was used to immobilize the perfluoroperhydrophenanthrene (PFPP) lubricant, which prevents non-specific adhesion. Samples were also incubated with human umbilical vein endothelial cells (RFP-HUVECs) in media or in human whole blood allowing the functionalized surfaces to specifically capture HUVECs, while repelling other biospecies.

3.3.2. Surface chemical composition of fluorine – presence of TPFS

X-ray photoelectron spectroscopy (XPS) was performed to confirm the presence of the TPFS molecule on the silane treated glass surfaces and the fluorine atom % was quantified for each sample treated with different ratios of APTES:TPFS (***Figure 3.2***a). In the CVD treated samples, there was a correlation between the atom % of fluorine and the volume % of TPFS used in the modification process. Samples treated with 100% TPFS had the highest atom % of fluorine (51.9 ± 3.4 atom %), and the atom % of fluorine decreased by decreasing the volume % of TPFS, with samples treated with 5% TPFS (95% APTES) having the lowest amount of fluorine (12.3 ± 9.5 atom %) compared with other ratios. In contrast to CVD treated samples, LPD treated samples showed no defined relationship between the fluorine atom % and the different silane ratios used in the reaction (***Supplementary Figure 3.1*a**).

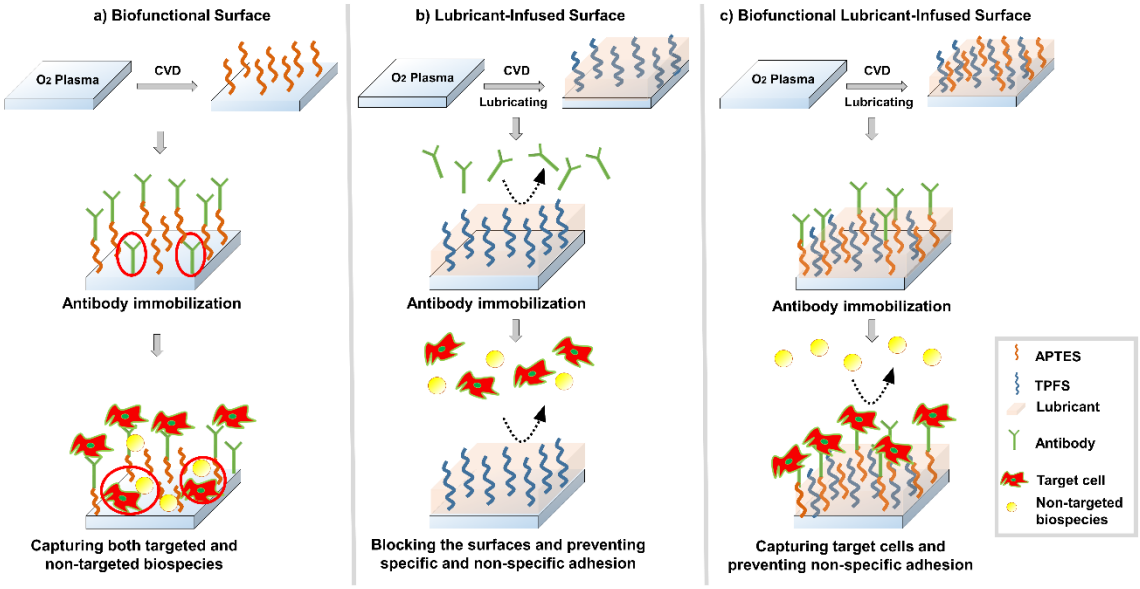

Figure 3.1 Schematic representation of creating (a) biofunctional, (b) lubricant-infused, and (c) biofunctional lubricant-infused surfaces using chemical vapor deposition (CVD) or liquid phase deposition (LPD) of silanes. (**a**) Surfaces are treated with 100% APTES molecule. Therefore, nonspecific adhesion of antibodies, cells, and other biospecies is observed on these surfaces even when applying conventional blocking strategies. (**b**) Omniphobic lubricant-infused slippery surfaces are generated by modifying the surfaces of the oxygen plasma treated samples with 100% TPFS using either CVD or LPD and, subsequently, adding the PFPP lubricant layer. These surfaces act as blocked surfaces with no biofunctional properties and prevent antibodies and cells from adhering to the surface. (**c**) By creating mixed SAMs using different ratios of APTES and TPFS molecules, biofunctional lubricant-infused surfaces (BLIS) are created. These surfaces simultaneously prevent nonspecific adhesion and promote targeted cell adhesion.

3.3.3. Quantification of amine groups on the mixed silane SAMs

Amine groups on the glass surfaces treated with the CVD or LPD technique were quantified using fluorescence imaging after labelling the surfaces with FITC, an amine reactive fluorophore (***Figure 3.2b*** and ***c***). The treated surfaces were imaged using a fluorescence microscope and the green fluorescence intensity was quantified using ImageJ. In the CVD treated group, samples modified with 100% APTES had the highest fluorescence intensity compared with other groups. The FITC fluorescence intensity decreased as the amount of APTES used in the reaction decreased. In contrast to CVD treated samples, with LPD treated samples, the FITC intensity did not correlate with the ratio of APTES used in the reaction (***Supplementary Figure 3.1b*** and ***c***).

3.3.4. Sliding and contact angle measurements

To evaluate the omniphobic slippery properties of the treated samples, sliding and contact angle measurements were performed using a 5 µL droplet of deionized (DI) water, as described in the methods section. Similar to surfaces treated with 100% TPFS, CVD and LPD samples treated with mixed ratios of APTES and TPFS had sliding angles as low as

5° (***Figure 3.2d*** and ***Supplementary Figure 3.1d***). This finding suggests that mixing APTES with TPFS does not compromise the slippery properties of the surface. In both CVD and LPD treated groups, the droplet did not slide on samples that were treated with 100% APTES (sliding angle >90 °).

The static contact angle measurements of the control and treated glass surfaces (prior to adding the lubricant layer) are shown in ***Figure 3.2*****e** and **f** and ***Supplementary Figure 3.1e*** and ***f***. Similar to surfaces treated with 100% TPFS, CVD and LPD samples with mixed silanes had mean static contact angles above 100°. Results obtained from the water sliding and contact angle measurements confirm that surfaces treated with mixed SAMs retain their omniphobic slippery properties and the presence of a minimum amount of TPFS during the modification step (as low as 5 volume %) is sufficient to preserve the omniphobic slippery characteristics (contact angle >100° and sliding angle <10°). In an effort to find the lower limit, we tried TPFS ratios lower than 5% (down to 1%), none of which showed slippery properties which could mainly be due to not having enough fluorine groups on the surface in order to lock in the lubricant layer.

3.3.5. Immobilization of anti-CD34 antibody

The omniphobic slippery surfaces were further functionalized with Alexa Fluor 488 conjugated anti-CD34 antibody. Antibody immobilized surfaces were imaged using fluorescence microscopy and the fluorescence intensity of the surfaces was quantified using ImageJ. As seen in ***Figure 3.3a*** and ***b***, in the CVD-treated samples, the amount of anti-CD34 antibody attached to the surface increases by increasing the amount of APTES in the reaction. Samples treated with 100% APTES showed the highest amount of antibody binding (78.74 ± 9.42 a.u.), while those treated with 95% and 75% APTES exhibited progressively less binding (53.35 ± 14.45 a.u. and 36.89 ± 16.53 a.u., respectively). There was minimal anti-CD34 antibody immobilization on surfaces treated with 50% APTES. With LPD-treated surfaces, there was no correlation between the amount of immobilized antibody and the percentage of APTES used in preparing the mixed SAMs (***Supplementary Figure 3.2***). Similar to CVD treated samples; there was minimal anti-CD34 antibody immobilization on surfaces treated with 50% APTES using LPD.

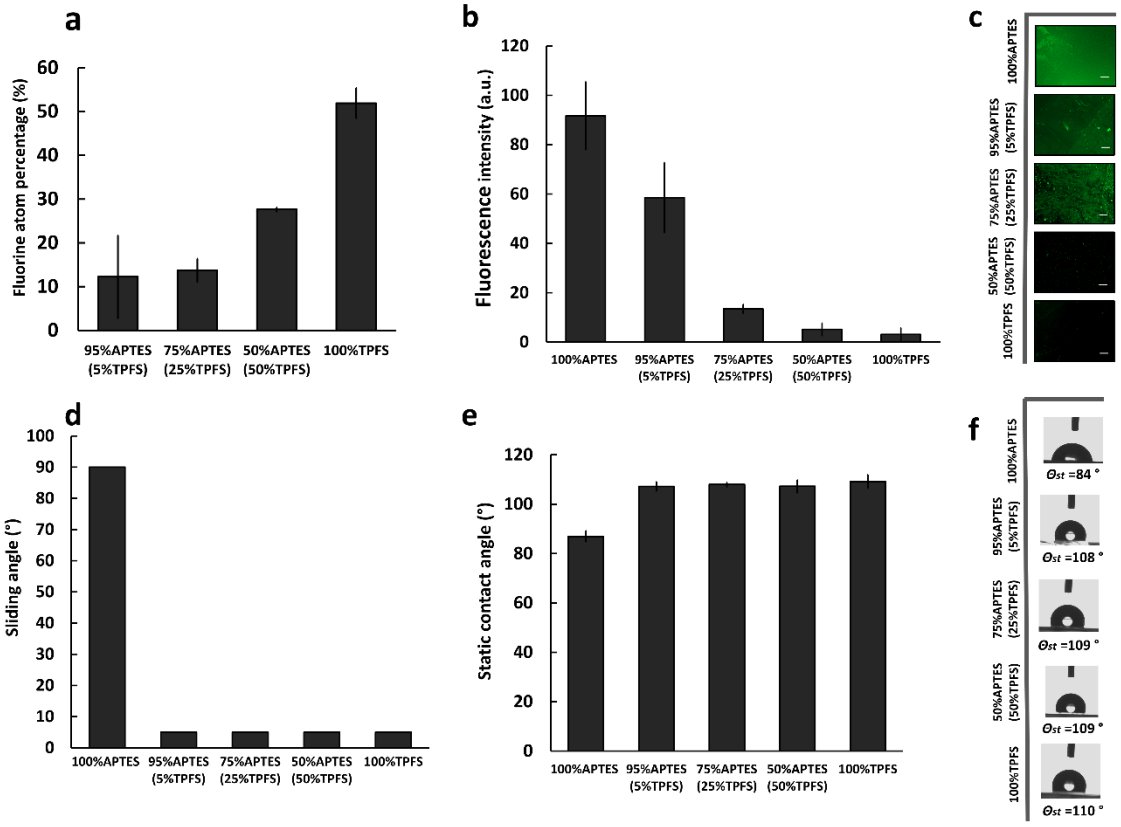

Figure 3.2 Assessing the chemical composition and the omniphobic slippery properties of the produced surfaces. (**a**) The presence of fluorine was confirmed and quantified using XPS analysis for samples treated with different ratios of APTES and TPFS. In the CVD-treated samples, the atom % of fluorine increased as the ratio of APTES to TPFS decreased. (**b**) The presence of APTES on surfaces coated with mixed APTES−TPFS or 100% APTES using CVD was evaluated using fluorescence microscopy after labeling them with a FITC-conjugated amine targeting dye. There was a clear correlation between the FITC fluorescence intensity and the amount of APTES used in the modification step. (**c**) Representative fluorescent images of FITC-labeled surfaces. (**d**) Sliding angle and (**e**) contact angle measurements were performed in order to evaluate the omniphobic slippery properties of the treated surfaces. Samples treated with 100% TPFS or mixed ratios of APTES and TPFS had sliding angles as low as 5 degrees and contact angles higher than 100 degrees. (**f**) Representative contact angle images of a 5 µL water droplet on treated glass surfaces before adding the lubricant coating. In all graphs, error bars show the means ± SD of at least three samples. The scale bars on the fluorescence images represent 100 µm.

3.3.6. RFP-HUVEC attachment and surface cell repellency properties – short-term experiments

The biofunctionality of developed surfaces was evaluated by incubating endothelial cells (RFP-HUVECs) with the anti-CD34 antibody functionalized surfaces. Endothelial cell attachment was investigated 24 hours after cell seeding and the average cell number per mm^2 was calculated after imaging the samples. As seen in ***Figure 3.4a***, in the CVD treated samples, there were more adherent cells on surfaces treated with 100% APTES (51 ± 8 cells/mm^2) than on those treated with 95% or 75% APTES (28 ± 6 and 26 ± 9 cells/mm^2,

respectively). Samples treated with 50% APTES had significantly fewer adherent cells (10 ± 8 cells/mm^2) compared with higher APTES ratios. Samples treated with 100% TPFS exhibited no cell attachment after 24 hours. In the LPD treated group, similar to CVD treated surfaces, samples treated with 100% TPFS were cell repellent and 100% APTES treated samples had the highest number of cells (61 ± 19 cells/mm^2) compared to 95% APTES, 75% APTES and 50% APTES treated surfaces (29 ± 11, 19 ± 10 and 13 ± 4 cells/mm^2, respectively) (***Supplementary Figure 3.3***).

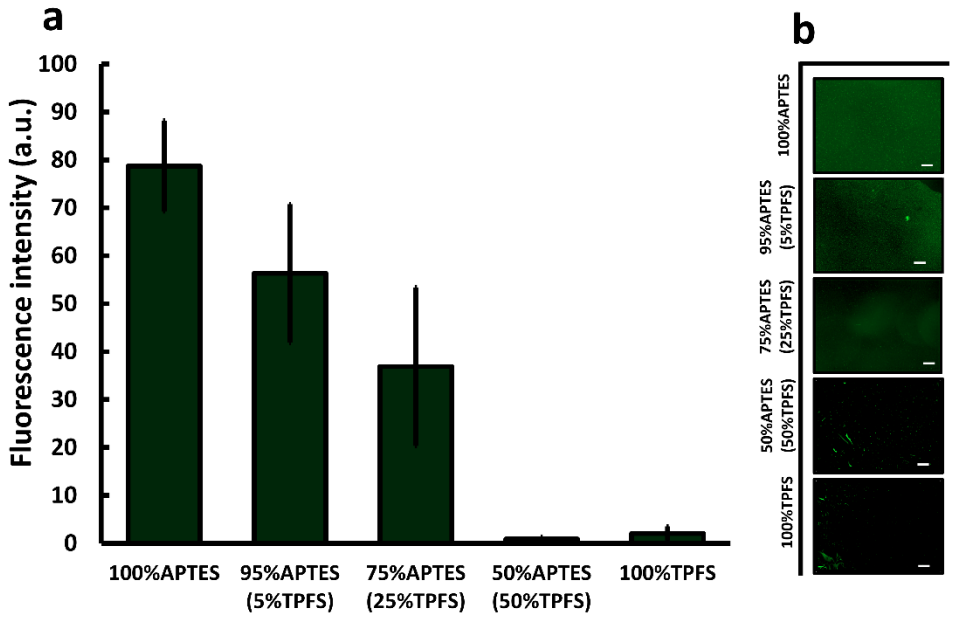

Figure 3.3 Anit-CD34 antibody immobilization on treated samples. (**a**) Surfaces treated with 100% APTES and mixed APTES−TPFS using CVD were functionalized with fluorescently labeled anti-CD34 antibody. By decreasing the amount of APTES used in the modification step, the fluorescence intensity of the immobilized antibody decreased. Samples treated with 100% TPFS (no amine groups) showed no antibody attachment. (**b**) Representative fluorescent images of anti-CD34 -functionalized surfaces. Error bars show the means ± SD of at least three samples. The scale bars on the fluorescence images represent 100 μm.

To further demonstrate superior blocking properties of BLIS, cell adhesion and repellency of different blocking agents were compared with the 100% TPFS treated samples (***Figure 3.4c*** and ***d***). Samples blocked using 100% TPFS, BSA or PLL-PEG (poly (L-lysine)-poly (ethylene glycol)) were incubated with cells for 24 hours and cell adhesion and growth were monitored. As seen in ***Figure 3.4c*** and *d*, lubricant-infused surfaces (100% TPFS) had significantly fewer adherent cells compared with samples blocked with BSA or PLL-PEG, both of which showed low repellency compared with the lubricant infused surfaces (LIS).

To study the potential *in vitro* cytotoxicity of the treated surfaces, cultured RFP-HUVECs were exposed to silanized surfaces for 48 hours and cell viability was assessed. There was

no significant decrease in cell viability suggesting that these surfaces are not toxic (***Supplementary Figure 3.4***).

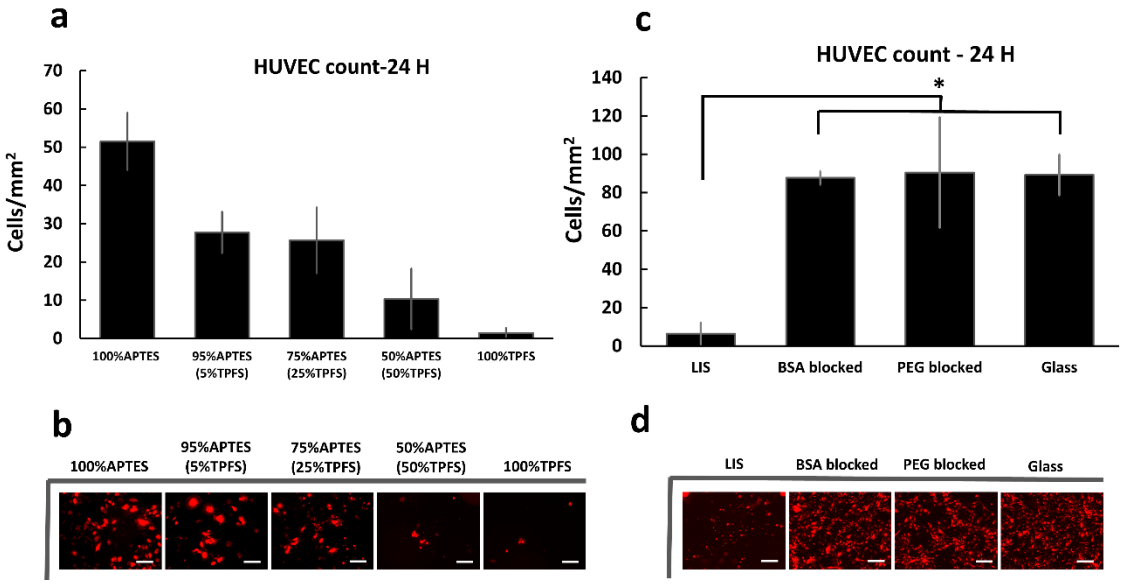

Figure 3.4 Investigating the RFP-HUVECs adhesion and interaction with silanized, anti-CD34-functionalized surfaces. (**a**) Treated surfaces were incubated with RFP-HUVECs for 24 h, and the cell adhesion and growth was investigated. All surfaces treated with TPFS were lubricated prior to the experiments. Cell attachment was decreased by decreasing the APTES:TPFS ratio. Cell count per surface area was highest in 100% APTES samples, which corresponds to the presence of a higher density of anti-CD34-antibody on these surfaces. 100% TPFS samples showed a minimum amount of cell attachment, confirming the repellency and omniphobic slippery properties of these surfaces. (**b**) Representative fluorescent images of surfaces incubated with RFP-HUVECs for 24 h. (**c**) The cell repellency properties of lubricant-infused surfaces (LIS) were compared to BSA or PLL−PEG-blocked substrates. LIS showed significantly less cell attachment compared to BSA or PLL−PEG-blocked surfaces. (d) Representative fluorescent images of surfaces incubated with RFP-HUVECs for 24 h. Error bars show the means ± SD of at least three samples. *Significant difference when comparing the results from 100% TPFS blocked surfaces with surfaces blocked using other techniques ($P < 0.001$). The scale bars on the fluorescence images are 20 μm.

3.3.7. Selecting the optimized treatment method and APTES:TPFS ratio

Overall, the CVD treatment method yielded more consistent results than the LPD method, and the surface chemical composition and the amount of TPFS and APTES present on the surface were better controlled with the CVD method. Although LPD is a widely used technique for creating SAMs of silanes [227], results obtained from the surface characteristic measurements show that the surface chemical composition and the amount of TPFS and APTES present on the surface could be better controlled using the CVD technique whereas controlling the silane deposition on the surface proved to be more challenging when using the LPD method (***Figure 3.2*** and ***Figure 3.3***). Previous studies have also shown that CVD is more effective and reproducible than LPD in generating

homogenous silanized layers [178], [227], [263]. This is likely due to self-polymerization of the silanes in the liquid phase, and as a result the formation of multilayers on the surface [264].

With CVD treated samples, there was no significant difference between samples treated with 95% and 75% APTES in terms of biofunctionality and repellency. In contrast, treatment with 50% APTES reduced biofunctionality. Therefore, in order to better evaluate the biofunctionality and omniphobic properties of the designed surfaces, we conducted further experiments on CVD treated samples with 75%-25% APTES-TPFS ratio in plasma and human whole blood and the results were compared with samples treated with 100% APTES, 100% TPFS, or other control samples. In order to confirm that our designed BLISs provide a generic platform compatible with other antibodies, we functionalized our surfaces with unconjugated anti-CD144 antibody, another endothelial cell specific antibody and investigated the cell growth, viability and endothelial function over a period of 5 days. Live/dead cell viability assay was also performed on these surfaces after 6 days of cell culture. The repellency properties of our designed substrates were further investigated by performing additional blood experiments and platelet and FITC-fibrinogen adhesion assays and the results were compared to the control samples.

3.3.8. Sliding and contact angle experiments using human whole blood

Surfaces treated with 100% or 75% APTES, or with 100% TPFS were lubricated with PFPP and a droplet of human blood was then added to the surface. Surfaces were tilted and the movement and sliding of the blood droplet was monitored. As seen in ***Supplementary movie 1***, similar to the results obtained from water sliding angle measurements, samples treated with mixed silanes or with 100% TPFS exhibited excellent slippery properties as evidenced by low sliding angles and immediate sliding of the blood droplet. The omniphobic slippery properties of samples treated with a mixture of APTES and TPFS were found to be comparable to omniphobic lubricant-infused surfaces created using 100% TPFS reported in other studies [174], [178], [179]. In contrast, the blood droplet did not slide on samples treated with 100% APTES and these samples did not exhibit blood repellency properties. After removing the blood droplets from the surfaces, a visible layer of blood remained on the 100% APTES treated samples. In contrast, significantly less blood remained on the surfaces of samples treated with 100% TPFS or 75% APTES (***Figure 3.5a***).

We also monitored the morphology of the blood droplet in contact with the treated surface. As seen in ***Figure 3.5a***, blood droplets remained spherical and had a significantly higher contact angle on samples treated with 75% APTES or 100% TPFS than on samples treated

with 100% APTES. On the latter surfaces, the blood droplets no longer remained spherical but spread to cover the entire surface area.

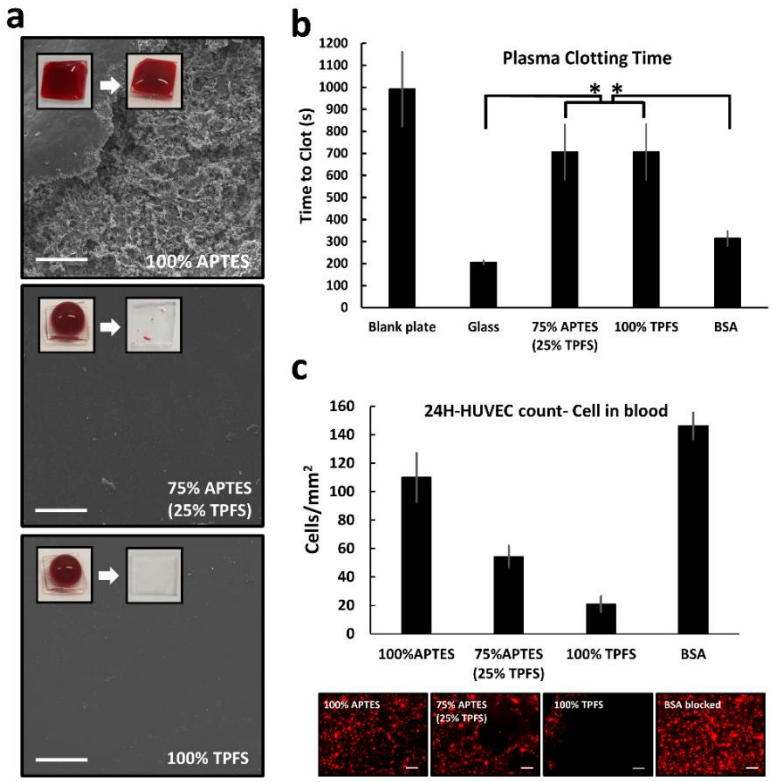

Figure 3.5 Investigating the blood and protein interaction with optimized biofunctional lubricant-infused surfaces. (**a**) Photographs (top) and SEM images taken from samples incubated with human whole blood indicate that samples treated with mixed silanes or 100% TPFS have excellent blood repellency properties, and no clot or blood cell adhesion was observed on them. (**b**) Plasma clotting assay results show no significant difference between the clotting times of samples treated with 75% APTES (25% TPFS) and those treated with 100% TPFS. In addition, both treated groups had significantly higher clotting times compared to untreated glass slides and glass slides treated with BSA. (**c**) Samples were incubated with RFP-HUVEC−blood mixture for 24 h, and cell adhesion was investigated. These results indicate that biofunctional lubricant-infused surfaces remain functional, retain their repellency properties in complex biological environments, and are able to capture the target cells from human whole blood. Error bars show the means ± SD of at least three samples. *Significant difference when comparing the results from different groups ($P < 0.001$). The scale bars are 200 μm on the fluorescence images and 50 μm on the SEM images.

3.3.9. Plasma clotting assay

Plasma clotting assays were performed on BLISs (75% APTES, 25% TPFS) to investigate their antithrombotic activity compared with samples that were blocked with BSA, or 100% TPFS (***Figure 3.5b***). Samples were covered with a 100 μL aliquot of citrated human plasma and incubated at 37 °C for 10 min prior to initiating clotting as explained in the methods section. As seen in Figure 5b, clotting times with samples treated with mixed silanes or 100% TPFS were significantly longer than those with untreated glass slides or glass slides

treated with BSA (706 ± 123, 706 ± 124, 205 ± 8 and 314 ± 33 sec respectively). Therefore, treatment with mixed silanes (BLIS) attenuated clotting to a similar extent as treatment with the previously reported lubricant-infused surfaces (100% TPFS) [178].

3.3.10. Protein and blood cell attachment to treated surfaces in human whole blood-blood clotting assay experiment

To investigate the surface-blood interaction, samples were incubated with citrated human whole blood and the blood clotting was initiated by adding $CaCl_2$ to the solution. After fixing the samples in 4% formaldehyde, they were imaged using SEM to assess protein and blood cell adhesion. As seen in ***Figure 3.5a***, there was significantly less blood cell accumulation and blood clot formation on samples treated with 100% TPFS or 75% APTES than on samples treated with 100% APTES. No significant difference was seen in blood repellency properties when comparing the results from samples treated with 75% APTES and 100% TPFS, suggesting that the blood repellency properties of biofunctional lubricant-infused samples treated with mixed silanes are comparable to those entirely blocked using lubricant-infused surfaces (100% TPFS).

3.3.11. Specific cell capture in human whole blood

Targeted binding and the capability of the blood-contacting surfaces to capture the desired biomolecules from a complex biological environment such as blood is crucial in biomedical implants [54]. The capacity of BLIS to capture target cells from a RFP-HUVEC and blood mixture was investigated (***Figure 3.5c***). RFP-HUVECs spiked into human blood were incubated with the surfaces for 24 hours, during which cell adhesion and cell growth were monitored. As seen in Figure 5c, more cells adhered to samples treated with 100% APTES than to samples treated with mixed silanes. However, there was significantly more cell adhesion to samples treated with 75% APTES than to samples treated with 100% TPFS. BSA-blocked surfaces did not show cell repellency properties. The surfaces treated with 100% TPFS or mixed silane also outperformed conventional blocking agents such as BSA and PEG (***Figure 3.4*** and ***Figure 3.5***). While the 75% APTES (25% TPFS) surfaces showed biofunctional features by capturing RFP-HUVECs from blood, they were resistant towards blood cells (***Figure 3.5a***) and exhibited excellent targeting characteristics (***Figure 3.5c***).

3.3.12. Platelet repellency properties of biofunctional lubricant infused substrates

Human platelet repellency properties of functionalized and control surfaces was investigated. Substrates were incubated with activated human platelets for 1 hour, fixed with 2% formaldehyde and conjugated with FITC-PAC1 antibody (platelet-activated marker) and platelet adhesion was studied using fluorescence microscopy. As seen in

Figure 3.6a and ***c,*** 75% APTES (25% TPFS) treated samples significantly prevented non-specific adhesion of platelets and there was no significant difference seen when comparing the results with 100% TPFS blocked samples. In contrast, 100% APTES treated samples were not platelet repellent and had significantly more platelets adhered to their surfaces. ***Supplementary Figure 3.5*** shows the flow cytometry results confirming the binding of FITC-PAC1 antibody to activated platelets. Resting platelets did not bind to the platelet activated marker.

3.3.13. FITC-fibrinogen adhesion – plasma clotting assay

The antithrombotic and repellency properties of the optimized BLISs were further investigated and directly visualized by performing the clotting assay using plasma containing FITC-fibrinogen. Samples were incubated with citrated plasma containing FITC-fibrinogen and the clotting assay was initiated as previously described. After washing and fixing the samples, they were visualized using a fluorescence microscope and the fluorescent intensity of the adhered FITC-fibrinogen was calculated. As seen in ***Figure 3.6b*** and ***d***, 75% APTES (25% TPFS) treated substrates prevented clot and fibrinogen adhesion to the same extend as 100% TPFS treated samples and no significant difference was observed between these two groups. In contrast, a dense layer of FITC-fibrinogen was formed on 100% APTES treated samples, covering the entire surface and these surfaces did not show antithrombotic properties and had significantly more protein adhered to their surfaces compared with 100% TPFS and 75% APTES (25% TPFS) treated groups. These results were in line with results obtained from the plasma and human whole blood clotting experiments.

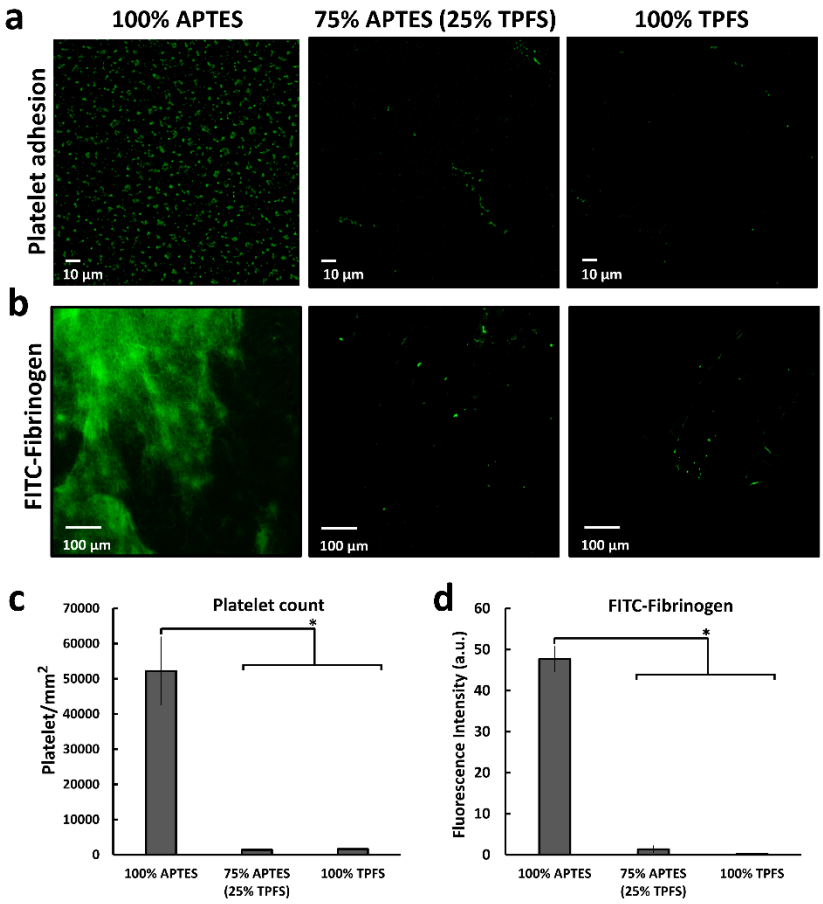

Figure 3.6 Investigating FITC−fibrinogen and platelet adhesion on treated surfaces. (**a**) Representative fluorescence images of activated platelets adhered to different treated substrates. Biofunctional lubricant-infused surfaces treated with 75% APTES (25% TPFS) showed excellent platelet repellency properties, and no significant difference was seen compared with 100% TPFS-lubricated samples. 100% APTES- treated substrates had significantly more platelets adhered to their surfaces compared with other treated groups. (b) Representative fluorescent images of FITC−fibrinogen attached to treated substrates. 75% APTES (25% TPFS) samples exhibited excellent protein repellency properties, to the same extent as 100% TPFS-treated samples. In contrast, a dense fibrinogen layer was formed on 100% APTES- treated samples. (**c**) Number of platelets/mm2 adhered to surfaces. (**d**) Fluorescence intensity of FITC−fibrinogen adhered to treated substrates. Error bars represent means ± SD of at least three samples. *Significant difference when comparing the results from different groups ($P < 0.005$).

3.3.14. Long-term cell adhesion and viability studies and the investigation of surface compatibility with anti-CD144

To demonstrate stability of the developed surfaces as well as their performance as a generic platform independent of the applied functional ligands, long-term cell study experiments with surfaces treated with unconjugated anti-CD34 or anti-CD144 antibodies were performed and HUVEC adhesion and cell compatibility of the surfaces with endothelial cell specific antibodies was investigated over a period of 5 days. Cells were further fixed and stained using Alexa Fluor 488-conjugated anti CD144 (VE-cadherin) antibody (green)

and Hoechst 33342 (blue) and were imaged using a confocal microscope (Zeiss LSM510 confocal laser scanning microscope) in order to better visualize their morphology and confluency (unconjugated antibodies were used for surface coating and Alexa Fluor 488-conjugated anti-CD144 antibody was used for immunofluorescent staining for VE-cadherin). Both anti-CD34 and anti-CD144 BLISs promoted endothelialization and cell growth and no significant difference was seen in the cell confluency and viability in 75% APTES (25 % TPFS) treated surfaces compared with 100% APTES treated samples after 5 days. The positive staining for Alexa Fluor 488-conjugated VE-cadherin confirmed the HUVEC phenotype for adherent cells and demonstrated the tight junctions formed between the endothelial cells and the successful formation of the endothelial layer on these surfaces (***Figure 3.7a*** and ***b***). In contrast to 75% APTES (25% TPFS) and 100% APTES treated surfaces, the 100% TPFS treated samples had significantly less cells adhered to their surfaces and they successfully prevented cell adhesion and growth and the lubricant-infused layer remained effective and successfully prevented non-specific adhesion of HUVECs during the 5 day cell experiments. The formation of cell junctions was not observed in 100% TPFS treated samples. Similar to previously reported studies which used anti-CD34 or anti-CD144 as endothelial cell specific markers [18], [38], [75], [265] our antibody coated surfaces showed rapid endothelialization and significantly increased endothelial cell capture and adhesion.

Live/dead cell staining assay was performed after 6 days of cell culture to evaluate the cytocompatibility of the treated surfaces. As seen in ***Figure 3.8***, 75% APTES (25% TPFS) samples functionalized with both anti-CD34 or anti-CD144 showed excellent compatibility with HUVECs, with live cell population being greater than 90%. No significant difference was seen when comparing the results with 100% APTES treated samples. The 100% TPFS treated samples blocked the surface and had few to no number of cells adhered to their surfaces.

The results obtained from the complimentary plasma clotting assay and cell studies, verify the successful integration of biofunctionality and specific targeting features on the surfaces created by the optimized ratio of mixed silanes.

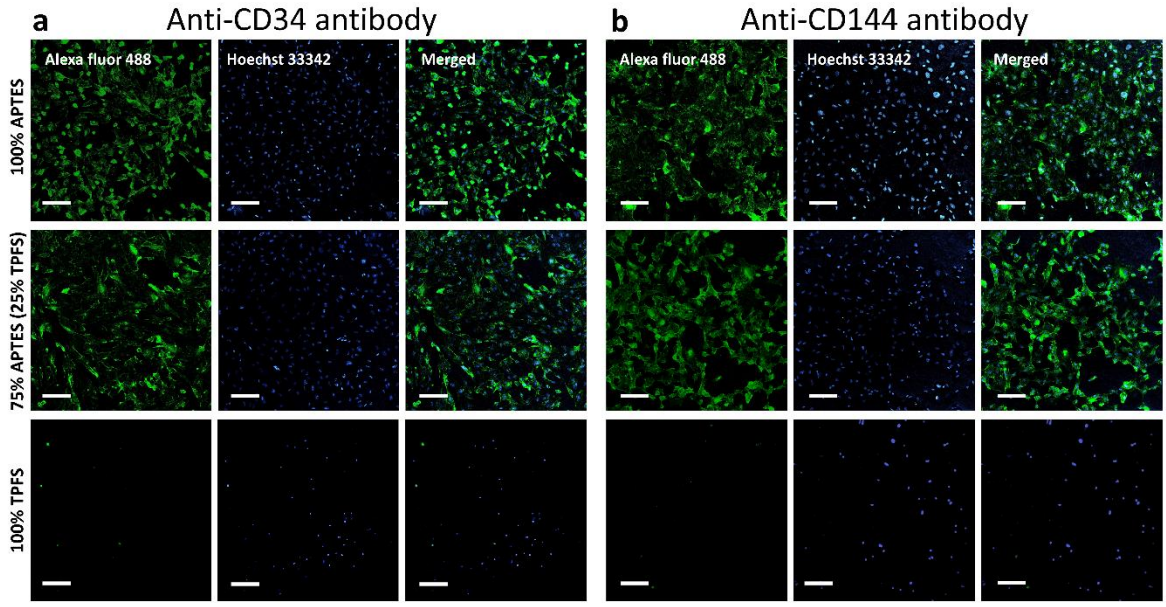

Figure 3.7 Long-term cell experiments conducted on anti-CD34- and anti-CD144-treated samples and the investigation of cell phenotype and cytocompatibility of the treated surfaces. Samples were functionalized with (**a**) anti-CD34 and (**b**) anti-CD144 antibodies and incubated with HUVECs for 5 days. The positive immunofluorescence staining for Alexa Fluor 488-conjugated VE-cadherin confirms the HUVEC phenotype for adherent cells. Both endothelial cell-specific antibodies promoted cell adhesion and endothelialization. The 100% TPFS- lubricated samples inhibited the nonspecific binding of cells and had significantly fewer adherent cells after 5 days compared to other treated substrates. The scale bars are 100 μm.

3.4. Conclusion

In summary, we have reported a method for successfully creating surfaces that are both biofunctional and lubricant-infused and are capable of preventing non-specific adhesion of biomolecules and cells while capturing target species in complex fluids such as blood. Different ratios of TPFS and APTES were used in this study in order to obtain the optimized surface properties where modified substrates remained omniphobic and slippery while having biofunctional domains integrated onto their surfaces. Both methods of CVD and LPD treatment showed promising results, however the results obtained using the CVD method were more consistent and we were able to better control the chemical properties of the modified surfaces obtained using this technique. Overall, the proposed technique is a straightforward and simple method that could be used to create biofunctional, lubricant-infused surfaces for different applications such as medical implants and biosensors, where both biofunctionality and prevention of non-specific adhesion are key and required features when utilizing these devices.

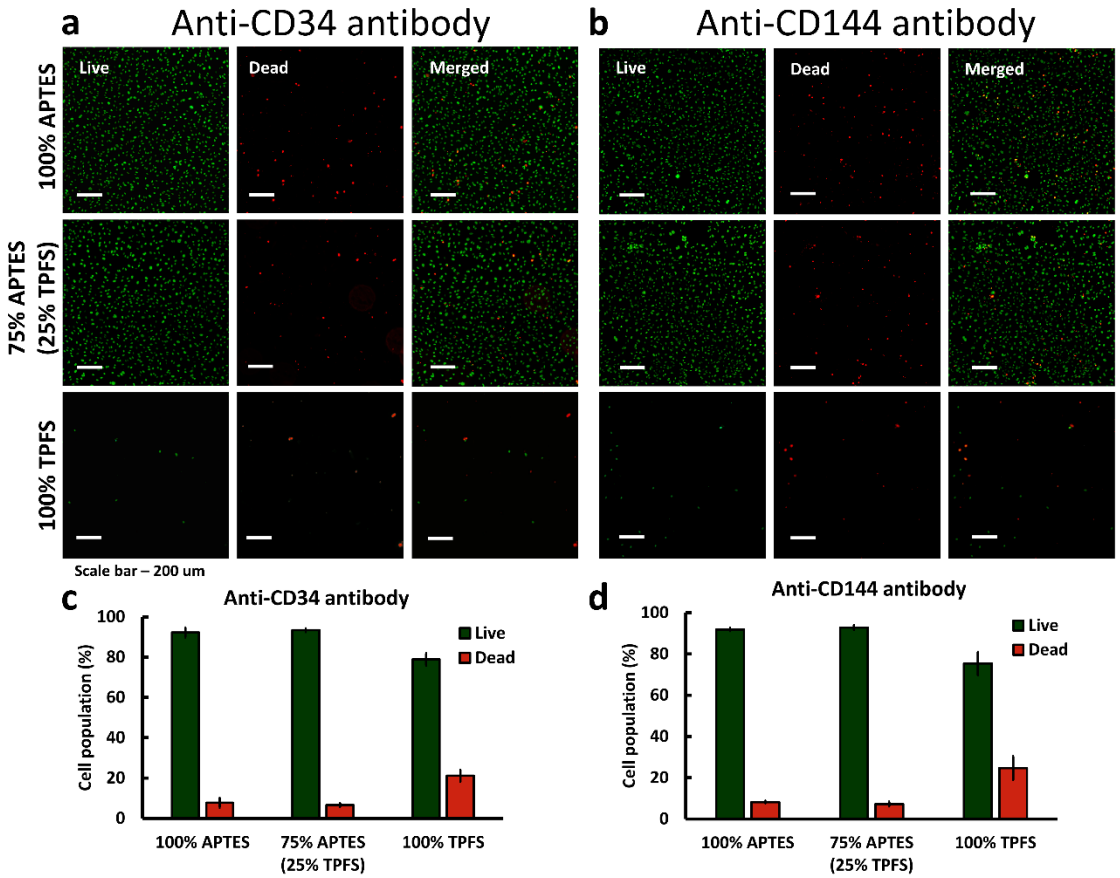

Figure 3.8 Live/dead cell population on 100% APTES, 75% APTES (25 % TPFS) and 100% TPFS treated surfaces. Samples treated with (**a**) unconjugated anti-CD34 or (**b**) unconjugated anti-CD144 antibody were incubated with HUVECs for 6 days and cell viability was assessed. The live cell population was greater than 90% for both biofunctional lubricant-infused and 100% APTES treated surfaces functionalized with either anti-CD34 or anti-CD144 antibody (**c** and **d**). Green: live cells, Red: dead cells. Error bars represent means ± SD of at least three samples. Scales bars on representative fluorescence images are 200 µm.

3.5. Materials and methods

3.5.1. Materials

Trichloro (1H,1H,2H,2H-perfluorooctyl) silane (TPFS), 3-aminopropyltriethoxy-silane (APTES), Triton X-100, phosphate Buffered Saline (PBS), bovine Serum Albumin (BSA), PLL-PEG, perfluoroperhydrophenanthrene (PFPP), N-(3-Dimethylaminopropyl)-N′-ethylcarbodiimide (EDC), N-Hydroxysuccinimide (NHS), sodium bicarbonate, 2-(N-Morpholino)ethanesulfonic acid (MES), FITC were purchased from Sigma–Aldrich (Oakville, Canada). Red Fluorescent Protein Expressing Human Umbilical Vein Endothelial Cells (RFP-HUVEC) were generously provided by Dr. P. Ravi Selvaganapathy's lab at McMaster University. Cell media kit (EGM-2 BelletKit) and trypsin neutralizing agent where purchased from Cedarlane (Burlington, Canada). Trypsin-EDTA (0.25%), phenol red and the MTT cell proliferation assay kit, unconjugated mouse

anti-human CD34 antibody, Alexa fluor 488-conjugated mouse anti-human anti-CD34 antibody, unconjugated mouse anti-human CD144 (VE-cadherin) antibody, Alexa fluor 488-conjugated mouse anti-human CD144 (VE-cadherin) antibody, Hoechst 33342 nucleic acid stain, cell viability imaging kit and methanol-free formaldehyde were purchased from Thermo Fisher Scientific (Waltham, United States). FITC mouse anti-human PAC1 antibody was purchased from BD Biosciences (New Jersey, United States). Plain glass slides were purchased from VWR (Radnor, United States). Whole blood and pooled citrated plasma was generated from blood samples collected from healthy donors as previously described [3]. All donors provided signed written consent. All procedures were approved by the McMaster University Research Ethics Board.

3.5.2. Initial activation of the surfaces using oxygen plasma treatment

Plain microscope glass slides were used as main substrates throughout the experiments. Prior to starting the surface modification process, glass slides were cut into small squares (about 0.5x0.5 cm2) using a carbide handheld glasscutter, washed with 100% ethanol, sonicated for 10 minutes and dried under nitrogen flow. Glass substrates were then put in plastic petri dishes, placed in an oxygen plasma cleaner (Harrick Plasma Cleaner, PDC-002, 230V) and exposed to high-pressure oxygen plasma for 5 minutes to functionalize their surfaces with hydroxyl groups.

3.5.3. Producing mixed SAMs of silanes using Chemical Vapor Deposition (CVD)

After removing the oxygen plasma-treated glass slides from the plasma cleaner, they were placed in a desiccator and droplets of TPFS and/or APTES were added in separately, reaching a total volume of 200 µL and placed beside the glass samples. After adding the proper amount of the silanes, the vacuum pump was turned on and the outlet valve of the desiccator was closed once a pressure of −0.08 MPa was reached in order to start the CVD process. Samples with three different ratios of 95% APTES (5% TPFS), 75% APTES (25% TPFS), and 50% APTES (50% TPFS) were prepared and samples containing 100% APTES or 100% TPFS were used as controls. The silanization reaction was carried out for 2 hours at room temperature. After the CVD step, glass slides were removed from the desiccator and placed in an oven at 60 ºC for a minimum of 12 hours in order to complete the reaction. Further, in order to ensure the removal of non-covalently attached silane molecules from the glass surfaces, they were sonicated for 10 minutes (VWR SympHony 97043-936 ultrasonic cleaner) and subsequently placed in a vacuum desiccator for 30 mins.

3.5.4. Producing mixed SAMs of silanes using Liquid Phase Deposition (LPD)

Glass slides were oxygen plasma treated as described above and then immediately incubated in a 50 mL plastic tube containing TPFS and/or APTES in anhydrous ethanol

solution (5% v/v). Similar to the CVD modification method, three different ratios of APTES and TPFS were prepared and samples made with 100% APTES or 100% TPFS were used as controls. The silane solutions containing the glass samples were stirred for 1 hour at room temperature and then the glass samples were removed from the solution, washed with 100% anhydrous ethanol and deionized water and ultimately 70% ethanol was used to complete the washing step. After drying the samples at room temperature, they were placed in the oven at 60ºC overnight for at least 12 hours. Similar to CVD treated samples, after removing the LPD treated glass slides from the oven, they were sonicated for 10 minutes and placed under vacuum for 30 mins in order to remove the non-covalently attached silane molecules.

3.5.5. X-ray photoelectron spectroscopy (XPS)

XPS was used to measure the surface chemical composition of the treated glass samples after CVD and LPD treatment. Three glass segments were used for each condition and means were determined. A Physical Electronics (PHI) Quantera II spectrometer equipped with an Al anode source for X-ray generation was used to record the XPS spectra (BioInterface Institute, McMaster University). XPS results were obtained at 45˚ take off angles with a pass energy of 280 eV. The atomic percentages of carbon, oxygen, fluorine and silicon was calculated using the instrument's software.

3.5.6. FITC labeling

Samples modified with the mixed silanes were further incubated with FITC in order to investigate the presence of APTES on the treated surfaces. A solution of 0.001 mg/mL FITC in carbonated buffer was prepared and 300 µL of the solution was added to each glass slide. Prior to adding the FITC solution on the glass samples, lubricant was added on samples that were prepared with both mixed ratios of TPFS and APTES in order to prevent physical adhesion of the FITC to the hydrophobic regions on the surface. Glass samples were incubated with the FITC solution overnight and they were washed with PBS and water after the incubation period. Samples were imaged using a Zeiss inverted fluorescent microscope (AX10) and the fluorescence intensity of FITC was quantified using ImageJ.

3.5.7. Water contact and Sliding angle measurements

In order to investigate the omniphobic slippery properties of the modified and control samples, their contact and sliding angles were measured using a 5 µL droplet of deionized water. Water sessile drop contact angle measurements were performed at room temperature using a Future Digital Scientific OCA20 goniometer (Garden City, NY). The contact angle goniometer was calibrated prior to each measurement.

Sliding angles were measured using a digital angle level (ROK, Exeter, UK). Prior to starting the measurements, silanized samples lubricated with PFPP were placed on the

calibrated level and a 5µL droplet of deionized water was placed on the glass surface. The level was gently angled until the droplet would start to move on the glass slide and the sliding angle was defined as the minimum angle required for droplets to start sliding on the glass substrate. For samples that the droplet failed to slide at angles of 90 degrees or higher, a sliding angle of 90 degrees was assigned. Measurements were performed on three different glass segments and means were determined.

3.5.8. Sliding angle and repellency measurements using human whole blood

The slippery and blood repellency properties of the optimized silane modified surfaces were measured using whole human blood. In this experiment, surfaces modified with 100% APTES, 75% APTES (25% TPFS), and 100% TPFS were tested and the results obtained from these surfaces were compared together. Initially, the surface area of the glass substrates was covered with a droplet of human blood and they were slowly tilted in order to force the blood droplet to slide off the glass substrates. In order to investigate the blood repellency properties and platelet adhesion, treated glass samples were incubated with citrated human whole blood and after initiating the clotting by adding $CaCl_2$, they were fixed in 4% formaldehyde and scanning electron microscope (SEM) was performed and the blood clot formation and blood cell attachment on these surfaces was investigated.

3.5.9. Surface functionalization using anti-CD34 or anti-CD144 antibodies

In order to make the silane modified surfaces biofunctional, samples with SAMs of mixed silanes or APTES were functionalized with anti-CD34 or anti-CD144 antibody using the carbodiimide crosslinker chemistry. Antibody solutions were prepared in 0.1 M MES buffer (1:500 dilution) and 2 mM EDC and 5 mM NHS was added in order to initiate the carbodiimide crosslinking reaction. Treated glass samples were placed inside the wells of a 48 well plate and in order to minimize the non-specific binding of the antibody, all samples that were modified with both TPFS were saturated with PFPP lubricant prior to adding the antibody solution. After removing the excess lubricant, each sample was incubated with 300 µL of the antibody solution for 2 hours at room temperature and later on incubated at 4 °C overnight. Samples were washed with PBS and DI water in order to remove the non-covalently attached antibodies and later on stored in PBS. All anti-body experiments were performed in the biosafety cabinet and samples were kept sterile.

3.5.10. Short and long-term cell experiments

After modifying the glass surfaces with unconjugated anti-CD34 or anti-CD144 antibodies, their biofunctionality and repellency properties were evaluated by investigating endothelial cell growth and attachment. Glass substrates that were placed in 48 well plates were incubated with 300 µL of RFP-HUVECs in cell media with a density of 1.5×10^5 cells/mL. Cell containing plates were placed in a 5% CO_2 incubator at 37 °C and samples were taken

out after 24 hours incubation time for short-term studies and after 5 days for long-term cell studies. In short-term cell studies, cells were washed with PBS x2 and imaged using a fluorescence microscope. In long-term cell studies, after washing the cells with PBS, adherent cells were fixed, permeabilized, blocked and stained with Alexa Fluor 488-conjugated VE-cadherin and Hoechst 33342 and imaged using a confocal microscope as further explained in the following sections. The potency of each surface for cell attachment and cell repellency was evaluated. Surfaces blocked using BSA, PLL-PEG or 100% TPFS with no lubricant were also investigated in short-term studies as controls and the results obtained from these surfaces were compared with other treated surfaces. Cell adhesion was also investigated in human whole blood. Modified surfaces were incubated with a cell/blood mixture for 24 hours and the same procedure as described above was used to evaluate the biofunctionality and repellency properties of the surfaces and their ability to capture cells from the blood/media mixture.

3.5.11. Plasma clotting assay with/without FITC-fibrinogen

Plasma clotting assay with/without FITC-fibrinogen was performed on glass substrates treated with the mixed silanes in order to investigate their anticoagulant properties and to see whether mixing the APTES and TPFS will compromise the anticoagulant properties of these surfaces. Based on the results obtained from initial experiments, 75% APTES (25% TPFS) was chosen as the optimized ratio between the two silanes and clotting assays were performed on this group of samples. The clotting time results and FITC-fibrinogen adhesion obtained from this group was compared to non-treated glass slides, samples treated with 100% TPFS and control substrates.

Treated and control glass slides were horizontally placed on the bottom of a 96 well plate and 100 µL aliquots of citrated human plasma were added to each well. In fibrinogen experiments, prior to adding the plasma to the samples, FITC conjugated fibrinogen (50 µg/ml) was added to the plasma solution and samples were incubated with plasma containing fibrinogen. Samples treated with TPFS were lubricated prior to adding the clotting media. After adding the citrated plasma to the wells, the plate containing the glass samples was incubated at 37 °C for 10 minutes and clotting was initiated by adding 100 µL of 20 mM HEPES (pH 7.4) containing 1M $CaCl_2$, yielding a final $CaCl_2$ concentration of 12.5 mM. Clot formation was assessed by monitoring absorbance at 405 nm at 10-sec intervals for 60 min using a SpectraMax plate reader (Molecular Devices). Clotting times were defined as the time to reach half-maximal absorbance and calculated by the instrument software from plots of absorbance *versus* time. In fibrinogen studies, after the clotting assay, samples were washed with PBS x2, fixed with 4% formaldehyde and imaged using

a fluorescence microscope. The fluorescence intensity of the FITC-fibrinogen adhered to the substrates was calculated using ImageJ.

3.5.12. Platelet adhesion on modified surfaces

Platelet adhesion was investigated using fluorescence imaging. Substrates were incubated with human platelets (1 mL of 1 x 10^8 platelet suspension in Tyrode's buffer) and the platelets were activated by adding 0.2 U/mL human thrombin in 2 mM $CaCl_2$. Samples were incubated with the platelet solution for 45 minutes, washed with PBS x2 and fixed with 2% formaldehyde in PBS prior to imaging. Later, activated, adherent platelets were stained using FITC-PAC1 antibody (platelet-activated marker, green), and platelet adhesion was directly visualized using fluorescence microscopy and the number of platelet/mm^2 was quantified using ImageJ.

3.5.13. Immunofluorescence staining with VE-cadherin and Hoechst 33342 nucleic acid staining

After incubating the anti-CD34 and anti-CD144 functionalized surfaces with HUVECs for 5 days, surfaces were washed twice with pre-warmed PBS and fixed with 4% methanol-free formaldehyde for 20 minutes. After removing the formaldehyde solution and washing the cells with PBS, adherent cells were permeabilized with 0.1% Triton in PBS for 15 minutes and blocked with BSA in PBS for 30 minutes to prevent non-specific binding. Subsequently they were stained with Alexa Fluor 488-conjugated VE-cadherin (green) and Hoechst 33342 nucleic acid stain (blue). After finishing the staining process, samples were washed with PBS and imaged using a confocal microscope (Zeiss LSM510 confocal laser scanning microscope).

3.5.14. Live/Dead cell viability assay

Cell viability was assessed using the live/dead cell viability assay kit after 6 days of cell culture. According to the manufacturer's instructions, cells were incubated with the live (NucBlue® Live reagent) and dead (NucGreen® Dead reagent) stains for 15 minutes and imaged using a fluorescence microscope. Cell viability was calculated by counting total vs dead cells using ImageJ.

3.5.15. *In vitro* cytotoxicity against RFP-HUVECs – MTT assay

RFP-HUVECs were grown in cell media and seeded with a density of 1.5 x 10^4 cells/mL in a 96 well plate. After 48 hours of culture, 300 µL fresh media and 30 µL of 12 mM MTT solution in PBS was added to each well and the well plate was incubated for an additional 4 hours at 37 °C. Subsequently, 150 µL DMSO was added to 75 µL of each well to dissolve the formazan crystals. Absorbance was measured at 570 nm wavelength on a SpectraMax plate reader. All measurements were repeated in triplicate.

3.5.16. Statistical analysis

All data are presented as means ± S.D. Each experiment condition was repeated at least three times. To access statistical significance between different groups, one-way analysis of variance (ANOVA) followed by post hoc analysis using Tukey's test was performed. P values less than 0.05 were considered statistically significant for all comparisons.

3.6. Supplementary Information

The Supporting movies referenced in the main body of the chapter are available on the ACS Publications website at DOI: 10.1021/acsnano.8b03938.

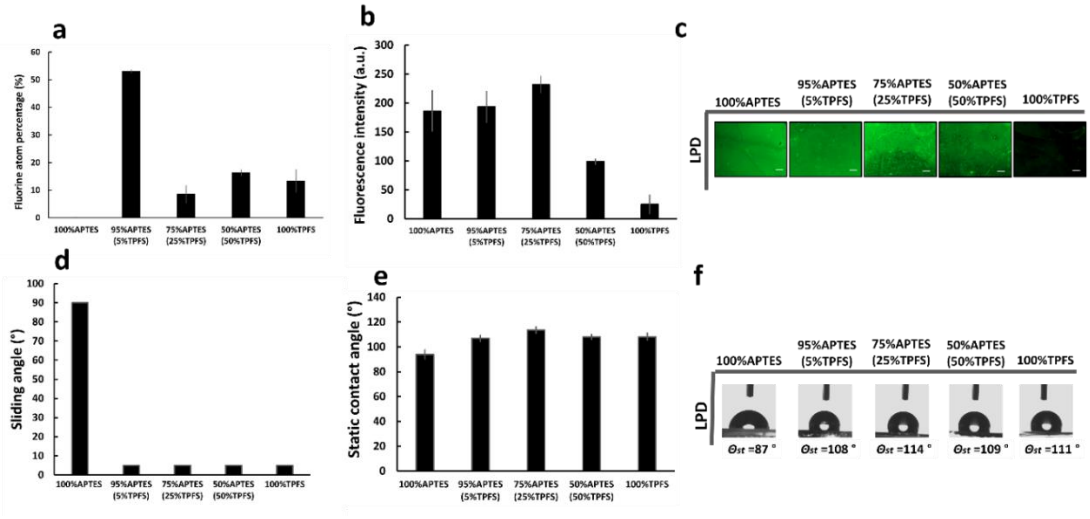

Supplementary Figure 3.1 Assessing the chemical composition and the omniphobic slippery properties of the modified surfaces using LPD. (a) Samples treated with different ratios of APTES and TPFS were analyzed using XPS and the fluorine atom % was calculated. In the LPD treated samples, no relationship was seen between the amount of TPFS used in the reaction and the atom % of fluorine measured by XPS. **(b)** The presence of APTES on surfaces treated with APTES and TPFS or 100% APTES was evaluated using fluorescence microscopy after labeling them with FITC. In the LPD treated samples, there was no correlation between the FITC fluorescence intensity and the amount of APTES used in the modification step. **(c)** Representative fluorescent images of FITC labeled surfaces. **(d)** Sliding angle and **(e)** contact angle measurements were performed in order to evaluate the omniphobic slippery properties of the treated surfaces. Samples treated with 100% TPFS or mixed ratios of APTES and TPFS, had sliding angles as low as 5 degrees and contact angles higher than 100 degrees. **(f)** Representative contact angle images of a 5 µL water droplet on treated glass surfaces before adding the lubricant coating. Bars show the means ± SD of at least three samples. The magnification bars on the fluorescence images are 100 µm.

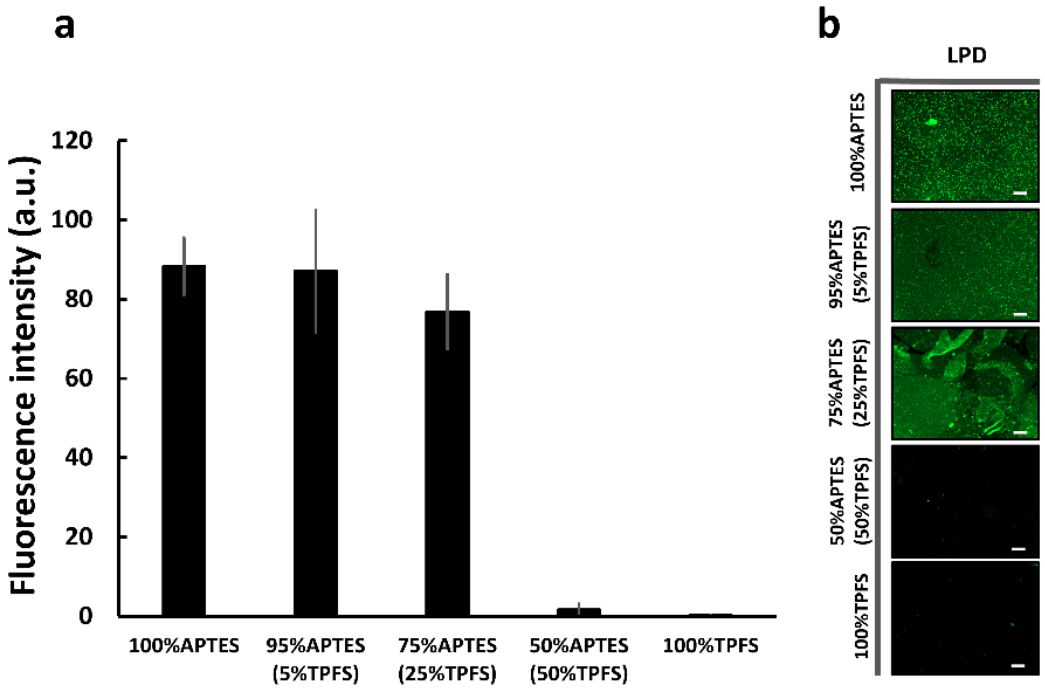

Supplementary Figure 3.2 Anit-CD34 antibody immobilization on LPD treated samples. (a) Samples treated with 100% APTES, mixed APTES and TPFS using the LPD method were biofunctionalized using fluorescently labeled anti-CD34 antibody. Similar to the results obtained from the FITC labeling experiments samples treated with 50% APTES (50% TPFS) did not show surface functionality compared to other samples treated with mixed silanes. Samples treated with 100% TPFS prevented non-specific adhesion of the antibody. **(b)** Representative fluorescent images of anti-CD34 functionalized surfaces are shown. Bars show the means ± SD of at least three samples. The magnification bars on the fluorescence images are 100 μm.

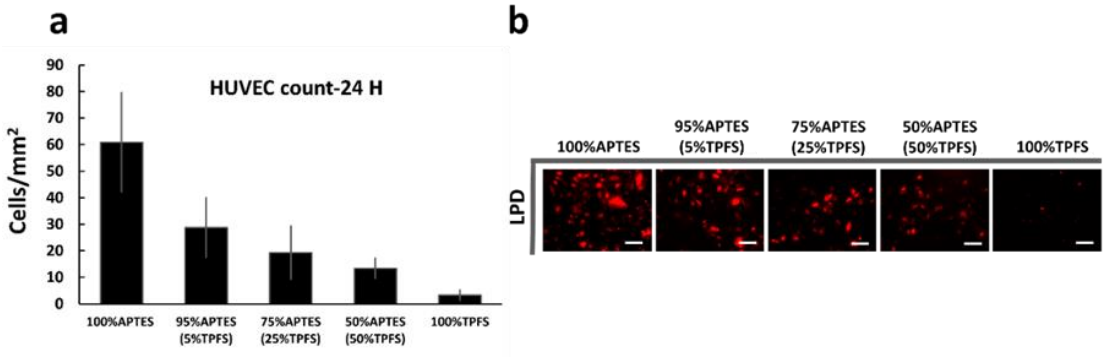

Supplementary Figure 3.3 Investigating the RFP-HUVECs adhesion and interaction with LPD silanized, anti-CD34 functionalized surfaces. (a) Treated surfaces were incubated with RFP-HUVECs for 24 hours and the cell adhesion and growth was investigated. All surfaces treated with TPFS were lubricated prior to starting the experiments. Cell attachment was decreased by decreasing the APTES:TPFS ratio. Cell count per surface area was highest in 100% APTES samples. 100% TPFS samples showed minimum amount of cell attachment, confirming the repellency and omniphobic slippery properties of these surfaces. **(b**) Representative fluorescence images of surfaces incubated with RFP-HUVECs for 24 hours. Bars show the means ± SD of at least three samples. The magnification bars on the fluorescence images are 20 µm.

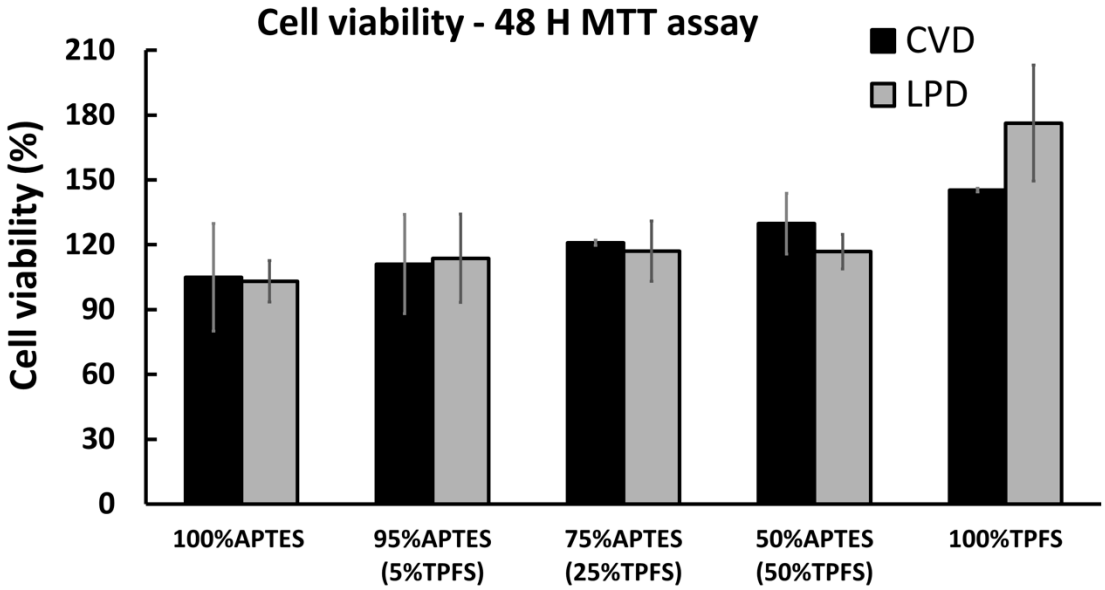

Supplementary Figure 3.4 *In vitro* cytotoxicity of silanized glass substrates incubated with RFP-HUVECs for 48 h. The cytotoxicity of the CVD and LPD treated surfaces was evaluated using the MTT assay after 48 hours of incubating the treated surfaces with RFP-HUVECs. No decrease in cell viability was observed upon exposing RFP-HUVECs to the silanized and control samples. Bars show the means ± SD of at least three samples.

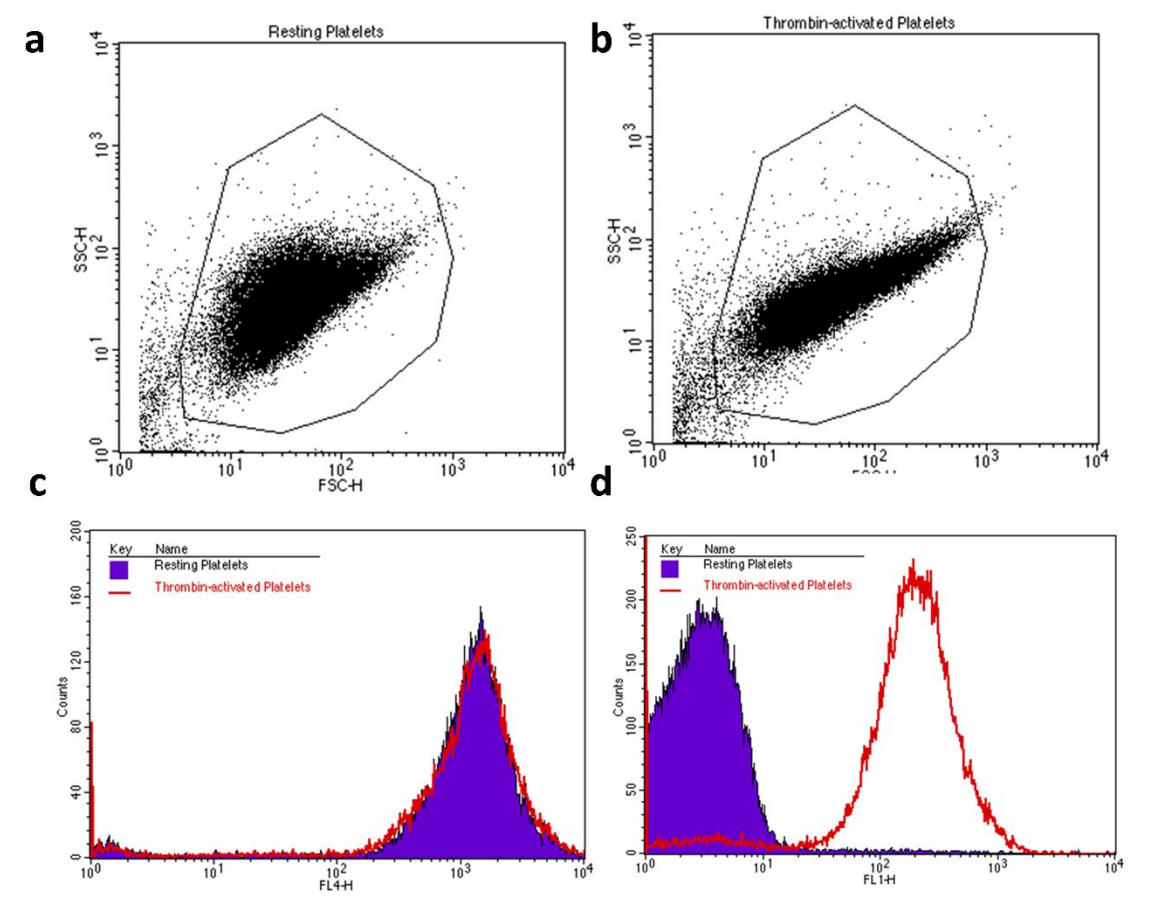

Supplementary Figure 3.5 Flow cytometry results of activated and resting platelets. (a) and **(b)** show the FSC&SSC comparison of resting and activated Platelets. **(c)** DiD binding to resting and activated Platelets. (**d**) FITC-PAC1 binding to resting and activated platelets. FITC-PAC1 did not bind to resting platelets and only activated platelets were conjugated to the antibody.

Chapter 4 *Lubricant-infused vascular grafts functionalized with silanized bio-inks suppress thrombin generation and promote endothelialization*

Preface

This study focuses on developing a novel and simplified modification technique for creating BLIS on ePTFE vascular grafts using silanized bio-inks. This study reports a technique that streamlines the modification procedure required to create functional BLIS and results in surfaces with excellent repellency properties and targeted-binding features. The created BLIPS were examined for their blood compatibility and ability to capture endothelial cells from human whole blood. The designed BLIPS were able to attenuate thrombin generation, blood clot formation and prevent protein and bacterial adhesion. In addition, the reported surfaces were able to effectively promote targeted binding and capture of endothelial cells from human whole blood.

Citation:

This research has been submitted to *Advanced Healthcare Materials.* Manuscript ID: adhm.201900753.

M. Badv, C. Alonso-Cantu, A. Shakeri, Z. Hosseinidoust, J. I. Weitz, T. F. Didar, "Lubricant-infused vascular grafts functionalized with silanized bio-inks suppress thrombin generation and promote endothelialization"

Relative Author Contributions

I prepared the samples, performed all experiments (except for the bacterial adhesion studies) and analyzed the data. The manuscript was written by myself and subsequently edited by my academic supervisor Dr. T. F. Didar, Dr. J. I. Weitz and Dr. Z. Hosseinidoust. C. Alonso-Cantu performed the bacterial adhesion studies. XPS measurements were done at the BioInterface Institute at McMaster University. The SEM was carried out at the Electron Microscopy Facility in the Health Science Centre at McMaster university. Marcia Reid from the Electron Microscopy Facility at McMaster is acknowledged for her great help and guidance in preforming the SEM imaging.

Note to Reader:

A supplementary section containing the additional figures and information referenced in the chapter is included at the end of the chapter.

4.1. Abstract

The ongoing problem with the thrombogenicity and poor tissue integration of synthetic vascular grafts demands the design of new surfaces that simultaneously suppress thrombosis and promote endothelialization. Lubricant-infused surfaces exhibit outstanding performance in preventing clot formation; however, their innate ability to completely block the surface, averts targeted binding of desired biomolecules. We report a new class of lubricant-infused expanded polytetrafluoroethylene (ePTFE) vascular grafts that prevent blood coagulation and concurrently promote endothelial cell adhesion. This is achieved by direct silanization of endothelial-specific ligands and subsequent conjugation of the silanized ligands to the ePTFE surface. Therefore, unlike conventional methods, we eliminated the need to chemically modify the ePTFE surface with a coupling agent, and as a result preserved the innate surface property of the ePTFE substrate. This is crucial for infiltrating the fluorine-based ePTFE substrate with a biocompatible lubricant and ultimately creating a functional and stable lubricant-infused layer. Compared to commercially available grafts and the ones coated using conventional methods, our developed grafts significantly attenuate thrombin generation and promote endothelialization in human whole blood.

4.2. Introduction

Cardiovascular disease, including heart attack and stroke, is the number one cause of death and disability worldwide, accounting for at least one-third of all deaths each year [34], [266], [267]. Ischemic cardiovascular diseases such as coronary and peripheral artery diseases, caused by atherosclerosis (plaque buildup inside arteries), are responsible for more than half of these deaths.[12] Expanding atherosclerotic plaques compromise blood flow and plaque rupture and superimposed thrombosis causes arterial occlusion [265]. Maneuvers to open blocked arteries include angioplasty and stenting, or endovascular or surgical bypass grafting [265]. Although the use of autologous vessels remains the standard of care, more than one third of the patients do not have available or suitable vessels [17], [18], due to pre-existing vascular diseases or prior vascular surgeries [19]–[21]. This shortage in viable autologous vessels has led to the development and utilization of synthetic graft alternatives constructed from synthetic polymers such as ePTFE [17], [268]. Vascular grafts, especially those of small diameter, are prone to occlusion because of thrombosis and neointimal hyperplasia [16], [77]. Thrombosis on the luminal surface of vascular grafts compromises blood flow and hinders coverage by endothelial cells [18]. Such coverage is critical for long-term graft patency because of the antithrombotic properties of endothelial cells [16], [267]. Hence, the development of ePTFE vascular grafts that are both antithrombotic and promote endothelial cell adhesion and growth is of great interest.

Anticoagulant, blood compatible vascular prostheses have been developed with immobilized heparin [29]–[34], synthetic or natural polymers such as poly (ethylene glycol) (PEG) [25]–[27], zwitterionic polymers [241], [242], poly-sulfobetaine [83], [217], bovine serum albumin (BSA) [240] and human albumin [221]. These surfaces show promising results but suffer from limitations such as depletion, degradation and loss of anticoagulant properties over time [23], [181]. Furthermore, the excessive hydrophilicity of some of these coatings has shown to limit the formation of an endothelial layer [54].

Immobilized lubricant-infused layers provide a highly effective and stable approach for elimination of non-specific adhesion of proteins and cells onto surfaces [174], [175], [177], [178], [181], [182], [185], [188]. Such surfaces are synthesized by chemically modifying the substrate with a perfluorosilane monolayer and infiltrating the silane layer with a biocompatible perfluorocarbon lubricant [174]. The strong intermolecular interactions between surface fluorine molecules and the lubricant layer creates a stable, slippery omniphobic lubricant-infused substrate [174], [179], [249]. Substrates of ePTFE, a synthetic fluorocarbon-based polymer composed of tetrafluoroethylene (C_2F_4) monomer chains [54], eliminate the need for a perfluorosilane monolayer and can be saturated with a fluorinated lubricant such as perfluoroperhydrophenanthrene (PFPP) to generate lubricant-infused surfaces that resist non-specific adhesion and repel bacteria, thereby reducing the risk of device-associated infection [175]. Despite the advantages of lubricant-coated ePTFE surfaces in preventing non-specific adhesion, they suffer from the same drawback of other repellent surfaces and blindly prevent all biomolecules from interacting with the surface and as a result avert targeted binding of endothelial cells. This is problematic for ePTFE vascular grafts since promoting endothelial cell adhesion is crucial in order to prevent thrombosis and to accelerate endothelialization and tissue integration of the implant [50], [67]. Therefore, additional surface modification steps are required to render non-silanized ePTFE surfaces both biocompatible and biofunctional in terms of promoting endothelial cell deposition, without interrupting the lubricant-infused layer.

Limited progress has been made in integrating both blood biocompatibility and endothelialization on lubricant-infused surfaces [40]. Generating SAMs using silane coupling agents such as 3-aminopropyltriethoxy-silane (APTES) [35], [37], [67], [74] and utilizing the functional terminal for covalent bonding of biomolecules is a widely used method for creating biofunctional platforms [75], [250]. However, this chemical modification technique results in coating the entire binding surface with the silane coupling agent and ultimately changing the surface chemical properties of the substrate [89]. This is particularly troublesome for creating non-silanized, lubricant-infused ePTFE substrates,

since the presence of the surface fluorine layer is crucial to stabilize and lock-in the liquid lubricant onto the surface.

In this study, we introduce a new class of ePTFE vascular grafts developed using a one-step, top-down approach to create biofunctional lubricant-infused ePTFE surfaces (BLIPS). This is achieved by first, functionalizing the endothelial cell specific protein (anti-CD34 antibody) with the APTES coupling agent in solution, followed by purification of the produced APTES-protein complex and then covalently attaching silanized anti-CD34 antibodies (CD34-APTES) to the hydroxyl-terminated ePTFE surface. This approach simplifies the currently available surface modification techniques and obviates the need for chemically modifying the entire ePTFE substrate with a coupling agent and/or other adhesive polymers in order to covalently attach the biomarker. As a result, the proposed method retains the surface chemical properties of the ePTFE surface, which is crucial for stabilizing the lubricant layer and creating a biofunctional lubricant-infused ePTFE substrate. Further, the physical and chemical properties, biofunctionality and hemocompatibility of the BLIPS were evaluated and compared with lubricated (L) and non-lubricated (NL) control ePTFE (Control-L and Control-NL respectively) and CD34 functionalized, lubricated and non-lubricated ePTFE surfaces modified using the conventional technique. Compared with these surfaces, BLIPS exhibit significantly enhanced capacity to suppress thrombin generation and effectively promote endothelial cell adhesion in whole blood.

4.3. Results

4.3.1. Creating biofunctional lubricant-infused ePTFE substrates (BLIPS)

To create BLIPS (***Figure 4.1d***), medical grade ePTFE vascular grafts were first oxygen plasma treated to generate hydroxyl functional groups on their surfaces. Biofunctional ePTFE substrates were then created by incubating the hydroxyl activated ePTFE substrates with APTES silanized anit-CD34 antibody solution (CD34-APTES). In contrast to existing methods for creating biofunctional substrates, in which the substrate is entirely coated with one or several coupling agents, in our novel approach, the focus was shifted to the antibody and the carboxyl groups (COOH) present on the antibody were functionalized with the APTES coupling agent by the carbodiimide cross-linker chemistry. For comparison, ePTFE substrates were also biofunctionalized using conventional modification techniques (***Figure 4.1c***) wherein APTES-SAMs were created on the oxygen plasma treated ePTFE substrates using chemical vapour deposition (CVD) and activated using EDC/NHS carbodiimide crosslinking chemistry. The anti-CD34 antibody was then immobilized on the APTES-treated ePTFE substrate (APTES-SAM-CD34). Surfaces from both groups were lubricated with PFPP lubricant prior to use and results were compared with non-lubricated

biofunctional surfaces and lubricated and non-lubricated control ePTFE substrates (***Figure 4.1a*** and ***b***).

Oxygen plasma-treated surfaces exhibited a significantly higher ($P = 0.003$) oxygen atomic percentage (at%) compared with control ePTFE substrates (7.7 ± 0.9 and 0.1 ± 0.1 % respectively), as confirmed by X-ray photoelectron spectroscopy (XPS) (***Figure 4.2*****a** and **b**). Oxygen plasma treatment resulted in a non-significant reduction in the fluorine at% compared with control (66.7 ± 0.6 and 50.8 ± 2.5 respectively). In contrast, APTES-SAM treated ePTFE surfaces showed significantly lower fluorine at% on their surface (17.1 ± 6.7) compared with control substrates and oxygen plasma treated surfaces ($P < 0.03$). The fluorine/carbon (F/C) ratio was significantly lower ($P < 0.02$) on APTES-SAM treated surfaces (0.4 ± 0.2) than on control (2.0 ± 0.1) or plasma treated samples (1.2 ± 0.1).

The ePTFE substrates with the PFPP lubricant exhibited a significant decrease in sliding angles over the bare ePTFE surface, showing an average sliding angle of 14.2 ± 1.9 degrees (***Figure 4.2c***). After oxygen plasma treatment, the ePTFE substrates sliding angles increased to 26.5 ± 5.1 degrees. Droplets did not slide on lubricant infused APTES-SAM surfaces and these surfaces did not show slippery properties (***Figure 4.2c***), similar to non-lubricated control ePTFE samples. Both control and oxygen plasma treated surfaces exhibited hydrophobic properties and had static contact angles higher than 100 degrees (115.4 ± 2.8 and 105.2 ± 7.1 respectively). In contrast, APTES-SAM treated surfaces, were hydrophilic and exhibited an average static contact angle of 77.4 ± 9.2 degrees (***Figure 4.2d***).

Biomolecule silanization procedure was optimized and evaluated using BSA as a model protein and APTES conjugation was assessed using mass spectrometry (MS). Silanized BSA-APTES molecules were prepared, dialyzed and lyophilized. As illustrated in ***Supplementary Figure 4.1***, the mass spectra obtained from standard and silanized BSA-APTES powder showed a shift in molecular mass with silanized BSA-APTES compared with non-modified BSA (68105 m/z and 67010 m/z respectively), which indicates successful covalent attachment of APTES molecules to BSA. A similar procedure was then used for silanizing CD34 antibody and creating CD34-APTES functionalized ePTFE surfaces. To evaluate the stability of the biofunctionalized surfaces, CD34 treated surfaces were subjected to multiple washing steps in 1% Tris-buffered saline tween (TBST) over a 2-week period. The fluorescence images revealed the presence and stability of the anti-CD34 antibody on both APTES-SAM-CD34 and CD34-APTES treated samples after 2 weeks of incubation in 1% TBST and no significant decrease in fluorescence intensity was observed on these surfaces. However, there was a significant decrease in the fluorescence intensity of samples coated with the antibody through physical adsorption ($P < 0.05$, ***Figure***

4.2f). Control, APTES-SAM-CD34, and CD34-APTES treated surfaces exhibited similar surface topography and structure on SEM analysis and there were no obvious differences between treated surfaces and control ePTFE samples (***Figure 4.2e***).

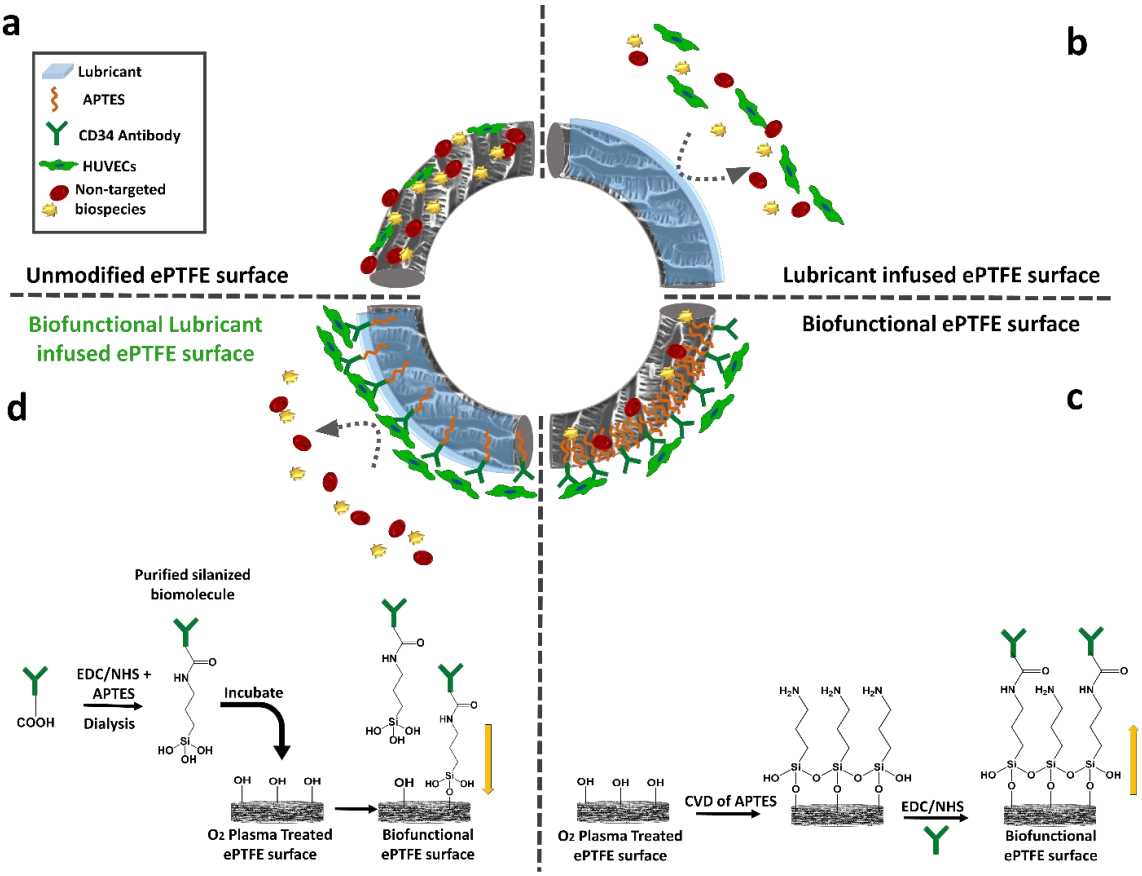

Figure 4.1 Schematic representation of the different modification steps on the ePTFE surface. **(a)** Control ePTFE grafts. Untargeted biospecies attach to unmodified ePTFE surfaces and these surfaces do not show anticoagulant or blocking properties. (**b)** Lubricant-infused ePTFE grafts. When lubricating the ePTFE control substrates, a lubricant-infused surface can be obtained that both prevents specific and non-specific adhesion of cells and biospecies. (**c)** APTES-CVD treated surfaces biofunctionalized with anti-CD34 antibody. The ePTFE surfaces are functionalized using the conventional technique were the substrate is completely coated with APTES (the coupling agent) using CVD and further, the CD34 antibody is immobilized on the surface. These surfaces promote endothelial cell adhesion but do not have blocking properties. (**d)** Biofunctional lubricant-infused ePTFE substrates (BLIPS). ePTFE surfaces are oxygen plasma treated and functionalized with CD34-APTES antibodies and infiltrated by a lubricant layer. The BLIPS prevent non-specific adhesion and promote specific binding of endothelial cells.

4.3.2. ePTFE-induced thrombin generation

To investigate the anti-thrombotic properties of the biofunctional and/or lubricant-infused surfaces, thrombin generation was performed in the absence (background) or presence of

lubricated and non-lubricated control and lubricated and non-lubricated APTES-SAM-CD34 and CD34-APTES treated ePTFE samples (***Figure 4.3a*** and ***b***). Lubricant-infused ePTFE substrates, functionalized with silanized anti-CD34 antibody (CD34-APTES-L) significantly prolonged the lag time and time to peak thrombin ($P < 0.001$) and significantly reduced peak thrombin, velocity index and endogenous thrombin potential (ETP) compared with non-modified control, APTES-SAM-CD34-L and APTES-SAM-CD34-NL, and CD34-APTES-NL treated surfaces ($P < 0.001$). In fact, biofunctional lubricant-infused CD34-APTES-L surfaces suppressed thrombin generation to background levels. In contrast, all other treated groups and control samples significantly increased thrombin generation above the background.

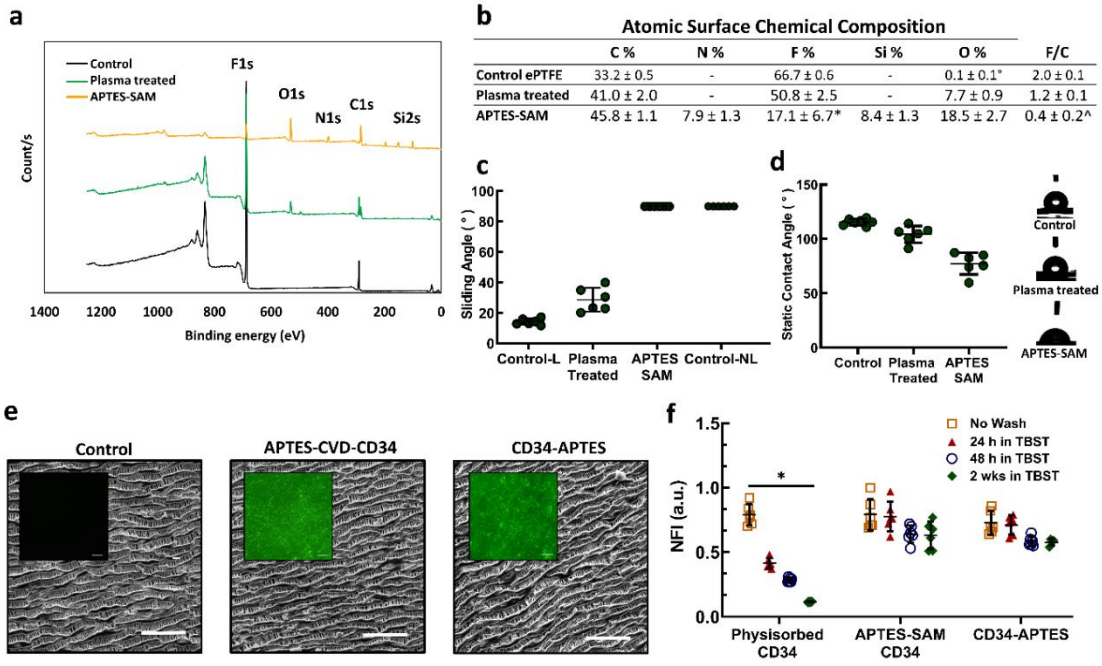

Figure 4.2 The surface chemical composition and the physical properties of the control and modified surfaces. (a) A representative graph and **(b)** the corresponding table of the surface at% of different elements present on the ePTFE substrate before and after each modification step. After oxygen plasma treating the ePTFE grafts for 5 minutes, the at% of the oxygen increased significantly compared with control ePTFE (°P=0.003), which indicates the presence of hydroxyl functional groups on ePTFE grafts. No significant difference was seen in the fluorine at% of oxygen plasma treated surfaces when comparing the results with the control ePTFE grafts. In contrast, when adding the APTES monolayer, the amount of surface fluorine significantly decreased compared with control and oxygen plasma treated surfaces (*P < 0.03). The at% of nitrogen (N) and silicon (Si) confirm the presence of APTES on the surface. In addition, the F/C ratio was significantly lower in APTES-SAM surfaces compared with control and oxygen plasma treated substrates (^P < 0.02). **(c)** Sliding angle and (**d)** contact angle results of unmodified, oxygen plasma treated and APTES treated surfaces. (**e)** Fluorescence microscopy and SEM was performed on anti-CD34 treated surfaces in order to confirm the binding of the antibody to the ePTFE surfaces and to investigate the morphology of the surface after each modification step. Scale bars are 100 µm on both fluorescent and SEM images. (**f)** The stability and covalent attachment of the CD34-APTES

and APTES-SAM-CD34 was confirmed by washing the substrates and incubating them with 1% TBST for up to 2 weeks. In contrast to CD34-APTES and APTES-SAM-CD34 surfaces, the fluorescence intensity of physiosorbed antibodies significantly decreased during the washing steps (*P < 0.05).

The potency of the lubricant layer in reducing thrombin generation was observed when comparing the lubricated and non-lubricated results in CD34-APTES treated groups. CD34-APTES-L samples significantly prolonged the lag time, time to peak thrombin and reduced peak thrombin and ETP compared with nonlubricated CD34-APTES samples. In contrast, thrombin generation with lubricated and nonlubricated APTES-SAM-CD34 treated samples was similar (***Figure 4.3a*** and ***b***).

a

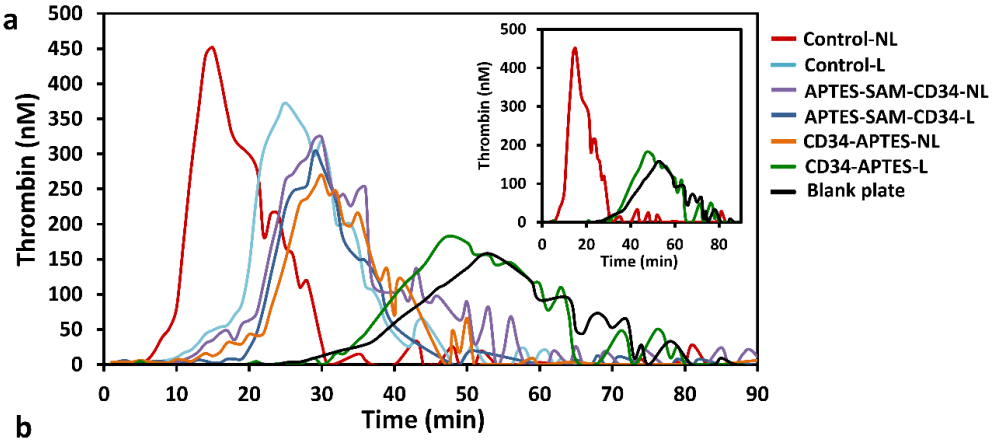

b

Parameter/Condition	Lag Time (min)	Peak Thrombin (nM)	Time to Peak Thrombin (min)	Velocity Index (nM/min)	ETP (nM.min)
Control-NL	8.2 ± 0.9$^{*‡θ°}$	443.2 ± 36.6$^{*‡¥°}$	14.9 ± 2.5$^{*‡°}$	74.9 ± 25.3$^{*‡¥°}$	7190.1 ± 561.6*‡
Control-L	12.9 ± 1.9*‡	357.9 ± 36.4*‡	21.3 ± 5.8*‡	45.0 ± 17.9*‡	6877.1 ± 658.2*‡
APTES-SAM-CD34-NL	13.4 ± 4.3*‡	337.8 ± 90.3*‡	25.0 ± 11.5*‡	48.2 ± 34.1*‡	6340.2 ± 718.8^{ǁ‡}
APTES-SAM-CD34-L	19.8 ± 4.0*‡	300.1 ± 39.5*‡	33.3 ± 10.2*‡	33.6 ± 22.2^{Λ}	6379.6 ± 715.5^{ǁ‡}
CD34-APTES-NL	14.8 ± 3.3*‡	330.8 ± 80.6*‡	27.8 ± 8.8*‡	34.9 ± 21.1^{Λ}	6601.2 ± 716.3*‡
CD34-APTES-L	25.6 ± 4.7	195.4 ± 53.4	49.5 ± 12.6	11.3 ± 7.4	5410.2 ± 627.0
Blank Plate	27.4 ± 5.7	165.9 ± 34.7	48.9 ± 7.8	8.3 ± 3.0	4185.6 ± 604.7

Figure 4.3 Effect of different modification techniques on ePTFE-induced thrombin generation. (a) A representative thrombin vs. time plot is shown. (**b)** Thrombin generation parameters were determined in empty wells or wells containing control or modified ePTFE surfaces. Values represent means ± SD of at least 12 samples. CD34-APTES-L treated surfaces significantly suppressed thrombin generation compared to control and other treated groups. *P < 0.001 and ^{ǁ}P < 0.05 compared with CD34-APTES-L. ‡P < 0.001 and ^{Λ}P < 0.05 compared with Blank plate. $^{¥}$P < 0.008 and ^{θ}P < 0.05 compared with Control + L. °P < 0.005 compared with APTES-SAM-CD34- L, NL and CD34-APTES-NL.

In addition to the lubricant, the anti-CD34 antibody with or without the lubricant layer significantly suppressed thrombin generation compared with nonlubricated control samples. Samples functionalized with anti-CD34 antibody significantly reduced peak

thrombin and velocity index ($P < 0.005$) and significantly prolonged the lag time and time to peak thrombin compared with Control-NL samples ($P < 0.005$) (***Figure 4.3a*** and ***b***).

4.3.3. Blood cell and bacterial repellency properties of control and modified ePTFE surfaces

The repellency and blocking properties of the control and coated surfaces were investigated by incubating the ePTFE substrates with re-calcified human whole blood or *Staphylococcus aureus* MW2 (***Figure 4.4***). In the blood clotting experiments, based on visual investigation and changes in sample weights, CD34-APTES-L samples induced the least blood clot formation compared with control and other treated groups (***Figure 4.4a*** and ***b***). In addition, based on SEM analysis there was less protein and blood cell adhesion to CD34-APTES-L than to the other surfaces (***Figure 4.4c***). In contrast, protein and blood clot deposition on Control-NL samples was greater than that on Control-L and lubricated and non-lubricated CD34-APTES and APTES-SAM-CD34 samples and the SEM images revealed the formation of a dense clot layer with adherence of large amounts of blood cells on Control-NL surfaces. In keeping with the thrombin generation data, the addition of the lubricant layer did not significantly affect the anticoagulant and repellency properties of APTES-SAM-CD34 samples nor did it affect the clot mass or blood cell adhesion. However, when comparing the lubricated and non-lubricated samples from the control and CD34-APTES treated groups, adding the lubricant layer significantly decreased clot mass, and protein and blood cell adhesion on these surfaces. In addition, the presence of the anti-CD34 antibody significantly reduced blood clot formation and cell adhesion. Samples treated with the antibody using both modification techniques had significantly less blood clot and blood cells adhered to their surfaces when compared to Control-NL samples (***Figure 4.4***).

Adding a lubricant layer significantly decreased bacterial adhesion compared with the non-lubricated samples in the control groups (ePTFE with no APTES or CD34) (***Figure 4.4d***). Coating the ePTFE surfaces with the CD34-APTES-L layer created surfaces that were essentially bacteria-repellent, showing no bacterial attachment and, upon longer incubation, no biofilm formation. However, lubricating ePTFE surfaces that were coated with APTES-SAM-CD34 completely compromised bacterial repellency and significantly more bacteria adhered to those surfaces compared with lubricated or non-lubricated ePTFE or lubricated surfaces coated with CD34-APTES (***Figure 4.4d***), demonstrating another superior property offered by our novel surface functionalization method.

4.3.4. Short-term cell studies - Bioactivity and endothelial cell capture

In short-term studies, human umbilical vein endothelial cells (HUVECs) were incubated with cells for 24 h and cell capture and adhesion were investigated. As seen in ***Figure 4.5***, Control-L samples blocked the ePTFE surfaces, significantly inhibited cell adhesion and

growth compared with Control-NL samples (0.8 ± 0.5 and 9.6 ± 1.6 cell/mm^2 respectively; P = 0.006). Control-NL ePTFE surfaces showed significantly less cell adhesion compared with lubricated and non-lubricated CD34-APTES surfaces and lubricated APTES-SAM-CD34 surfaces. As seen in the fluorescence and SEM images (***Figure 4.5a*** and ***b***), cells were individually adherent to the Control-NL surfaces and assumed a spherical shape, whereas cells adherent to anti-CD34 functionalized surfaces were elongated and well spread. Addition of the lubricant layer enhanced cell spreading on the CD34 functionalized, APTES-SAM-CD34-L and CD34-APTES-L surfaces compared with non-lubricated surfaces.

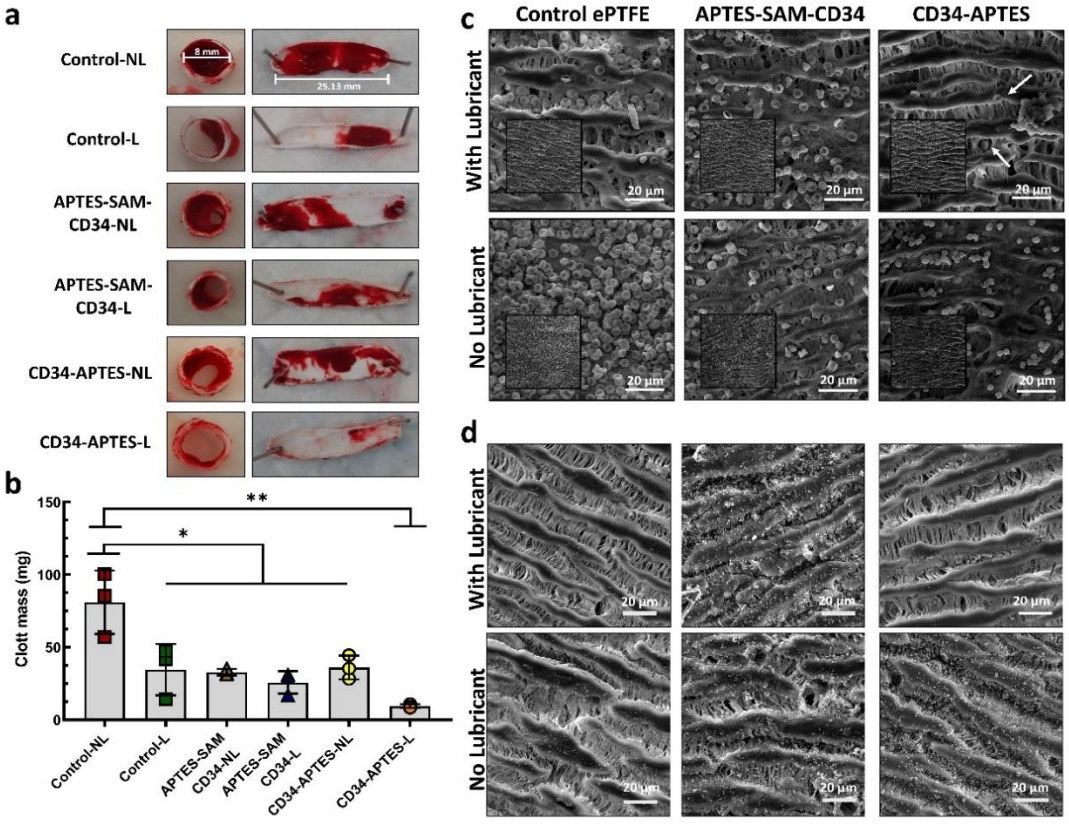

Figure 4.4 Blood clot formation and bacteria and blood cell adhesion on modified and control ePTFE surfaces. (a) Images of blood clot formation and adhesion on ePTFE vascular grafts incubated with human whole blood. (**b)** Human whole blood clot mass attached to modified and control ePTFE grafts. BLIPS had significantly less blood clot adhered to their surfaces compared to other treated and control groups. (**c)** SEM images of ePTFE grafts, after the human whole blood clotting experiment. (**d)** SEM images of bacteria adhesion and biofilm formation studies on control and treated ePTFE surfaces. Bars show means ± SD of at least three samples. *P < 0.05 and **P < 0.005.

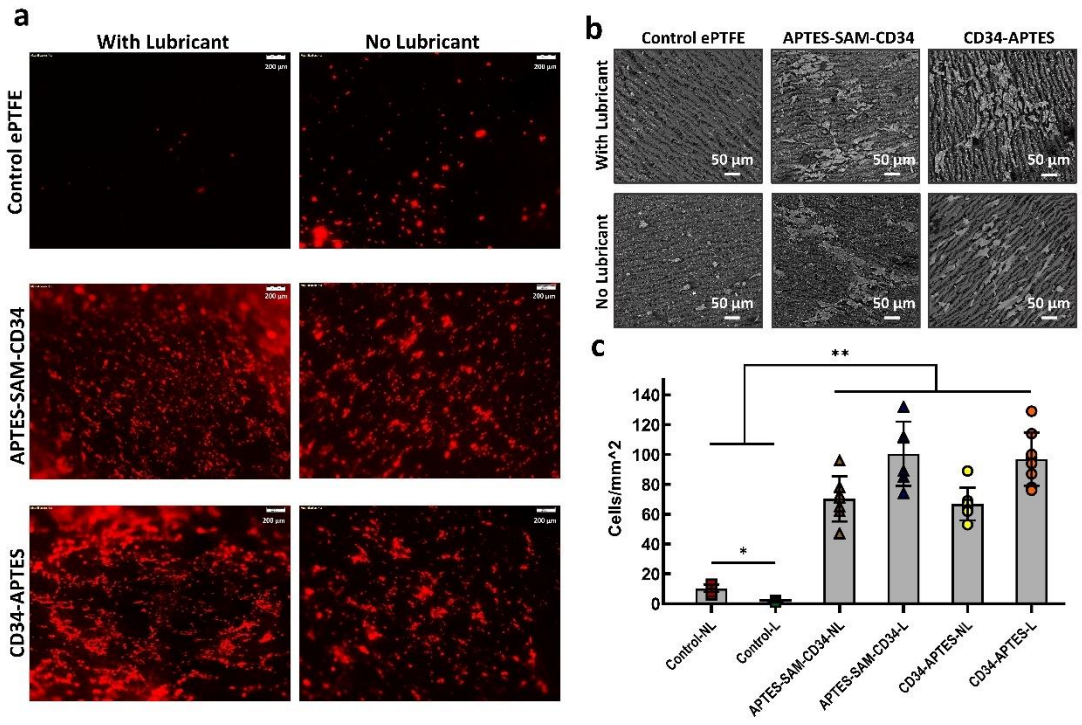

Figure 4.5 Short-term endothelial cell studies on control and CD34 modified surfaces. (a) Representative fluorescence images of the RFP-HUVECs adhered to the ePTFE samples. Treated and control surfaces were incubated with RFP-HUVECs for 24 hours and cell adhesion was investigated. (**b)** SEM images of the cell treated ePTFE surfaces. (**c)** Cell count per mm^2 was significantly lower in Control-L and Control-NL when compared to CD34 treated surfaces. Control-L samples blocked the surface and had significantly less cells compared to Control-NL samples. Bars show the means ± SD of at least three samples. *P < 0.05 and **P < 0.001.

4.3.5. Long-term cell studies in human whole blood – Investigation of cell phenotype, cytocompatibility and endothelialization

BLIPS (CD34-APTES-L) were incubated with a cell-blood mixture for 4 days and cell capture from blood and the formation of a confluent and functional endothelial layer was investigated (***Figure 4.6a***). As shown in both confocal and SEM images in ***Figure 4.6b***, CD34-APTES-L surfaces were capable of capturing HUVECs from human whole blood after 4 days of incubation. The positive staining for VE-cadherin (green) confirmed the HUVEC phenotype of adherent cells and provided evidence of tight junctions between cells consistent with the formation of a confluent monolayer. The porous morphology of the ePTFE substrates influenced the orientation of the adherent cells. Thus, endothelial cells aligning along the dense features present on the ePTFE surface (***Figure 4.6a*** and ***b***). Compared with non-modified control ePTFE substrates, BLIPS had significantly more cells adherent to their surfaces than control ePTFE samples, which showed scattered cells and negative staining for VE-cadherin. In contrast to CD34-APTES-L and non-lubricated

control samples, lubricant-infused control ePTFE substrates showed excellent non-specific adhesion properties and prevented adhesion of HUVECs after 4 days which is advantageous for preventing coagulation but a significant drawback for endothelialization and tissue integration.

4.4. Discussion

Preventing non-specific adhesion of biomolecules and concurrently promoting endothelialization are two critical and inseparable features required for the optimal performance of synthetic vascular grafts [40]. Due to the thrombogenicity and poor endothelialization of synthetic vascular grafts, there is a pressing need for designing new surface coatings that would improve both the hemocompatibility and biofunctionality of the medical implants. Although extensive research has been devoted to this area, integrating these two essential features on a single platform still remains a challenge [40]. Here, we report for the first time a novel method for creating biofunctional lubricant-infused ePTFE grafts that prevent thrombin generation and clot formation and promote endothelial cell adhesion. In this technique, ePTFE substrates were biofunctionalized with a novel method using silanized anti-CD34 antibodies (silanized bio-inks) and subsequently lubricated with a fluorocarbon-based lubricant, creating a bio-targeting interface with excellent repellency properties. This novel surface modification method preserved the surface chemical properties of the ePTFE substrate, allowing the lubricant layer to infiltrate the ePTFE surface and, as a result, creating a stable, lubricant-infused layer. In addition, the anti-CD34 antibody preserved its innate function as an endothelial cell specific marker [38], [75], [265], once immobilized on ePTFE surfaces and coated with lubricant, as indicated by the high degree of cell-cell interaction exhibited by the lubricated biofunctionalized surfaces. This indicates that the presence of the lubricant layer does not block the antibody and prevent the cells from being captured by the cell capturing ligand. This was also observed in our previous study where anti-CD34 antibody functional lubricant-infused surfaces were generated by creating a SAM using a mixture of TPFS and APTES molecules on glass substrates [182]. In contrast to our previous work where APTES anchors present on the TPFS/APTES SAM were utilized for anti-CD34 immobilization, in this work, we eliminated the need for modifying the substrate with coupling agents and simplified the biofunctionalization process by silanizing the anti-CD34 antibodies and directly conjugating them to hydroxyl terminated ePTFE substrates.

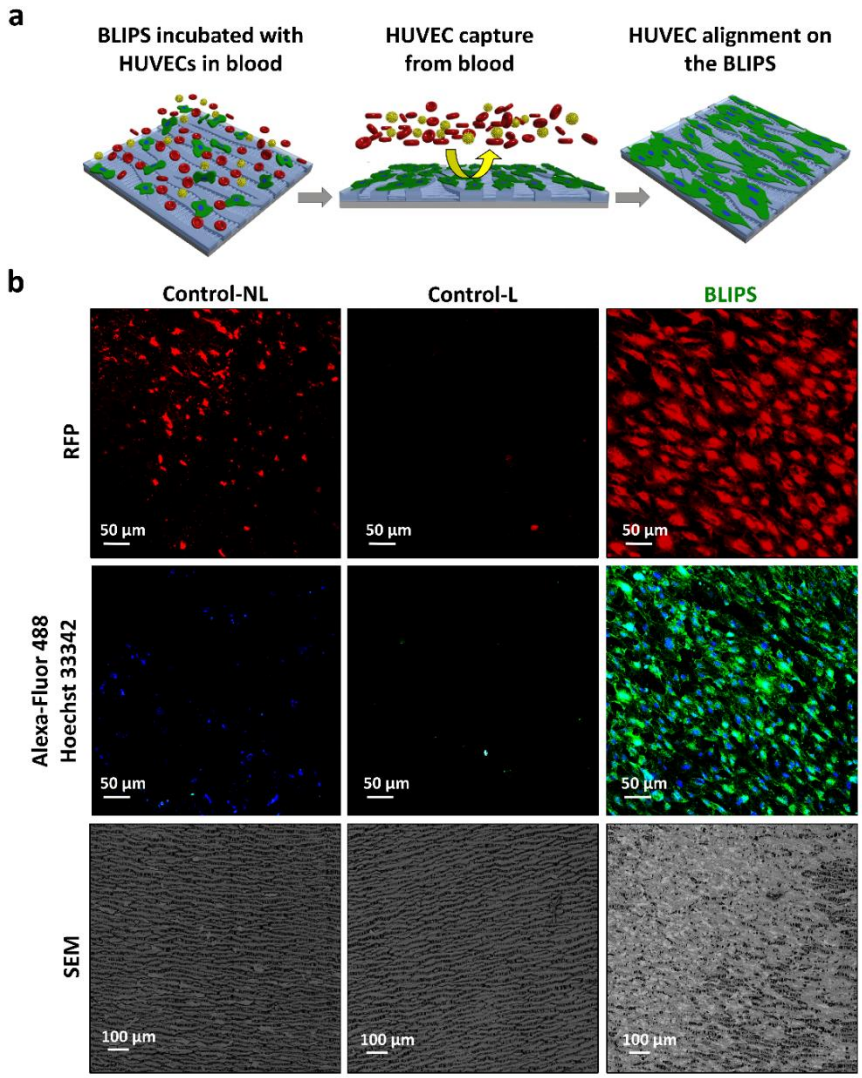

Figure 4.6 Long-term cell studies in blood on BLIPS and lubricated and non-lubricated control samples. (a) Schematic representation of endothelial cell capture and adhesion from whole blood and the alignment of cells along the dense features present on the CD34-APTES-L ePTFE surface. **(b)** Fluorescent and SEM images obtained from long-term cell experiments. ePTFE grafts were incubated with RFP-HUVECs for 4 days and endothelial cell adhesion and the formation of a confluent endothelial layer and cell phenotype of the treated surfaces was investigated. The positive immunofluorescence staining for Alexa Fluor 488-conjugated VE-cadherin (green) confirm the HUVEC phenotype for adherent cells. In contrast to control and lubricant-infused ePTFE surfaces, the optimized BLIPS promoted cell adhesion and the formation of a confluent endothelial layer was observed on these surfaces. The Control-L samples inhibited the non-specific binding of cells and had significantly fewer adherent cells after 4 days compared to other treated substrates.

When looking at the results obtained from the XPS measurements, it was evident that by modifying the ePTFE surface using the conventional method where the surface is entirely coated with an APTES layer using CVD, the surface fluorine at% and the F/C ratio significantly decreased. The optimal performance of slippery lubricant-infused surfaces

relies on the strong fluorine-fluorine interactions induced between the liquid lubricant and the fluorine molecules present on the substrate [178], [269]. Coating the ePTFE layer with a SAM of APTES, prevents the intermolecular interaction between the ePTFE surface and the lubricant layer, therefore, these surfaces are unable to lock-in the lubricant layer and create lubricant-infused surfaces. In addition, generating uniform silane monolayers using silane coupling agents are challenging and difficult to establish [270] and since not all silane-coupling molecules present on the coated surface will be utilized for biomolecule immobilization, the remaining non-reacted moieties could act as active sites for non-specific adhesion [271]. This is mainly troublesome in synthetic vascular grafts and other medical implants where preventing non-specific adhesion of biomolecules and cells is critical.

Lubricant-infused slippery surfaces are best known for their outstanding ability in preventing non-specific adhesion of biomolecules and cells [174], [178], [179]. In our experiments, lubricant-infused surfaces exhibited significantly lower thrombin generation and non-specific adhesion of HUVECs and bacteria compared with non-lubricated control ePTFE substrates, as expected. In addition to the lubricant layer, the anti-CD34 antibody potentiates the antithrombotic properties, because ePTFE substrates treated with both CD34-APTES and the APTES-SAM-CD34 significantly reduced thrombin generation and blood adhesion compared with non-modified control ePTFE surfaces (Control-NL). This phenomenon has also been observed in other studies where anti-CD34 antibody is used as an endothelial cell specific marker to increase endothelial cell capture and adhesion [35], [153]–[155]. Those studies reported increased hemocompatibility and less platelet adhesion on surfaces coated with anti-CD34 antibody biomarker.

4.5. Conclusion

In summary, we have reported a novel method for creating BLIPS using silanized anti-CD34 antibodies. This method simplifies currently available surface modification techniques for immobilizing biomolecules, reduces the steps required to obtain a biofunctional surface and eliminates the need for coating the surface of the biomaterial substrate with a coupling agent for attaching the biomolecule. Our CD34-APTES immobilized, lubricant-infused ePTFE substrates blocked non-specific adhesion of proteins, bacteria and cells and promoted endothelialization, the two main characteristics required to maximize the patency of permanent medical implants. This modification technique can be applied to other biomarkers, using different coupling agents and can be tailored towards different biomedical applications where biofunctionality and targeted binding are of importance.

4.6. Experimental Section

4.6.1. Materials

Perfluoroperhydrophenanthrene (PFPP), 3-aminopropyltriethoxy-silane (APTES), N-(3-Dimethylaminopropyl)-N′-ethylcarbodiimide (EDC), N-Hydroxysuccinimide (NHS), 2-(N-Morpholino) ethanesulfonic acid (MES), spectra-por float-a-lyzer G2 dialysis tubes were purchased from Sigma–Aldrich (Oakville, Canada). Alexa Fluor-488 conjugated mouse anti-human CD34 antibody and trypsin-EDTA (0.25%), Alexa Fluor 488-conjugated mouse anti-human CD144 (VE-cadherin) antibody, Hoechst 33342 nucleic acid stain and methanol-free formaldehyde were purchased from ThermoFisher Scientific (Massachusetts, United States). Red Fluorescent Protein Expressing Human Umbilical Vein Endothelial Cells (RFP-HUVEC) were generously donated by Dr. P. Ravi Selvaganapathy's lab at McMaster University. Cell media kit (EGM-2 BelletKit) and trypsin neutralizing agent where purchased from Cedarlane (Burlington, Canada). The thrombin-directed fluorescent substrate, Z-Gly-Gly-Arg-AMC, was purchased from Bachem (Bubendorf, Switzer- land). ePTFE vascular grafts were kindly provided by Hamilton Health Sciences (Hamilton, ON). Human whole blood and pooled citrated plasma was generated from blood samples collected from healthy donors as previously described [3]. A signed written consent was collected from donors and all procedures were approved by the McMaster University Research Ethics Board.

4.6.2. Preparing APTES functionalized anti-CD34 antibodies (CD34-APTES)

Anti-CD34 antibodies were silanized with APTES using the EDC/NHS carbodiimide crosslinker chemistry. The anti-CD34 antibody solution was prepared with a 1:100 ratio (5 µg/mL) in 0.1 M MES buffer (pH 5.5). In order to initiate the crosslinking chemistry, EDC and NHS solutions were added to the antibody mixture, leading to a concentration of 1mM EDC and 3 mM NHS. While the mixture was being stirred APTES (1% v/v) was added to the solution. The CD34-APTES solution was mixed for 2 hours and further transferred to float-a-lyzer dialysis membranes (molecular weight cut off 3.5-5 kDa) for purification. The solution was dialyzed for a minimum of six cycles.

4.6.3. Initial activation of ePTFE surfaces using oxygen plasma

Prior to modifying the ePTFE surfaces using the two techniques, hydroxyl functional groups were created on their surfaces using an oxygen plasma machine (Harrick Plasma Cleaner, PDC-002, 230 V). ePTFE samples were exposed to high-pressure oxygen plasma for 5 minutes. The hydroxyl groups generated on the ePTFE substrates were used to covalently attach APTES or CD34-APTES molecules onto the surface.

4.6.4. Creating anti-CD34 antibody functionalized ePTFE surfaces using CVD of APTES

After removing the hydroxyl functionalized ePTFE substrates from the plasma machine, they were placed in a vacuum desiccator and a droplet of 200 µL of APTES was added on a glass slide and placed beside the ePTFE samples. The vacuum pomp was turned on and after reaching a pressure of -0.085 MPa, the outlet valve was closed and the CVD of the APTES was initiated. The silanization was carried out for 4 hours at room temperature. Once the silanization step was completed, the APTES functionalized ePTFE substrates were removed from the desiccator and placed in an oven set at 60 °C for 12 hours. After removing the APTES functionalized ePTFE samples from the oven, they were glued to the bottom of the wells of a 96 well plate using a medical grade silicon adhesive (Silbione, Bluestar Silicones, Burlington, ON). Further, the substrates were biofunctionalized with the anti-CD34 antibody using the carbodiimide crosslinker chemistry. Anti-CD34 antibody solution with a concentration of 5 µg/mL in 0.1 M MES buffer (pH 5.5) was prepared and 1 mM EDC and 3 mM NHS was added to the antibody solution in order to initiate the EDC/NHS reaction. The solution was added to the APTES treated ePTFE substrates and the samples were incubated with the antibody solution overnight. After removing the solution, samples were rinsed with PBS in order to remove the physically bonded antibodies from the surface. CD34 attachment was investigated using a fluorescence microscope (Zeiss Primovert upright fluorescent microscope) and the green fluorescence intensity was quantified using ImageJ. The stability of the anti-CD34 antibody coated surfaces was investigated by washing the surfaces with 1% TBST several times and incubating the modified substrates with the buffer up to 2 weeks. Surfaces were imaged after each washing step and the fluorescence intensity was calculated using ImageJ. Results obtained from the stability experiments were compared with surfaces that were coated with the antibody through physical adsorption.

4.6.5. Creating biofunctional ePTFE surfaces using APTES silanized anti-CD34 antibody

In this technique, oxygen plasma treated ePTFE surfaces were functionalized with APTES treated antibodies (CD34-APTES). Oxygen plasma treated ePTFE substrates were incubated with the purified CD34-APTES solution overnight at 37 ºC. After removing the antibody solution, ePTFE substrates were washed with PBS in order to remove non-bonded antibodies from the surface. The CD34 attachment and the stability of the coating was investigated as described above.

4.6.6. X-ray photoelectron spectroscopy (XPS)

XPS was used to assess the surface chemical composition of the ePTFE surfaces before and after each modification technique. Three ePTFE substrates were subjected to XPS analysis for each condition and means were calculated. XPS measurements were performed by BioInterface Institute at McMaster University. The raw data were analyzed using the instrument software and the atom percentages of carbon, oxygen, fluorine, silicon, nitrogen was calculated.

4.6.7. Contact and sliding angle measurements

The contact and sliding angles of the treated and control ePTFE surfaces were measured in order to investigate their lubricant-infused properties before and after each modification step. A Future Digital Scientific OCA20 goniometer (Garden City, NY) was used to measure water sessile drop contact angles of the substrates (BioInterface Institute, McMaster University). Sliding angles were measured using a digital angle level (ROK, Exeter, UK). Prior to starting the sliding angle measurements, ePTFE samples were lubricated with PFPP and a 5µL droplet of deionized water was placed on their surface. The sliding angle was defined as the minimum angle required for droplets to start moving on the surface once the level was tilted. If the droplet failed to slide at angles of 90 degrees or higher, a sliding angle of 90 degrees was assigned to that sample. Measurements were performed in triplicates and the means were calculated.

4.6.8. Scanning electron microscopy (SEM)

SEM was performed on ePTFE samples in order to investigate the endothelial cell and bacteria adhesion, blood-cell interaction and clot formation on control and modified surfaces. Samples were fixed in 2% glutaraldehyde (2% v/v in 0.1M sodium cacodylate buffer) overnight. The samples were rinsed twice in buffer solution, post-fixed in 1% osmium tetroxide in 0.1M sodium cacodylate buffer for 1 hour and then dehydrated through a graded ethanol series. While the samples were immersed in 100% ethanol, they were transferred to the chamber of a Leica EM CPD300 critical point dryer (Leica Mikrosysteme GmbH, Wien, Austria). The dried samples were mounted onto SEM stubs with double-sided carbon tape. The samples on stubs were then placed in the chamber of a Polaron Model E5100 sputter coater (Polaron Equipment Ltd., Watford, Hertfordshire) and approximately 4 nm of gold was deposited onto the samples. Samples were then removed from the sputter coater and SEM imaging (JSM- 7000 F) was performed at 10 kx, 5 kx and 1 kx magnification.

4.6.9. Thrombin generation assay

A fluorogenic thrombin generation assay was used to compare the effect of different modification techniques on ePTFE-induced thrombin generation. Control and treated

ePTFE substrates were cut into 6 mm discs using a biopsy punch (Integra Miltex, Plainsboro, NJ) and glued to the bottom of the uncoated 96 well flat-bottom plates (Evergreen Scientific, Rancho Dominguez, CA) using a medical grade silicon adhesive (Silbione, Bluestar Silicones, Burlington, ON). To wells with or without the ePTFE discs, 80 µL of plasma and 20 µL of 0.02 M HEPES buffer was added. After incubating the plates for 10 minutes at 37 degrees, 100 µL aliquots of 1 mM Z-Gly-Gly-Arg-AMC in HBS containing 25 mM $CaCl_2$ was added to each well. The substrate hydrolysis was monitored using a FlexStation 3 fluorescence plate reader (Molecular Devices, Sunnyvale, CA) at 1 minute intervals for 90 minutes at excitation and emission wavelengths of 360 and 460 nm, respectively, and the emission cut-off filter of 455 nm. Thrombin generation results were analysed using Technothrombin TGA evaluation software (Vienna, Austria) and the assay was calibrated with the Technothrombin TGA CAL SET according to manufacturer's instructions (Technoclone). Peak thrombin (nM), time to peak thrombin (min), lag time to initial thrombin generation (min), the area under the curve or endogenous thrombin potential (ETP, nM.min), and velocity index (nM/min) were determined using the instrument software.

4.6.10. Assessing the bioactivity of ePTFE grafts - Endothelial cell adhesion and growth

The bioactivity, endothelial cell adhesion and the ability of the surfaces to create an endothelial layer was investigated by incubating the control and modified surfaces with endothelial cells for short (24 h) and long-term (4 days) periods. Control and anti-CD34 antibody treated ePTFE surfaces were cut into 6 mm disks, a size chosen to cover the bottom of 96-well plates and glued to the bottom of the wells. To each well, 150 µL of RFP-HUVEC solution with a concentration of 2 x 10^5 cell/mL was added. In the long-term cell studies the surfaces were incubated with a cell-blood mixture. Prior to adding the cell solution, samples that required lubricant were infiltrated with PFPP for 10 minutes. Further, the ePTFE plus cell containing plates were placed in an incubator at 37 °C and 5% CO_2 for the required incubation time. After taking out the samples from the incubator, surfaces were washed with pre-warmed cell media (3x) in order to remove the non-adhered cells, fixed with 4% methanol free formaldehyde and imaged using a confocal microscope and SEM. In the long-term cell study experiments cells were stained using Alexa Fluor 488-conjugated anti CD144 (VE-cadherin) antibody (green) and Hoechst 33342 (blue) in order to study cell phenotype of the treated surfaces. The number of adherent cells/area and the potency of the surfaces to create an endothelial layer was investigated.

4.6.11. Blood clot formation and blood cell repellency properties in human whole blood

The blood repellency and anti-clotting properties of the control and modified ePTFE surfaces were accessed using re-calcified human whole blood. ePTFE grafts were cut into 7 mm thick rings, pre-weighed and placed around the walls of a 48 well plate, leaving the center of the well unobstructed. Lubricated and non-lubricated ePTFE samples were used as controls. To each well, 200 µL of citrated whole blood was added and further, the blood was re-calcified by adding 200 µL of 20 mM HEPES (pH 7.4) containing 1 M $CaCl_2$, yielding a final $CaCl_2$ concentration of 12.5 mM. The grafts were incubated with re-calcified blood for 2 hours at room temperature. The blood clot containing ePTFE grafts were gently removed from the wells briefly blotted on an absorbent bench pad and weighed. The blood clot mass was calculated by subtracting the initial and final weighs of the ePTFE grafts. Further, ePTFE grafts were fixed in 4% formalin and subjected to SEM imaging in order to assess the clot adhesion and blood cell repellency properties of the surfaces.

4.6.12. Bacterial adhesion experiments

Staphylococcus aureus MW2 biofilms were grown on control and treated ePTFE surfaces for 48 hours under agitation at 37 ºC in TSB enriched with 0.2% sodium citrate, 0.6% yeast extract, and 0.5% glucose. Treated and control ePTFE vascular grafts were cut into 6 mm discs and glued to the bottom of the wells of a 96 well plate to keep them submerged. After incubation, the substrates were removed and washed once with PBS, fixed and dried for SEM imaging.

4.6.13. Statistical analysis

Data are presented as means ± S.D in all Figures. Data were statistically analyzed by one-way analysis of variance (ANOVA) followed by post hoc analysis using Bonferroni's test in **Figure 3b, Figure 4b** and **5c** and unpaired, two-tailed t-test for **Figures 2b** and **2f**. P values less than 0.05 were considered statistically significant for all comparisons.

4.7. Supplementary Information

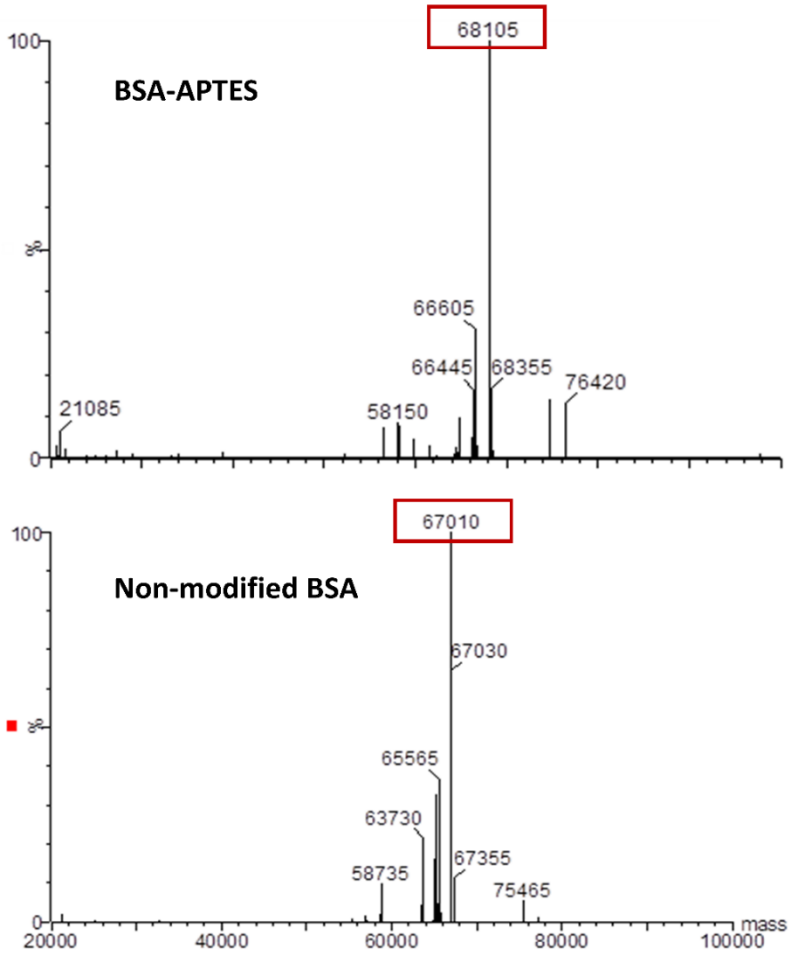

Supplementary Figure 4.1 Mass spectrometry (MS) results of non-modified and APTES silanized BSA (BSA-APTES). BSA was silanized with APTES using the EDC/NHS carbodiimide crosslinker chemistry. The BSA solution was prepared with a concentration of 5 mg/mL in 0.1 M MES buffer (pH 5.5). In order to initiate the crosslinking chemistry, EDC and NHS solutions were added to the antibody mixture, leading to a concentration of 1mM EDC and 3 mM NHS. While the mixture was being stirred, APTES (1% v/v) was added to the solution. The BSA solution was mixed for 2 hours and further transferred to dialysis membranes (molecular weight cut off 3.5-5 kDa) for purification. After a minimum of 6 cycles of dialyzing, the BSA-APTES solution was transferred to 50 mL falcon tubes and lyophilized until a dried and purified powder was obtained. The obtained BSA-APTES powder was dissolved in a H_2O/Acetonitrile/formic acid solvent (0.1 mg/mL) and subjected to MS. The mass spectra obtained from non-modified and BSA-APTES powder showed a shift in molecular mass with silanized BSA-APTES compared with non-modified BSA (68105 m/z and 67010 m/z respectively). This indicates successful covalent attachment of APTES molecules to BSA. The results also show the monodispersity of the BSA-APTES solution.

Chapter 5 *Fluorinated biofunctional lubricant-infused PET grafts with built-in functional groups prevent non-specific adhesion and promote endothelialization*

Preface

In this chapter fluorinated biofunctional lubricant-infused PET surfaces are created using a novel method where hydroxyl groups are first generated on fluorosilanized PET substrates using a secondary plasma treatment technique and then biofunctionalized using APTES silanized bio-inks. The hemocompatibility and biofunctionality of our developed surfaces were tested by performing thrombin generation, blood clot formation and endothelial cell adhesion studies and the results were compared to control PET grafts. Our developed PET vascular grafts were able to prevent thrombin generation and blood clot formation and promote endothelial cell adhesion and growth.

Relative Author Contributions

I prepared the samples, performed all experiments and analyzed the data. The manuscript was drafted by myself and subsequently edited by my academic supervisor Dr. Didar. XPS measurements were done at the BioInterface Institute at McMaster University. The SEM was carried out at the Electron Microscopy Facility in the Health Science Centre at McMaster university. Marcia Reid from the Electron Microscopy Facility at McMaster is acknowledged for her great help and guidance in preforming the SEM imaging.

Note to Reader:

This manuscript is under preparation and will soon be submitted to a per-reviewed journal. M. Badv, J. I. Weitz, T. F. Didar, “Fluorinated biofunctional lubricant-infused PET grafts with built-in functional groups prevent non-specific adhesion and promote endothelialization”

5.1. Introduction

Synthetic vascular grafts made of biostable polymers such as ePTFE and PET are widely used as alternatives to autologous vessels for replacing obstructed or diseased arteries [21], [72]. Despite their prevalence, these grafts suffer from low patency rates, because of their thrombogenicity and poor biofunctionality, leading to graft occlusion and explantation [77], [81], [132]. In order to overcome these limitations, recent research has focused on designing new surface coatings that increase the hemocompatibility and cell interaction on these surfaces. These modification techniques mainly involve coating the surfaces with synthetic, bioinert polymers [25]–[28], natural proteins [75], [153], [236], [239] and antithrombotic agents such as heparin [29]–[34]. In addition, coating the surfaces with endothelial cell specific markers [35]–[38] and vascular endothelial growth factors [39], [40] have also been explored to improve their endothelial cell-specific capturing features. Despite the extensive research devoted to this area, designing a suitable surface coating that integrates both hemocompatibility and endothelial cell capture on a single platform still remains a challenge.

The recent concept of lubricant-infused surfaces has gained extensive attention as a potential surface coating for biomaterials and blood-contacting devices [174], [179], [246]. Surfaces coated using this modification technique, possess excellent repellency properties and have been successfully applied as surface blockers to prevent nonspecific adhesion of cells and biospecies [174], [175], [178]. The solid surface and the infiltrating lubricant layer are the two main components present in a lubricant-infused system that interact and work together to create a stable yet dynamic and repellent interface. More specifically, in order to successfully create such surfaces, the underlying substrate needs to have a high chemical affinity for the lubricant-infused layer [272], [273]. Fluorine-based lubricant-infused surfaces, created by exploiting the strong intermolecular interactions between the fluorine atoms present on fluorinated substrates and perfluorocarbon-based lubricants are one of the most common lubricant-infused systems that have been explored for biomedical applications [178], [185]. These surface coatings can be achieved by either exploiting the innate chemical properties of fluorine-based solid surfaces such as ePTFE [175], [179] or by chemically modifying the surface with a fluorosilane based self-assembled monolayer [176], [178].

Despite the promising results obtained from the lubricant-infused surfaces, substrates modified using this technique all suffer from one mutual drawback, and that is the lack of biofunctionality and strongly preventing all biomolecules from interacting with the surface. This limitation is troublesome for permanent medical implants such as vascular grafts, where tissue integration and endothelial cell capture play a significant role in the

performance and patency of the device. In our recent studies, we intended to overcome this limitation by designing a new class of LIS that biofunctionality and targeted binding were integrated in the lubricant-infused platform, without compromising the repellency properties of the surface [182]. In our first study, fluorine-based biofunctional lubricant-infused surfaces (BLIS) were generated by creating SAMs of a 3-aminopropyltriethoxysilane (APTES)-Trichloro (1H, 1H, 2H, 2H-perfluorooctyl) silane (TPFS) mixture using CVD and further, utilizing the APTES coupling agents for biomarker immobilization. APTES was chosen as the silane coupling agent for biomolecule immobilization since this molecule has extensively been used for generating functional interfaces for biomolecule immobilization in the past [203], [204]. In our second study (unpublished: Badv *et al.*, "Lubricant-infused vascular grafts functionalized with silanized bio-inks suppress thrombin generation and promote endothelialization", submitted to *AHM*, Manuscript ID: adhm.201900753) we took this challenge further and created biofunctional lubricant infused ePTFE surfaces by exploiting the innate chemical properties of the ePTFE surface and eliminating the need for chemically modifying the substrate with silane molecules. In this study, the fluorine atoms present on the ePTFE surface were utilized for stabilizing the fluorocarbon lubricant layer and biofunctional features were added by functionalizing the hydroxyl terminated ePTFE surfaces with APTES-silanized biomarkers. Both surfaces created using these two techniques revealed excellent repellency and bio-targeting features.

PET vascular grafts have shown satisfactory results when employed in large diameter vessels, however, due to their thrombogenicity and poor cellular infiltration, they exhibit low-patency rates and poor patient outcomes when utilized in small-diameter vessels [69], [95]. The hydrophobicity of PET surfaces, hinders endothelial cell interaction and growth, which leads to platelet adhesion and clot formation [19], [21]. To combat these issues, extensive research has been devoted to developing new surfaces coatings that would improve cell interaction and hemocompatibility on these surfaces, however limited success has been made in designing straightforward, stable and durable coatings that would integrate both these requirements on one platform.

Here, we report a new class of biofunctional lubricant-infused PET surfaces, generated by combining and tuning the two modification techniques used in our previous studies. Fluorinated biofunctional lubricant infused PET surfaces (FBLIS) were created by initially adding the appropriate chemical groups onto the PET surface via creating a SAM of TPFS and further, generating functional groups on the fluorinated surface by exposing the fluorinated PET surfaces to a brief secondary oxygen plasma treatment. Moreover, the fluorinated, hydroxyl-terminated PET surfaces were biofunctionalized by covalently

attaching the APTES silanized anti-CD34 antibody bio-inks (created using carbodiimide crosslinker chemistry using N-(3-Dimethylaminopropyl)-N′-ethylcarbodiimide (EDC) and N-Hydroxysuccinimide (NHS)) to hydroxyl groups generated on the surface and the modification procedure was completed by infiltrating the surfaces with a fluorocarbon-based lubricant. In this technique we further simplified our modification procedure by circumventing the need for mixing the two fluoro and aminosilane molecules to our surfaces. The developed PET-based FBLIS grafts were tested for hemocompatibility and biofunctionality by performing thrombin generation, blood clot adhesion and endothelial cell adhesion studies and the results were compared with control PET and lubricant-infused PET surfaces.

5.2. Results and Discussion

In order to create FBLIS (***Figure 5.1***), a SAM of TPFS was created on hydroxyl terminated PET surfaces (PET-FS) as explained in methods.

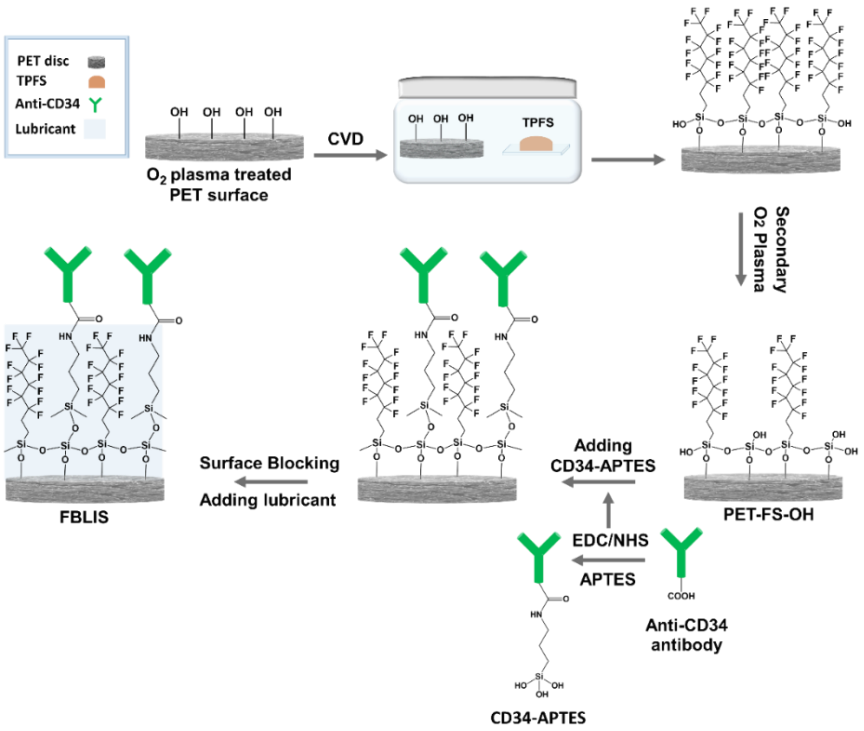

Figure 5.1 Schematic representation of creating fluorinated, biofunctionalized lubricant-infused PET surfaces (FBLIS) using silanized CD34-APTES antibodies. PET surfaces were initially oxygen plasma treated and further CVD treated using trichloro (1H,1H,2H,2H-perfluorooctyl) silane (TPFS). A secondary oxygen plasma treatment was applied on the TPFS treated surfaces in order to partially etch the TPFS layer and generate hydroxyl groups on the surface (PET-FS-OH). Further, premade, CD34-APTES functionalized antibodies were covalently attached to the hydroxyl functionalized TPFS treated surfaces using EDC/NHS chemistry. In the final step, biofunctionalized surfaces were blocked by adding perfluoroperhydrophenanthrene (PFPP) lubricant to the surfaces and FBLIS were generated.

Later, fluorinated PET surfaces were briefly exposed to a secondary oxygen plasma treatment in order to partially etch the fluorosilane layer and induce hydroxyl functional groups. Further, fluorinated, hydroxyl terminated PET surfaces (PET-FS-OH) were biofunctionalized using premade, APTES silanized anti-CD34 antibodies. In contrast to our previously reported technique for creating BLIS [182], in this method we significantly simplified the coating process by eliminating the need for pre-treating the surface with a mixture of amino and fluorosilane molecules through creating fluorinated surfaces with "built-in" hydroxyl functional groups by briefly exposing the fluorosilanized PET surfaces to a secondary plasma treatment. In addition, the PET-FS-OH surfaces were biofunctionalized by immobilizing pre-silanized bio-inks on their surfaces (unpublished: Badv *et al.*, "Lubricant-infused vascular grafts functionalized with silanized bio-inks suppress thrombin generation and promote endothelialization", submitted to *AHM*, Manuscript ID: adhm.201900753).

In order to confirm the presence of the initial fluorosilane monolayer added to the surfaces and the efficiency of the secondary plasma treatment technique performed to partially etch the fluorosilane layer, X-ray photoelectron spectroscopy (XPS) measurements were conducted on control, fluorosilanized and secondary oxygen plasma treated samples and the atomic percentage (at%) of fluorine (F), carbon (C) and oxygen (O) was assessed and the F/O ratio was calculated for each sample. As seen in ***Figure 5.2a***, the significant increase ($P < 0.001$) in the F/O ratio after performing the CVD treatment on PET samples confirms the presence of the fluorosilane layer on PET-FS surfaces. In addition, the significant decrease ($P < 0.001$) in the F/O ratio after performing the secondary plasma treatment (from 0.96 ± 0.04 to 0.46 ± 0.04 respectively), confirms the partial removal of the fluorosilane layer and the formation of hydroxyl functional groups on PET-FS-OH surfaces**.**

Plasma modification is one of the most common, straightforward and effective techniques used to change the surface properties of different biomaterials such as ePTFE and PET [88]. This technique allows the surfaces to bind with different atmospheric gases and as a result alters the surface chemical properties of the biomaterial [21], [87], [88]. In addition, studies have shown that by tuning the plasma power and type of gas used in the plasma modification procedure, the modification could be applied to a shallow depth of the surface, leaving the bulk properties of the substrates unaltered, something that should be considered when modifying the surfaces of blood-contacting devices [89], [90], [178]**.**

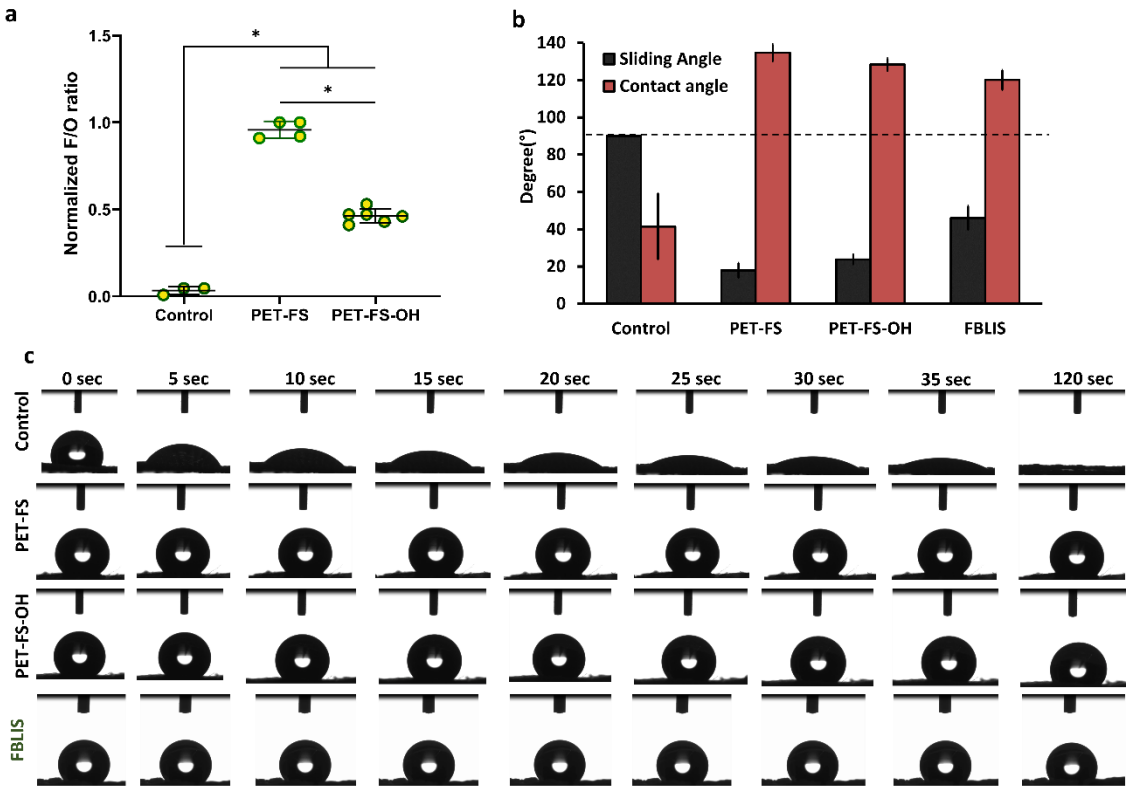

Figure 5.2 The surface chemical composition and the contact and sliding angle measurements of control-PET, PET-FS, PET-FS-OH and FBLIS surfaces. (a) The at% of fluorine and oxygen was assessed using XPS. The presence of fluorine after CVD treating the substrates with TPFS, confirms the formation of the fluorosilane self-assembled monolayer (SAM) on the PET surfaces. After conducting the secondary oxygen plasma treatment on the PET-FS surfaces, the F/O ratio decreased significantly (*$P < 0.001$). This confirms the partial removal of the fluorosilane layer and formation of the hydroxyl groups on the surface. **(b)** Sliding and contact angle measurements on control, lubricant-infused and FBLIS confirm the slippery properties of the substrates. Samples treated with TPFS, had significantly higher contact angles compared to control PET surfaces. **(c)** The water-substrate interaction was investigated at different time points after adding a 5 µl droplet on the surfaces and the contact angle was measured. In contrast to the control PET surfaces, the water droplet was not absorbed onto the surfaces of PET-FS, PET-FS-OH and FBLIS substrates even after 120 seconds.

Sliding and contact angle measurements were performed on control PET, PET-FS, PET-FS-OH and FBLIS surfaces to test their water repellency and slippery properties. As seen in ***Figure 5.2b*** **and** ***c***, control PET surfaces did not reveal slippery properties and the water droplet was pinned to the surface (did not slide) and started to get absorbed onto the surface after 5 seconds. In contrast, PET-FS, PET-FS-OH and FBLIS surfaces had slippery and water repellency properties by exhibiting low sliding angles (18 ± 4, 24 ± 3 and 46 ± 6 degrees respectively) and high contact angles (135 ± 4, 128 ± 3 and 120 ± 5 respectively) and were able to maintain the water droplet on their surfaces even after 120 seconds. When comparing the results with PET-FS samples, the water repellency properties of PET-FS-

OH and FBLIS surfaces decreased. The increase in the sliding angle and decrease in the contact angle after plasma treating and biofunctionalizing the PET-FS substrates with silanized anti-CD34 antibody could be attributed to the presence of hydroxyl groups and hydrophilic biomolecules on the PET surface. Hydroxyl groups are strongly hydrophilic and polar functional groups and their presence affects the physical surface properties (sliding and contact angle properties) of the substrate [274].

Thrombin generation was performed on control and modified PET surfaces in order to investigate their antithrombogenicity (***Figure 5.3a* and *b***). All fluorosilanized samples were lubricated prior to performing the test. Lubricated PET-FS surfaces significantly prolonged lag time and time to peak thrombin ($P \leq 0.001$) and significantly reduced thrombin generation and velocity index ($P \leq 0.001$) when compared with unmodified control PET surfaces. These results confirm that fluorinated, lubricant-infused PET surfaces express excellent blocking properties, and the coating significantly enhances the hemocompatibility of the grafts, similar to previously reported LIS coatings [174], [178].

a

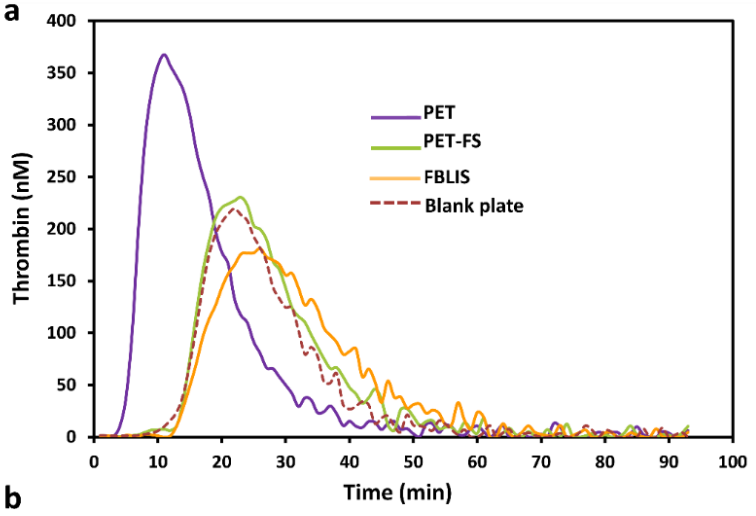

b

Parameter/Condition	PET	PET-FS	FBLIS	Blank Plate
Lag Time (min)	5.9 ± 0.5 *α	13.42 ± 2.5*	**17.67 ± 3.3**	12.42 ± 1.5*
Peak Thrombin (nM)	322.16 ± 33.6*α	250.51 ± 43.6ǂ	**201.95 ± 46.1**	214.50 ± 33.5
Time to Peak Thrombin (min)	9.17 ± 0.9 *α	21.75 ± 5.6 ǂ	**27.58 ± 6.1**	23.33 ± 3.8
Velocity Index (nM/min)	110.60 ± 42.6*α	39.13 ± 22.9	**24.55 ± 13.9**	22.78 ± 12.3
ETP (nM.min)	4246 ± 531	4426 ± 284	**4317 ± 472**	3920 ± 191

Figure 5.3 Investigating thrombin generation and clot formation on modified and control surfaces. (a) A representative thrombin vs. time plot is shown. **(b)** Thrombin generation parameters were determined in empty wells or wells containing control or modified PET surfaces. FBLIS treated surfaces significantly suppressed thrombin generation compared with control PET and PET-FS surfaces. Values represent means ± SD of 12 samples. *$P < 0.0001$ and ǂ$P < 0.05$ compared with FBLIS. ᵅ$P \leq 0.001$ compared with PET-FS.

The hemocompatibility of the FBLIS surfaces and their ability to prevent clot formation and blood-cell adhesion was further investigated by performing whole blood clotting assay. Citrated human whole blood was added to control and treated PET surfaces and the clotting assay was initiated by adding $CaCl_2$ to the solution. After incubating the samples with the blood mixture for 2 hours, blood clot formation and blood cell adhesion was investigated using SEM imaging (***Figure 5.4a***). As seen in the SEM images and photographs obtained from the samples, control PET surfaces did not reveal blood-repellency properties and a significant amount of blood clot and blood cell adhesion was observed on these surfaces. In contrast, both PET-FS and FBLIS surfaces exhibited excellent blocking and blood-repellency properties and minimum amounts of blood clot or cell adhesion was observed on these surfaces. Similar to the results obtained from our previous study [182] and studies reported by others [75], [159], [160], it could be concluded that, in addition to promoting endothelial cell adhesion, anti-CD34 antibody attenuates clot formation and enhances the repellency and anticoagulant properties of the coated surfaces. The exact mechanism is unclear and further studies need to be conducted in order to better understand the pathway(s) involved in the antithrombotic properties of this biomolecule.

Lastly, endothelial cell adhesion and growth was investigated on FBLIS, that were modified with an endothelial cell specific antibody (anti-CD34 antibody) and the results were compared with control PET and PET-FS surfaces. The biofunctional and control surfaces were incubated with RFP-HUVECs in blood for 2 days and cell adhesion and growth were studied using fluorescence microscopy. As seen in ***Figure 5.4b***, FBLIS remained bioactive and were able to capture endothelial cells and promote cell-cell interaction and growth when compared with control PET and PET-FS surfaces. Moreover, PET-FS surfaces exhibited excellent blocking properties by attenuating cell adhesion compared with biofunctional and control samples. PET samples with no cell specific marker showed endothelial cell adhesion to some extent, which could be attributed to the porosity and the knitted structure of the PET vascular graft. Clinically available PET surfaces consist of polyester fibers that are produced in either woven or knitted patterns [95]. Knitted PET grafts, which were also used in this study, have a looser structure and higher porosity compared to woven grafts. In contrast to woven grafts that are highly impermeable, the high porosity between the fibers of the knitted grafts encourages cell infiltration and ingrowth [275]. In addition to the porous structure of the knitted PET grafts, when comparing the results obtained from control PET and FBILS, it is evident that adding biofunctionality and cell specific markers to these surfaces could magnify and further enhance their cell permeability and targeted cell capturing features.

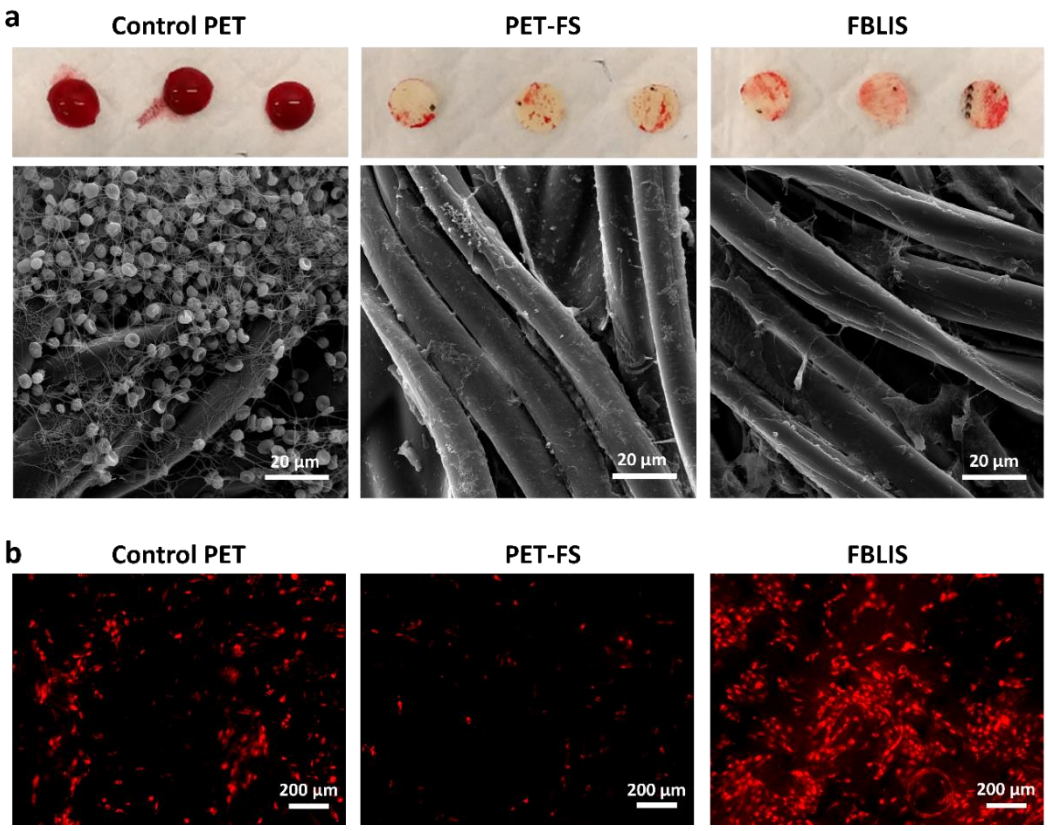

Figure 5.4 Investigating the blood-repellency and endothelial cell adhesion properties of PET, PET-FS and FBLIS surfaces. **(a)** Human whole blood clot formation on control-PET, PET-FS and FBLIS. The optimized FBLIS and Lubricant infused surfaces significantly reduced clot formation and blood cell adhesion compared to unmodified control substrates. **(b)** FBLIS surfaces, functionalized with anti-CD34 antibody promoted endothelial cell adhesion and capture from human whole blood. In contrast a low number of cells were adhered to PET-FS surfaces. Control PET surfaces showed a higher number of cell adhesion compared to PET-FS surfaces, however cell-cell interactions and the formation of an endothelial layer was not observed on these surfaces.

5.3. Conclusion

In conclusion we have reported a straightforward and simple method for creating fluorinated biofunctional lubricant-infused PET grafts with "built-in" chemical functional groups. PET vascular grafts modified with our developed coating significantly attenuated thrombin generation and promoted endothelial cell adhesion when compared with uncoated PET grafts. Our purposed modification technique eliminates the need for coating the surface with silane coupling agents for biomolecule immobilization and the required chemical moieties are generated using a post plasma modification technique, resulting in fluorinated surfaces containing "built-in" functional groups. This technique could be applied to other biomaterials and different plasma gases could be used in order to generate different chemical groups on the surface for biomolecule immobilization.

5.4. Materials and methods

5.4.1. Materials

Alexa Fluor 488 conjugated mouse anti-human CD34 antibody and trypsin-EDTA (0.25%) were purchased from ThermoFisher Scientific (Massachusetts, United States). Trichloro (1H, 1H, 2H, 2H-perfluorooctyl) silane (TPFS), perfluoroperhydrophenanthrene (PFPP), 3-aminopropyltriethoxy-silane (APTES), N-(3-Dimethylaminopropyl)-N′-ethylcarbodiimide (EDC), N-Hydroxysuccinimide (NHS), 2-(N-Morpholino) ethanesulfonic acid (MES), spectra-por float-a-lyzer G2 dialysis tubes were purchased from Sigma–Aldrich (Oakville, Canada). Red Fluorescent Protein Expressing Human Umbilical Vein Endothelial Cells (RFP-HUVEC) were generously donated by Dr. P. Ravi Selvaganapathy's lab at McMaster University. Cell media kit (EGM-2 BelletKit) and trypsin neutralizing agent where purchased from Cedarlane (Burlington, Canada). The thrombin-directed fluorescent substrate, Z-Gly-Gly-Arg-AMC, was purchased from Bachem (Bubendorf, Switzer- land). Dacron (Polyethylene terephthalate, PET) vascular grafts were kindly provided by Hamilton Health Sciences (Hamilton, ON). Whole human blood and pooled citrated plasma was generated from blood samples that were collected from healthy donors. All donors provided a signed written consent prior to collecting their blood and all procedures were approved by the McMaster University Research Ethics Board.

5.4.2. Surface modification of PET substrates

5.4.2.1. Generating hydroxyl terminated PET substrates

Prior to functionalizing the PET surfaces with TPFS and creating a TPFS-SAM, hydroxyl functional groups were generated on their surfaces using oxygen plasma (Harrick Plasma Cleaner, PDC-002, 230 V). PET samples were cut into appropriate disc sizes using a biopsy punch and exposed to high-pressure oxygen plasma for 2 minutes.

5.4.2.2. Preparation of fluorosilanized PET surfaces using CVD

After removing the oxygen plasma-treated PET discs from the plasma cleaner, they were immediately placed in a desiccator connected to a vacuum pump and on a glass slide, 400 µL of TPFS was added and placed beside the PET substrates. The vacuum pump was turned on and once a pressure of −0.085 MPa was reached, the exit valve of the desiccator was closed, and the CVD process was initiated. The CVD silanization procedure was carried out for about 5 hours at room temperature. After the CVD step, PET surfaces were removed from the desiccator and placed in an oven at 60 °C overnight in order to complete the condensation step.

5.4.2.3. Secondary oxygen plasma treatment of TPFS functionalized PET surfaces

After removing the fluorosilanized PET samples (PET-FS) from the oven, substrates were exposed to a secondary oxygen plasma treatment for 10 seconds in order to partially etch the fluorine SAM layer and to create hydroxyl functional groups on the fluorosilanized surface (***Figure 5.1***). The fluorinated, hydroxyl functionalized surfaces (PET-FS-OH) were then removed from the plasma machine and glued to the bottom of the wells of a 96 well plate using a medical grade silicon adhesive (Silbione, Bluestar Silicones, Burlington, ON). PET-FS surfaces with no secondary plasma treatment were used as controls. All fluorosilanized surfaces were lubricated using PFPP lubricant prior to preforming further experiments.

5.4.2.4. Creating biofunctional PET surfaces using APTES silanized anti-CD34 antibody (FBLIS)

Prior to functionalizing the hydroxyl functionalized, PET-FS surfaces with anti-CD34 antibody, anti-CD34 antibody was silanized with APTES using EDC/NHS chemistry, as described in *Chapter 4*. In summary, the chemical reaction was carried out in 0.1 M MES buffer (pH 5.5) for 2 hours. Initially, anti-CD34 antibody was added to the MES buffer yielding to a concentration of 5 µg/mL and then 1 mM EDC and 3 mM NHS was added to the solution. In a subsequent step, APTES was added to the mixture (1% v/v) and the solution was left stirring at room temperature for 2 hours. The solution mixture was transferred to dialysis membranes (molecular weight cut off 3.5-5 kDa) and dialyzed for four to six cycles in order to purify the antibody mixture and remove the non-reacted APTES molecules and other impurities present in the solution. Fluorosilanized, hydroxyl functionalized PET substrates (PET-FS-OH) were then incubated with the purified CD34-APTES solution overnight in order to obtain CD34-APTES functionalized PET-FS surfaces (FBLIS). After removing the antibody solution, PET substrates were washed with PBS in order to remove non-bonded antibodies from the surface.

5.4.3. Surface characterization of PET modified substrates

5.4.3.1. XPS

XPS was used to assess the surface chemical composition of the PET surfaces after the fluorosilanized and secondary oxygen plasma treatment steps. Three PET substrates were subjected to XPS analysis for each condition and means were calculated. XPS spectra were recorded using a Physical Electronics (PHI) Quantera II spectrometer (Biointerfaces Institute, McMaster University). The raw data were analyzed using the instrument software and the atomic percentages of carbon, oxygen, fluorine, silicon and chlorine were calculated.

5.4.3.2. Contact and sliding angle measurements

The contact and sliding angles of the control PET, PET-FS, PET-FS-OH and FBLIS surfaces were measured as previously described (unpublished: Badv *et al.*, "Lubricant-infused vascular grafts functionalized with silanized bio-inks suppress thrombin generation and promote endothelialization", submitted to *AHM*, Manuscript ID: adhm.201900753) with some modifications. Briefly, a Future Digital Scientific OCA20 goniometer (Garden City, NY) was used to measure the water sessile drop contact angles of the substrates. After placing the droplet on the control and modified PET surfaces, images were taken in 5 second intervals in order to study the water repellency properties of the PET modified surfaces and their ability to prevent the water droplet from getting adsorbed onto the surface. The contact angles were measured once the droplet would touch the PET surface (at 0 seconds). Sliding angles were measured using a digital angle level (ROK, Exeter, UK). Prior to starting the measurements, PET samples were lubricated with PFPP and a 5µL droplet of deionized water was placed on their surface. The sliding angle was defined as the minimum angle required for droplets to start sliding on the surface, once the level was tilted. If the droplet failed to slide at angles of 90 degrees or higher, a sliding angle of 90 degrees was assigned to that sample.

5.4.3.3. SEM imaging

SEM was performed on PET samples in order to investigate the blood-cell interaction and clot formation on control and modified surfaces. Samples were fixed in 2% glutaraldehyde (2% v/v in 0.1M sodium cacodylate buffer) overnight and rinsed twice in buffer solution, post-fixed in 1% osmium tetroxide in 0.1M sodium cacodylate buffer for 1 hour and then dehydrated through a graded ethanol series. The samples were then transferred to the chamber of a Leica EM CPD300 critical point dryer (Leica Mikrosysteme GmbH, Wien, Austria) and flushed with liquid CO_2. The dried samples were mounted onto SEM stubs with double-sided carbon tape and then placed in the chamber of a Polaron Model E5100 sputter coater (Polaron Equipment Ltd., Watford, Hertfordshire) in order to be sputter coated with approximately 4 nm of gold. Samples were then removed from the sputter coater and SEM imaging (JSM- 7000 F) was performed.

5.4.4. Thrombin generation assay

A fluorogenic thrombin generation assay was used to compare the effect of different modification techniques on thrombin generation. Control and treated PET substrates were cut into 6 mm discs using a biopsy punch (Integra Miltex, Plainsboro, NJ) and glued to the bottom of the uncoated 96 well flat-bottom plates (Evergreen Scientific, Rancho Dominguez, CA) using a medical grade silicon adhesive (Silbione, Bluestar Silicones, Burlington, ON). 80 µL of plasma and 20 µL of 0.02 M HEPES buffer was added to the

wells with or without the PET discs. After incubating the plates at 37 degrees for 10 minutes, to each well, 100 µL aliquots of 1 mM Z-Gly-Gly-Arg-AMC in HBS containing 25 mM $CaCl_2$ was added. The substrate hydrolysis was monitored using a FlexStation 3 fluorescence plate reader (Molecular Devices, Sunnyvale, CA) at 1-minute intervals for 120 minutes at excitation and emission wavelengths of 360 and 460 nm, respectively, and the emission cut-off filter of 455 nm. Thrombin generation results were analysed using Technothrombin TGA evaluation software (Vienna, Austria). Lag time to initial thrombin generation (min), peak thrombin (nM) and time to peak thrombin (min), the area under the curve or endogenous thrombin potential (ETP, nM.min), and velocity index (nM/min) were determined and calculated using the instrument's software.

5.4.5. Blood clot formation and blood cell repellency properties in human whole blood

The blood repellency and anti-clotting properties of the control and modified PET surfaces were accessed using re-calcified human whole blood. PET grafts were cut into 6 mm in diameter discs and placed at the bottom of the wells of a 96 well plate. Lubricated and non-lubricated PET samples were used as controls. To each well, 100 µL of citrated blood was added and further, the blood clotting was initiated by re-calcifying the blood by adding 100 µL of 1M $CaCl_2$ in HEPES. The PET discs were incubated with re-calcified blood for 2 hours at room temperature and were gently removed from the wells, briefly blotted on an absorbent bench pad and fixed in 2% glutaraldehyde (2% v/v in 0.1M sodium cacodylate buffer) overnight. Further, PET grafts were subjected to SEM imaging in order to assess the clot and blood cell adhesion on their surfaces.

5.4.6. Assessing the bioactivity of PET grafts - Endothelial cell adhesion and growth from human whole blood

The bioactivity, endothelial cell adhesion and the ability of the FBLIS surfaces to capture endothelial cells was investigated, and the results were compared to control and PET-FS surfaces. Control, PET-FS and anti-CD34 antibody treated PET surfaces were cut into 6 mm disks. To each well, 150 µL of RFP-HUVEC + blood solution with a concentration of 2 x 10^5 cell/mL was added, and the plate was placed in an incubator at 37 °C and 5% CO_2 for 2 days. Prior to adding the cell solution, samples that required lubricant were infiltrated with PFPP and the excess amount of lubricant was removed immediately before adding the cell solution. After the 2-day incubation time, surfaces were washed with pre-warmed cell media (3x) in order to remove the non-adhered cells, fixed using 4% formalin in PBS and imaged using an upright fluorescence microscope. The number of cells/area attached to each substrate and the potency of the surfaces to create an endothelial layer was investigated.

Chapter 6 *Concluding remarks and future directions*

In this thesis, various surface modification techniques were designed and developed to address the complications and challenges associated with blood-contacting medical implants. These challenges mainly include the low hemocompatibility and high thrombogenicity of these surfaces, as well as their poor biofunctionality and inability to promote endothelial cell adhesion and tissue integration on their surfaces. Hemocompatibility and endothelialization are two inseparable and crucial features that are required when designing surface coatings for permanent medical implants. The techniques developed in this thesis allow the integration of both these features on a single platform, resulting in surface coatings that simultaneously attenuate clot formation, prevent non-specific adhesion and promote endothelial cell integration and growth. The proposed research objectives were fully achieved in this thesis and the significant outcomes to acknowledge are summarized below:

A non-invasive and straightforward modification procedure for creating LIS, compatible with polymeric substrates was developed in *Chapter 2*. The modification procedure required for creating LIS on flat substrates that do not have the appropriate chemical affinity to stabilize the desired lubricant-layer was developed, optimized and applied to polymeric catheters, resulting in surfaces with excellent antithrombotic and repellency properties.

In *Chapter 3*, for the first time, we impregnated lubricant-infused surfaces with biofunctional features and created biofunctional lubricant-infused surfaces that exhibited excellent biotargeting and repellency properties. In this developed method, surfaces were modified with a mixture of amino (APTES) and fluorosilane (TPFS) molecules and by tuning the ratio between these two silane molecules we were able to create lubricant-infused surfaces that not only had excellent repellency properties and prevented non-specific adhesion, but also promoted targeted binding of cells and biomolecules. In our designed surfaces, the APTES molecules present on the SAM were used for endothelial cell-specific antibody immobilization and the fluorosilane molecules stabilized the fluorocarbon-based lubricant, resulting in a biofunctional, lubricant-infused layer.

In *Chapter 4*, we successfully created biofunctional lubricant-infused surfaces on medical grade ePTFE vascular grafts and further simplified the developed modification procedure in *Chapter 3*. In this work, we aimed to create biofunctional lubricant-infused ePTFE surfaces without the need of chemically modifying the ePTFE substrate with silane molecules and as a result preserving the chemical properties of the ePTFE grafts. In order

to do so, we developed a novel method (*patent filed*) where instead of the base substrate, endothelial cell-specific markers were silanized using APTES molecules and directly immobilized on ePTFE substrates. This novel technique streamlines the modification procedure required to create biofunctional lubricant-infused surfaces and results in surfaces with excellent antithrombotic properties and targeted-binding features. Moreover, our developed procedure for creating silanized bio-inks could be applied to different biomarkers and can be used in several biomedical related applications.

Our developed method for creating biofunctional lubricant-infused surfaces was not limited to ePTFE surfaces that had innate chemical properties for stabilizing fluorinated lubricants and in *Chapter 5* we further modified our technique and optimized our procedure for non-fluorinated substrates such as PET. In this Chapter we describe a novel method (*patent filed*) for creating fluorinated biofunctional lubricant-infused PET surfaces that exhibit excellent biofunctionality and antithrombotic properties. In this work, instead of creating a SAM using both APTES and TPFS molecules, we simplified the modification procedure by partially etching the fluorine SAM layer created on the PET surface by exposing the surface to a secondary oxygen plasma treatment and substituting the fluorine molecules with hydroxyl functional groups. Further, the fluorinated, hydroxyl terminated, lubricant-infused surfaces were biofunctionalized using the silanized bio-inks created in *Chapter 4*, resulting in stable fluorinated biofunctional lubricant-infused PET surfaces that attenuated thrombin generation and promoted endothelial cell adhesion.

Overall, the work presented in this thesis describes strategies to optimize the fabrication process for generating lubricant-infused surfaces and novel techniques to integrate biofunctionality into lubricant-infused systems, demonstrating significant improvements in cell capture, targeted-binding and the prevention of non-specific adhesion. In addition to the publications, two patents have been filed from the research done in this thesis.

Moving forward we are planning on performing more *in vitro* and *in vivo* experiments in order to investigate the short-term and long-term stability and performance of our modified surfaces in different conditions. Firstly, we aim to evaluate the stability and biofunctionality of our coated surfaces and investigate their hemocompatibility and ability to attenuate blood clot formation under flow conditions. The *in vitro* cell specificity of the biofunctional lubricant-infused surfaces will be further investigated, by co-immobilizing the surfaces with other cell types (e.g. smooth muscle cells (SMCs)). The biofunctional lubricant-infused ePTFE or PET surfaces should be capable of capturing endothelial cells under flow conditions and forming a confluent endothelial layer.

Lastly, our ultimate goal is to investigate the short (*e.g.* 2-4 weeks) and long-term (*e.g.* 6-24 weeks) performance of our designed biofunctional lubricant-infused surfaces *in vivo* in both small (*e.g.* rats) and large (*e.g.* pigs) animal models. In these experiments we will be looking at endothelial cell capture, adhesion and endothelialization and investigate platelet adhesion, activation, thrombin-antithrombin complexes (TAT), and clot formation on our designed surfaces. Further, neointimal hyperplasia will be studied by looking at SMC adhesion and growth and preforming histopathological and morphometric analysis on the explanted vascular grafts.

References

[1] I. H. Jaffer, J. C. Fredenburgh, J. Hirsh, and J. I. Weitz, "Medical device-induced thrombosis: What causes it and how can we prevent it?," *J. Thromb. Haemost.*, vol. 13, no. S1, pp. S72–S81, 2015.

[2] C. J. Wilson, R. E. Clegg, D. I. Leavesley, and M. J. Pearcy, "Mediation of Biomaterial–Cell Interactions by Adsorbed Proteins: A Review," *Tissue Eng.*, vol. 11, no. 1–2, pp. 1–18, Jan. 2005.

[3] J. W. Yau, A. R. Stafford, P. Liao, J. C. Fredenburgh, R. Roberts, and J. I. Weitz, "Mechanism of catheter thrombosis: Comparison of the antithrombotic activities of fondaparinux, enoxaparin, and heparin in vitro and in vivo," *Blood*, vol. 118, no. 25, pp. 6667–6674, 2011.

[4] J. L. Orford *et al.*, "Safety and efficacy of aspirin, clopidogrel, and warfarin after coronary stent placement in patients with an indication for anticoagulation," *Am. Heart J.*, vol. 147, no. 3, pp. 463–467, 2004.

[5] E. G. Butchart *et al.*, "Recommendations for the management of patients after heart valve surgery," *Eur. Heart J.*, vol. 26, no. 22, pp. 2463–2471, 2005.

[6] R. Gbyli, A. Mercaldi, H. Sundaram, and K. A. Amoako, "Achieving Totally Local Anticoagulation on Blood Contacting Devices," *Adv. Mater. Interfaces*, vol. 5, no. 4, pp. 1–16, 2018.

[7] G. Conn, A. G. Kidane, G. Punshon, R. Y. Kannan, G. Hamilton, and A. M. Seifalian, "Is there an alternative to systemic anticoagulation, as related to interventional biomedical devices?," *Expert Rev. Med. Devices*, vol. 3, no. 2, pp. 245–261, 2006.

[8] I. Reviakine *et al.*, "Stirred, shaken, or stagnant: What goes on at the blood–biomaterial interface," *Blood Rev.*, vol. 31, no. 1, pp. 11–21, 2017.

[9] Y. Misawa, "Valve-related complications after mechanical heart valve implantation," *Surg. Today*, vol. 45, no. 10, pp. 1205–1209, 2014.

[10] T. Bourguignon *et al.*, "Risk factors for valve-related complications after mechanical heart valve replacement in 505 patients with long-term follow up.," *J. Heart Valve Dis.*, vol. 20, no. 6, pp. 673–680, 2011.

[11] L. H. Edmunds, "Thrombotic and Bleeding Complications of Prosthetic Heart Valves," *Ann. Thorac. Surg.*, vol. 44, no. 4, pp. 430–445, 1987.

[12] World Health Organization "WHO," "A global brief on Hyper tension Silent killer, global public health crisis," 2013.

[13] World Health Organization, "WHO | World Heart Day," *WHO*, 2018. [Online]. Available: https://www.who.int/cardiovascular_diseases/world-heart-day/en/. [Accessed: 05-Apr-2019].

[14] A. J. Epstein, D. Polsky, F. Yang, L. Yang, and P. W. Groeneveld, "Coronary Revascularization Trends in the United States, 2001-2008," *JAMA*, vol. 305, no. 17,

p. 1769, May 2011.

[15] D. E. Bloom *et al.*, "The Global Economic Burden of Noncommunicable Diseases," *Progr. Glob. Demogr. Aging Work. Pap.*, no. 87, 2012.

[16] K. Wang *et al.*, "Functional Modification of Electrospun Poly(ε-caprolactone) Vascular Grafts with the Fusion Protein VEGF-HGFI Enhanced Vascular Regeneration," *ACS Applied Materials and Interfaces*, vol. 9, no. 13. pp. 11415–11427, 2017.

[17] J. M. Bastijanic *et al.*, "In vivo evaluation of biomimetic fluorosurfactant polymer-coated expanded polytetrafluoroethylene vascular grafts in a porcine carotid artery bypass model," *J. Vasc. Surg.*, vol. 63, no. 6, pp. 1620-1630e4, 2016.

[18] A. K. Ranjan, U. Kumar, A. A. Hardikar, P. Poddar, P. D. Nair, and A. A. Hardikar, "Human blood vessel-derived endothelial progenitors for endothelialization of small diameter vascular prosthesis," *PLoS One*, vol. 4, no. 11, 2009.

[19] D. B. Shi, W. G. Fu, H. B. He, and Y. Q. Wang, "Small-diameter vascular grafts for bypass surgery," *J. Clin. Rehabil. Tissue Eng. Res.*, vol. 11, no. 43, pp. 8781–8784, 2007.

[20] A. J. Melchiorri, N. Hibino, and J. P. Fisher, "Strategies and techniques to enhance the in situ endothelialization of small-diameter biodegradable polymeric vascular grafts.," *Tissue Eng. Part B. Rev.*, vol. 19, no. 4, pp. 292–307, 2013.

[21] M. A. Hiob, S. She, L. D. Muiznieks, and A. S. Weiss, "Biomaterials and Modifications in the Development of Small-Diameter Vascular Grafts," *ACS Biomater. Sci. Eng.*, vol. 3, no. 5, pp. 712–723, 2017.

[22] S. de Valence *et al.*, "Long term performance of polycaprolactone vascular grafts in a rat abdominal aorta replacement model," *Biomaterials*, vol. 33, no. 1, pp. 38–47, 2012.

[23] C. Nie, L. Ma, C. Cheng, J. Deng, and C. Zhao, "Nanofibrous Heparin and Heparin-Mimicking Multilayers as Highly Effective Endothelialization and Antithrombogenic Coatings," *Biomacromolecules*, vol. 16, no. 3, pp. 992–1001, 2015.

[24] M. Fischer, M. F. Maitz, and C. Werner, *Coatings for biomaterials to improve hemocompatibility*. Elsevier Ltd., 2017.

[25] K. M. Hansson *et al.*, "Whole blood coagulation on protein adsorption-resistant PEG and peptide functionalised PEG-coated titanium surfaces," *Biomaterials*, vol. 26, no. 8, pp. 861–872, 2005.

[26] D. E. Heath and S. L. Cooper, "Design and characterization of PEGylated terpolymer biomaterials," *J. Biomed. Mater. Res. - Part A*, vol. 94, no. 4, pp. 1294–1302, 2010.

[27] W. B. Tsai, Y. H. Chen, and H. W. Chien, "Collaborative cell-resistant properties of polyelectrolyte multilayer films and surface PEGylation on reducing cell adhesion to cytophilic surfaces," *J. Biomater. Sci. Polym. Ed.*, vol. 20, no. 11, pp. 1611–1628,

2009.

[28] K. Ishihara, "Blood-Compatible Surfaces with Phosphorylcholine-Based Polymers for Cardiovascular Medical Devices," *Langmuir*, p. acs.langmuir.8b01565, Aug. 2018.

[29] P. H. Lin, C. Chen, R. L. Bush, Q. Yao, A. B. Lumsden, and S. R. Hanson, "Small-caliber heparin-coated ePTFE grafts reduce platelet deposition and neointimal hyperplasia in a baboon model," *J. Vasc. Surg.*, vol. 39, no. 6, pp. 1322–1328, 2004.

[30] J. M. M. Heyligers *et al.*, "Heparin immobilization reduces thrombogenicity of small-caliber expanded polytetrafluoroethylene grafts," *J. Vasc. Surg.*, vol. 43, no. 3, pp. 587–591, 2006.

[31] F. P. Seib, M. Herklotz, K. A. Burke, M. F. Maitz, C. Werner, and D. L. Kaplan, "Multifunctional silk-heparin biomaterials for vascular tissue engineering applications," *Biomaterials*, vol. 35, no. 1, pp. 83–91, 2014.

[32] J. Zhao *et al.*, "Improving blood-compatibility via surface heparin-immobilization based on a liquid crystalline matrix.," *Mater. Sci. Eng. C. Mater. Biol. Appl.*, vol. 58, pp. 133–41, 2016.

[33] Z. Yang *et al.*, "The covalent immobilization of heparin to pulsed-plasma polymeric allylamine films on 316L stainless steel and the resulting effects on hemocompatibility," *Biomaterials*, vol. 31, no. 8, pp. 2072–2083, Mar. 2010.

[34] R. A. Hoshi, R. Van Lith, M. C. Jen, J. B. Allen, K. A. Lapidos, and G. Ameer, "The blood and vascular cell compatibility of heparin-modified ePTFE vascular grafts," *Biomaterials*, vol. 34, no. 1, pp. 30–41, 2013.

[35] A. Tan *et al.*, "An Anti-CD34 Antibody-Functionalized Clinical-Grade POSS-PCU Nanocomposite Polymer for Cardiovascular Stent Coating Applications: A Preliminary Assessment of Endothelial Progenitor Cell Capture and Hemocompatibility," *PLoS One*, vol. 8, no. 10, pp. 1–14, 2013.

[36] J. I. Rotmans *et al.*, "In vivo cell seeding with anti-CD34 antibodies successfully accelerates endothelialization but stimulates intimal hyperplasia in porcine arteriovenous expanded polytetrafluoroethylene grafts," *Circulation*, vol. 112, no. 1, pp. 12–18, 2005.

[37] S. Petersen, A. Strohbach, R. Busch, S. B. Felix, K. P. Schmitz, and K. Sternberg, "Site-selective immobilization of anti-CD34 antibodies to poly(l -lactide) for endovascular implant surfaces," *J. Biomed. Mater. Res. - Part B Appl. Biomater.*, vol. 102, no. 2, pp. 345–355, 2014.

[38] L. Chen, H. He, M. Wang, X. Li, and H. Yin, "Surface Coating of Polytetrafluoroethylene with Extracellular Matrix and Anti-CD34 Antibodies Facilitates Endothelialization and Inhibits Platelet Adhesion Under Sheer Stress," *Tissue Eng. Regen. Med.*, vol. 14, no. 4, pp. 359–370, 2017.

[39] R. J. Smith, M. T. Koobatian, A. Shahini, D. D. Swartz, and S. T. Andreadis, "Capture of endothelial cells under flow using immobilized vascular endothelial

growth factor," *Biomaterials*, vol. 51, pp. 303–312, 2015.

[40] S. Lu *et al.*, "Synthetic ePTFE grafts coated with an anti-CD133 antibody-functionalized heparin/collagen multilayer with rapid in vivo endothelialization properties," *ACS Appl. Mater. Interfaces*, vol. 5, no. 15, pp. 7360–7369, 2013.

[41] M. Sun *et al.*, "A correlation study of protein adsorption and cell behaviors on substrates with different densities of PEG chains," *Colloids Surfaces B Biointerfaces*, vol. 122, pp. 134–142, 2014.

[42] D. Cheng, Y. Wen, L. Wang, X. An, X. Zhu, and Y. Ni, "Adsorption of polyethylene glycol (PEG) onto cellulose nano-crystals to improve its dispersity," *Carbohydr. Polym.*, vol. 123, pp. 157–163, 2015.

[43] M. Ulbricht, H. Matuschewski, A. Oechel, and H.-G. Hicke, "Photo-induced graft polymerization surface modifications for the preparation of hydrophilic and low-proten-adsorbing ultrafiltration membranes," *J. Memb. Sci.*, vol. 115, no. 1, pp. 31–47, Jun. 1996.

[44] Y. S. Lin, V. Hlady, and C.-G. Gölander, "The surface density gradient of grafted poly(ethylene glycol): Preparation, characterization and protein adsorption," *Colloids Surfaces B Biointerfaces*, vol. 3, no. 1–2, pp. 49–62, Sep. 1994.

[45] J. Wang *et al.*, "Surface characterization and blood compatibility of poly(ethylene terephthalate) modified by plasma surface grafting," *Surf. Coatings Technol.*, vol. 196, no. 1-3 SPEC. ISS., pp. 307–311, 2005.

[46] S. Jo and K. Park, "Surface modification using silanated poly(ethylene glycol)s," *Biomaterials*, vol. 21, no. 6, pp. 605–616, 2000.

[47] J. H. Kim and S. C. Kim, "PEO-grafting on PU/PS IPNs for enhanced blood compatibility - Effect of pendant length and grafting density," *Biomaterials*, vol. 23, no. 9, pp. 2015–2025, 2002.

[48] K. Park, H. S. Shim, M. K. Dewanjee, and N. L. Eigler, "In vitro and in vivo studies of PEO-grafted blood-contacting cardiovascular prostheses," vol. 5063, 2012.

[49] Q. Zhang, C. Wang, Y. Babukutty, T. Ohyama, M. Kogoma, and M. Kodama, "Biocompatibility evaluation of ePTFE membrane modified with PEG in atmospheric pressure glow discharge," *J. Biomed. Mater. Res.*, vol. 60, no. 3, pp. 502–509, Jun. 2002.

[50] P. Qi, M. F. Maitz, and N. Huang, "Surface modification of cardiovascular materials and implants," *Surf. Coatings Technol.*, vol. 233, pp. 80–90, 2013.

[51] M. Shen *et al.*, "Inhibition of monocyte adhesion and fibrinogen adsorption on glow discharge plasma deposited tetraethylene glycol dimethyl ether," *J. Biomater. Sci. Polym. Ed.*, vol. 12, no. 9, pp. 961–978, 2001.

[52] L. Li, S. Chen, and S. Jiang, "Protein interactions with oligo(ethylene glycol) (OEG) self-assembled monolayers: OEG stability, surface packing density and protein adsorption," *J. Biomater. Sci. Polym. Ed.*, vol. 18, no. 11, pp. 1415–1427, 2007.

[53] J. B. Schlenoff, "Zwitteration: Coating surfaces with zwitterionic functionality to reduce nonspecific adsorption," *Langmuir*, vol. 30, no. 32, pp. 9625–9636, 2014.

[54] X. Ren *et al.*, "Surface modification and endothelialization of biomaterials as potential scaffolds for vascular tissue engineering applications," *Chem. Soc. Rev.*, vol. 44, no. 15, pp. 5680–5742, 2015.

[55] B. Y. Yu *et al.*, "Surface zwitterionization of titanium for a general bio-inert control of plasma proteins, blood cells, tissue cells, and bacteria," *Langmuir*, vol. 30, no. 25, pp. 7502–7512, 2014.

[56] L. Zheng, H. S. Sundaram, Z. Wei, C. Li, and Z. Yuan, "Applications of zwitterionic polymers," *React. Funct. Polym.*, vol. 118, no. March, pp. 51–61, 2017.

[57] P. Li *et al.*, "Hemocompatibility and anti-biofouling property improvement of poly(ethylene terephthalate) via self-polymerization of dopamine and covalent graft of zwitterionic cysteine," *Colloids Surfaces B Biointerfaces*, vol. 110, pp. 327–332, 2013.

[58] M. S. Bretscher and M. C. Raff, "Mammalian plasma membranes," *Nature*, vol. 258, no. 5530, pp. 43–49, 1975.

[59] R. F. A. Zwaal and A. J. Schroit, "Pathophysiologic Implications of Membrane Phospholipid Asymmetry in Blood Cells," *Blood*, vol. 89, no. 4, pp. 1121–1132, Apr. 1997.

[60] Y. Iwasaki and K. Ishihara, "Phosphorylcholine-containing polymers for biomedical applications," *Anal. Bioanal. Chem.*, vol. 381, no. 3, pp. 534–546, 2005.

[61] K. Ishihara, T. Ueda, and N. Nakabayashi, "Preparation of Phospholipid Polymers and Their Properties as Polymer Hydrogel Membranes," *Polymer Journal*, vol. 22, no. 5. pp. 355–360, 1990.

[62] T. Yoneyama, M. Ito, K. ichi Sugihara, K. Ishihara, and N. Nakabayashi, "Small diameter vascular prosthesis with a nonthrombogenic phospholipid polymer surface: Preliminary study of a new concept for functioning in the absence of pseudo- or neointima formation," *Artif. Organs*, vol. 24, no. 1, pp. 23–28, 2000.

[63] T. Yoneyama, K. Sugihara, K. Ishihara, Y. Iwasaki, and N. Nakabayashi, "The vascular prosthesis without pseudointima prepared by antithrombogenic phospholipid polymer," *Biomaterials*, vol. 23, no. 6, pp. 1455–1459, Mar. 2002.

[64] Y. Hong, S. H. Ye, A. Nieponice, L. Soletti, D. A. Vorp, and W. R. Wagner, "A small diameter, fibrous vascular conduit generated from a poly(ester urethane)urea and phospholipid polymer blend," *Biomaterials*, vol. 30, no. 13, pp. 2457–2467, 2009.

[65] L. Soletti *et al.*, "In vivo performance of a phospholipid-coated bioerodable elastomeric graft for small-diameter vascular applications," *J. Biomed. Mater. Res. - Part A*, vol. 96 A, no. 2, pp. 436–448, 2011.

[66] S. E. Sakiyama-Elbert and J. A. Hubbell, "Development of fibrin derivatives for

controlled release of heparin- binding growth factors," *J. Control. Release*, vol. 65, no. 3, pp. 389–402, 2000.

[67] G. Li, P. Yang, W. Qin, M. F. Maitz, S. Zhou, and N. Huang, "The effect of coimmobilizing heparin and fibronectin on titanium on hemocompatibility and endothelialization," *Biomaterials*, vol. 32, no. 21, pp. 4691–4703, 2011.

[68] X. Wang *et al.*, "Extracellular matrix inspired surface functionalization with heparin, fibronectin and VEGF provides an anticoagulant and endothelialization supporting microenvironment," *Appl. Surf. Sci.*, vol. 320, pp. 871–882, 2014.

[69] M. J. B. Wissink *et al.*, "Immobilization of heparin to EDC/NHS-crosslinked collagen. Characterization and in vitro evaluation," *Biomaterials*, vol. 22, no. 2, pp. 151–163, 2001.

[70] M. Hristov, W. Erl, and P. C. Weber, "Endothelial Progenitor Cells," *Arterioscler. Thromb. Vasc. Biol.*, vol. 23, no. 7, pp. 1185–1189, Jul. 2003.

[71] Q. Lin, X. Ding, F. Qiu, X. Song, G. Fu, and J. Ji, "In situ endothelialization of intravascular stents coated with an anti-CD34 antibody functionalized heparin-collagen multilayer," *Biomaterials*, vol. 31, no. 14, pp. 4017–4025, 2010.

[72] W. S. Choi *et al.*, "Enhanced Patency and Endothelialization of Small-Caliber Vascular Grafts Fabricated by Coimmobilization of Heparin and Cell-Adhesive Peptides," *ACS Appl. Mater. Interfaces*, vol. 8, no. 7, pp. 4336–4346, 2016.

[73] Y. Yao *et al.*, "Effect of sustained heparin release from PCL/chitosan hybrid small-diameter vascular grafts on anti-thrombogenic property and endothelialization," *Acta Biomater.*, vol. 10, no. 6, pp. 2739–2749, 2014.

[74] S. Meng *et al.*, "The effect of a layer-by-layer chitosan-heparin coating on the endothelialization and coagulation properties of a coronary stent system," *Biomaterials*, vol. 30, no. 12, pp. 2276–2283, 2009.

[75] J. Chen *et al.*, "Biofunctionalization of titanium with PEG and anti-CD34 for hemocompatibility and stimulated endothelialization," *J. Colloid Interface Sci.*, vol. 368, no. 1, pp. 636–647, 2012.

[76] J. H. Pang *et al.*, "In situ Endothelialization: Bioengineering Considerations to Translation," *Small*, vol. 11, no. 47, pp. 6248–6264, 2015.

[77] Y. M. Shin *et al.*, "Mussel-inspired immobilization of vascular endothelial growth factor (VEGF) for enhanced endothelialization of vascular grafts.," *Biomacromolecules*, vol. 13, no. 7, pp. 2020–2028, 2012.

[78] X. Qiu, B. L. P. Lee, X. Ning, N. Murthy, N. Dong, and S. Li, "End-point immobilization of heparin on plasma-treated surface of electrospun polycarbonate-urethane vascular graft," *Acta Biomater.*, vol. 51, pp. 138–147, 2017.

[79] K. Ishihara, H. Nomura, T. Mihara, K. Kurita, Y. Iwasaki, and N. Nakabayashi, "Why do phospholipid polymers reduce protein adsorption?," *J. Biomed. Mater. Res.*, vol. 39, no. 2, pp. 323–330, Feb. 1998.

[80] C. Chen, J. C. Ofenloch, Y. P. Yianni, S. R. Hanson, and A. B. Lumsden, "Phosphorylcholine coating of ePTFE reduces platelet deposition and neointimal hyperplasia in arteriovenous grafts," *J. Surg. Res.*, vol. 77, no. 2, pp. 119–125, 1998.

[81] P. Chevallier, R. Janvier, D. Mantovani, and G. Laroche, "In vitro biological performances of phosphorylcholine-grafted ePTFE prostheses through RFGD plasma techniques," *Macromol. Biosci.*, vol. 5, no. 9, pp. 829–839, 2005.

[82] M. C. Sin, S. H. Chen, and Y. Chang, "Hemocompatibility of zwitterionic interfaces and membranes," *Polym. J.*, vol. 46, no. 8, pp. 436–443, 2014.

[83] R. S. Smith *et al.*, "Vascular Catheters with a Nonleaching Poly-Sulfobetaine Surface Modification Reduce Thrombus Formation and Microbial Attachment," *Sci. Transl. Med.*, vol. 4, no. 153, pp. 153ra132-153ra132, 2012.

[84] Y. L. Liu, C. C. Han, T. A. C. Wei, and Y. Chang, "Surface-initiated atom transfer radical polymerization from porous poly(tetrafluoroethylene) membranes using the C-F groups as initiators," *J. Polym. Sci. Part A Polym. Chem.*, vol. 48, no. 10, pp. 2076–2083, 2010.

[85] W. Yang *et al.*, "Film thickness dependence of protein adsorption from blood serum and plasma onto poly(sulfobetaine)-grafted surfaces," *Langmuir*, vol. 24, no. 17, pp. 9211–9214, 2008.

[86] J. Ran, L. Wu, Z. Zhang, and T. Xu, "Atom transfer radical polymerization (ATRP): A versatile and forceful tool for functional membranes," *Prog. Polym. Sci.*, vol. 39, no. 1, pp. 124–144, Sep. 2013.

[87] A. Dekker, K. Reitsma, T. Beugeling, A. Bantjes, J. Feijen, and W. G. van Aken, "Adhesion of endothelial cells and adsorption of serum proteins on gas plasma-treated polytetrafluoroethylene," *Biomaterials*, vol. 12, no. 2, pp. 130–138, 1991.

[88] P. K. Chu, J. Y. Chen, L. P. Wang, and N. Huang, "Plasma-surface modification of biomaterials," *Mater. Sci. Eng. R Reports*, vol. 36, no. 5–6, pp. 143–206, Mar. 2002.

[89] A. I. Cassady, N. M. Hidzir, and L. Grøndahl, "Enhancing expanded poly(tetrafluoroethylene) (ePTFE) for biomaterials applications," *J. Appl. Polym. Sci.*, vol. 131, no. 15, 2014.

[90] M. M. Bilek and D. R. McKenzie, "Plasma modified surfaces for covalent immobilization of functional biomolecules in the absence of chemical linkers: Towards better biosensors and a new generation of medical implants," *Biophys. Rev.*, vol. 2, no. 2, pp. 55–65, 2010.

[91] F. R. Pu, R. L. Williams, T. K. Markkula, and J. A. Hunt, "Effects of plasma treated PET and PTFE on expression of adhesion molecules by human endothelial cells in vitro," *Biomaterials*, vol. 23, no. 11, pp. 2411–2428, 2002.

[92] M. Crombez, P. Chevallier, R. C. Gaudreault, E. Petitclerc, D. Mantovani, and G. Laroche, "Improving arterial prosthesis neo-endothelialization: Application of a proactive VEGF construct onto PTFE surfaces," *Biomaterials*, vol. 26, no. 35, pp. 7402–7409, 2005.

[93] K. Vallières, É. Petitclerc, and G. Laroche, "Covalent grafting of fibronectin onto plasma-treated PTFE: Influence of the conjugation strategy on fibronectin biological activity," *Macromol. Biosci.*, vol. 7, no. 5, pp. 738–745, 2007.

[94] T. Chandy, G. S. Das, R. F. Wilson, and G. H. R. Rao, "Use of plasma glow for surface-engineering biomolecules to enhance bloodcompatibility of Dacron and PTFE vascular prosthesis," *Biomaterials*, vol. 21, no. 7, pp. 699–712, 2000.

[95] L. Xue and H. P. Greisler, "Biomaterials in the development and future of vascular grafts," *J. Vasc. Surg.*, vol. 37, no. 2, pp. 472–480, 2003.

[96] S. Gore, J. Andersson, R. Biran, C. Underwood, and J. Riesenfeld, "Heparin surfaces: Impact of immobilization chemistry on hemocompatibility and protein adsorption," *J. Biomed. Mater. Res. - Part B Appl. Biomater.*, vol. 102, no. 8, pp. 1817–1824, 2014.

[97] M. S. Lord, W. Yu, B. Cheng, A. Simmons, L. Poole-Warren, and J. M. Whitelock, "The modulation of platelet and endothelial cell adhesion to vascular graft materials by perlecan," *Biomaterials*, vol. 30, no. 28, pp. 4898–4906, 2009.

[98] T. Liu *et al.*, "Surface modification with dopamine and heparin/poly-l-lysine nanoparticles provides a favorable release behavior for the healing of vascular stent lesions," *ACS Appl. Mater. Interfaces*, vol. 6, no. 11, pp. 8729–8743, 2014.

[99] P. Dong, W. Hao, X. Wang, and T. Wang, "Fabrication and biocompatibility of polyethyleneimine/heparin self-assembly coating on NiTi alloy," *Thin Solid Films*, vol. 516, no. 16, pp. 5168–5171, 2008.

[100] J. Laredo, L. Xue, V. A. Husak, J. Ellinger, and H. P. Greisler, "Silyl-heparin adsorption improves the in vivo thromboresistance of carbon-coated polytetrafluoroethylene vascular grafts," *Am. J. Surg.*, vol. 186, no. 5, pp. 556–560, 2003.

[101] J. Sanchez, G. Elgue, J. Riesenfeld, and P. Olsson, "Control of contact activation on end-point immobilized heparin: The role of antithrombin and the specific antithrombin-binding sequence," *J. Biomed. Mater. Res.*, vol. 29, no. 5, pp. 655–661, 1995.

[102] P. C. Begovac, R. C. Thomson, J. L. Fisher, A. Hughson, and A. Gällhagen, "Improvements in GORE-TEX® vascular graft performance by Carmeda® BioActive Surface heparin immobilization," *Eur. J. Vasc. Endovasc. Surg.*, vol. 25, no. 5, pp. 432–437, 2003.

[103] J. H. Jiang, L. P. Zhu, X. L. Li, Y. Y. Xu, and B. K. Zhu, "Surface modification of PE porous membranes based on the strong adhesion of polydopamine and covalent immobilization of heparin," *J. Memb. Sci.*, vol. 364, no. 1–2, pp. 194–202, 2010.

[104] Y. Byun, H. A. Jacobs, and S. Wan Kim, "Heparin surface immobilization through hydrophilic spacers: Thrombin and antithrombin III binding kinetics," *J. Biomater. Sci. Polym. Ed.*, vol. 6, no. 1, pp. 1–13, Jan. 1995.

[105] K. N. Pandiyaraj, V. Selvarajan, Y. H. Rhee, H. W. Kim, and S. I. Shah, "Glow

discharge plasma-induced immobilization of heparin and insulin on polyethylene terephthalate film surfaces enhances anti-thrombogenic properties," *Mater. Sci. Eng. C*, vol. 29, no. 3, pp. 796–805, 2009.

[106] C. J. Pan, Y. H. Hou, B. Bin Zhang, Y. X. Dong, and H. Y. Ding, "Blood compatibility and interaction with endothelial cells of titanium modified by sequential immobilization of poly (ethylene glycol) and heparin," *J. Mater. Chem. B*, vol. 2, no. 7, pp. 892–902, 2014.

[107] K. D. Park, T. Okano, C. Nojiri, and S. W. Kim, "Heparin immobilization onto segmented polyurethaneurea surfaces?effect of hydrophilic spacers," *J. Biomed. Mater. Res.*, vol. 22, no. 11, pp. 977–992, Nov. 1988.

[108] C. Nojiri *et al.*, "In vivo nonthrombogenicity of heparin immobilized polymer surfaces," *ASAIO Trans*, vol. 36, no. 3, pp. M168-72, 1990.

[109] Y. Shan, B. Jia, M. Ye, H. Shen, W. Chen, and H. Zhang, "Application of Heparin/Collagen-REDV Selective Active Interface on ePTFE Films to Enhance Endothelialization and Anticoagulation," *Artif. Organs*, vol. 42, no. 8, pp. 824–834, 2018.

[110] A. P. Zhu, Z. Ming, and S. Jian, "Blood compatibility of chitosan/heparin complex surface modified ePTFE vascular graft," *Appl. Surf. Sci.*, vol. 241, no. 3–4, pp. 485–492, 2005.

[111] G. C. Li, Q. F. Xu, and P. Yang, "Inhibiting smooth muscle cell proliferation via immobilization of heparin/fibronectin complexes on titanium surfaces," *Biomed. Environ. Sci.*, vol. 28, no. 5, pp. 378–382, 2015.

[112] K. Zhang, J.-A. Li, K. Deng, T. Liu, J.-Y. Chen, and N. Huang, "The endothelialization and hemocompatibility of the functional multilayer on titanium surface constructed with type IV collagen and heparin," *Colloids Surfaces B Biointerfaces*, vol. 108, no. 1, pp. 295–304, Aug. 2013.

[113] G. Li, F. Zhang, Y. Liao, P. Yang, and N. Huang, "Coimmobilization of heparin/fibronectin mixture on titanium surfaces and their blood compatibility," *Colloids Surfaces B Biointerfaces*, vol. 81, no. 1, pp. 255–262, 2010.

[114] J. Andersson, J. Sanchez, K. N. Ekdahl, G. Elgue, B. Nilsson, and R. Larsson, "Optimal heparin surface concentration and antithrombin binding capacity as evaluated with human non-anticoagulated blood in vitro," *J. Biomed. Mater. Res. - Part A*, vol. 67, no. 2, pp. 458–466, 2003.

[115] J. W. Yau *et al.*, "Corn trypsin inhibitor coating attenuates the prothrombotic properties of catheters in vitro and in vivo," *Acta Biomater.*, vol. 8, no. 11, pp. 4092–4100, 2012.

[116] S. Alibeik, S. Zhu, J. W. Yau, J. I. Weitz, and J. L. Brash, "Surface modification with polyethylene glycol-corn trypsin inhibitor conjugate to inhibit the contact factor pathway on blood-contacting surfaces," *Acta Biomater.*, vol. 7, no. 12, pp. 4177–4186, 2011.

[117] M. Heise *et al.*, "PEG-hirudin/iloprost Coating of Small Diameter ePTFE Grafts Effectively Prevents Pseudointima and Intimal Hyperplasia Development," *Eur. J. Vasc. Endovasc. Surg.*, vol. 32, no. 4, pp. 418–424, 2006.

[118] J. Li *et al.*, "Immobilization of Human Thrombomodulin to Expanded Polytetrafluoroethylene," *J. Surg. Res.*, vol. 105, no. 2, pp. 200–208, Jun. 2002.

[119] G. Wong, J. ming Li, G. Hendricks, M. H. Eslami, M. J. Rohrer, and B. S. Cutler, "Inhibition of experimental neointimal hyperplasia by recombinant human thrombomodulin coated ePTFE stent grafts," *J. Vasc. Surg.*, vol. 47, no. 3, pp. 608–615, 2008.

[120] Z. Zhou and M. E. Meyerhoff, "Preparation and characterization of polymeric coatings with combined nitric oxide release and immobilized active heparin," *Biomaterials*, vol. 26, no. 33, pp. 6506–6517, Nov. 2005.

[121] S. Alibeik, S. Zhu, J. W. Yau, J. I. Weitz, and J. L. Brash, "Modification of Polyurethane with Polyethylene Glycol-Corn Trypsin Inhibitor for Inhibition of Factor XIIa in Blood Contact," *J. Biomater. Sci. Ed.*, vol. 23, no. 15, pp. 1981–1993, 2012.

[122] S. Alibeik, S. Zhu, J. W. Yau, J. I. Weitz, and J. L. Brash, "Dual surface modification with PEG and corn trypsin inhibitor: Effect of PEG:CTI ratio on protein resistance and anticoagulant properties," *J. Biomed. Mater. Res. - Part A*, vol. 100 A, no. 4, pp. 856–862, 2012.

[123] S. W. Jordan and E. L. Chaikof, "Novel thromboresistant materials," *J. Vasc. Surg.*, vol. 45, no. 6 SUPPL., pp. 104–115, 2007.

[124] A. Kishida, Y. Ueno, N. Fukudome, E. Yashima, I. Maruyama, and M. Akashi, "Immobilization of human thrombomodulin onto poly(ether urethane urea) for developing antithrombogenic blood-contacting materials," *Biomaterials*, vol. 15, no. 10, pp. 848–852, 1994.

[125] C. Sperling, K. Salchert, U. Streller, and C. Werner, "Covalently immobilized thrombomodulin inhibits coagulation and complement activation of artificial surfaces in vitro," *Biomaterials*, vol. 25, no. 21, pp. 5101–5113, 2004.

[126] H. S. Han, S. L. Yang, H. Y. Yeh, J. C. Lin, H. L. Wu, and G. Y. Shi, "Studies of a novel human thrombomodulin immobilized substrate: Surface characterization and anticoagulation activity evaluation," *J. Biomater. Sci. Polym. Ed.*, vol. 12, no. 10, pp. 1075–1089, 2001.

[127] P.-Y. Tseng, S. S. Rele, X.-L. Sun, and E. L. Chaikof, "Membrane–mimetic films containing thrombomodulin and heparin inhibit tissue factor-induced thrombin generation in a flow model," *Biomaterials*, vol. 27, no. 12, pp. 2637–2650, Apr. 2006.

[128] Z. Qu *et al.*, "Immobilization of Actively Thromboresistant Assemblies on Sterile Blood-Contacting Surfaces," *Adv. Healthc. Mater.*, vol. 3, no. 1, pp. 30–35, 2014.

[129] Z. Qu *et al.*, "A biologically active surface enzyme assembly that attenuates

thrombus formation," *Adv. Funct. Mater.*, vol. 21, no. 24, pp. 4736–4743, 2011.

[130] R. Jiang, J. Weingart, H. Zhang, Y. Ma, and X. L. Sun, "End-point immobilization of recombinant thrombomodulin via sortase-mediated ligation," *Bioconjug. Chem.*, vol. 23, no. 3, pp. 643–649, 2012.

[131] A. De Mel, F. Murad, and A. M. Seifalian, "Nitric oxide: A guardian for vascular grafts?," *Chem. Rev.*, vol. 111, no. 9, pp. 5742–5767, 2011.

[132] A. de Mel, G. Jell, M. M. Stevens, and A. M. Seifalian, "Biofunctionalization of biomaterials for accelerated in situ endothelialization: A review," *Biomacromolecules*, vol. 9, no. 11, pp. 2969–2979, 2008.

[133] D. J. Smith *et al.*, "Nitric oxide-releasing polymers containing the [N(O)NO]-group," *J. Med. Chem.*, vol. 39, no. 5, pp. 1148–1156, 1996.

[134] S. K. Pulfer, D. Ott, and D. J. Smith, "Incorporation of nitric oxide-releasing crosslinked polyethyleneimine microspheres into vascular grafts," *J. Biomed. Mater. Res.*, vol. 37, no. 2, pp. 182–189, 1997.

[135] K. A. Mowery, M. H. Schoenfisch, J. E. Saavedra, L. K. Keefer, and M. E. Meyerhoff, "Preparation and characterization of hydrophobic polymeric films that are thromboresistant via nitric oxide release," *Biomaterials*, vol. 21, no. 1, pp. 9–21, 2000.

[136] X. Duan and R. S. Lewis, "Improved haemocompatibility of cysteine-modified polymers via endogenous nitric oxide," *Biomaterials*, vol. 23, no. 4, pp. 1197–1203, 2002.

[137] B. K. Oh and M. E. Meyerhoff, "Catalytic generation of nitric oxide from nitrite at the interface of polymeric films doped with lipophilic Cu(II)-complex: A potential route to the preparation of thromboresistant coatings," *Biomaterials*, vol. 25, no. 2, pp. 283–293, 2004.

[138] S. Hwang and M. E. Meyerhoff, "Polyurethane with tethered copper(II)-cyclen complex: Preparation, characterization and catalytic generation of nitric oxide from S-nitrosothiols," *Biomaterials*, vol. 29, no. 16, pp. 2443–2452, 2008.

[139] Z. Yang *et al.*, "Nitric oxide producing coating mimicking endothelium function for multifunctional vascular stents," *Biomaterials*, vol. 63, pp. 80–92, 2015.

[140] M. Deutsch, J. Meinhart, T. Fischlein, P. Preiss, and P. Zilla, "Clinical autologous in vitro endothelialization of infrainguinal ePTFE grafts in 100 patients: A 9-year experience," *Surgery*, vol. 126, no. 5, pp. 847–855, 1999.

[141] T. Fischlein, M. Deutsch, P. Zilla, J. Meinhart, and P. Preiss, "Clinical autologous in vitro endothelialization of infrainguinal ePTFE grafts in 100 patients: A 9-year experience," *Surgery*, vol. 126, no. 5, pp. 0847–0855, 2002.

[142] P. Fernandez, A. Deguette, L. Pothuaud, G. Belleannée, P. Coste, and L. Bordenave, "Quality control assessment of ePTFE precoating procedure for in vitro endothelial cell seeding," *Biomaterials*, vol. 26, no. 24, pp. 5042–5047, 2005.

[143] M. Avci-Adali, G. Ziemer, and H. P. Wendel, "Induction of EPC homing on biofunctionalized vascular grafts for rapid in vivo self-endothelialization - A review of current strategies," *Biotechnol. Adv.*, vol. 28, no. 1, pp. 119–129, 2010.

[144] M. Avci-Adali, N. Perle, G. Ziemer, and H. P. Wendel, "Current concepts and new developments for autologous in vivo endothelialisation of biomaterials for intravascular applications," *Eur. Cells Mater.*, vol. 21, pp. 157–176, 2011.

[145] N. Ferrara, H. Gerber, and J. LeCouter, "The biology of VEGF and its receptors," *Nat. Med.*, vol. 9, no. 6, pp. 669–676, Jun. 2003.

[146] A. Eichmann and M. Simons, "VEGF signaling inside vascular endothelial cells and beyond," *Curr. Opin. Cell Biol.*, vol. 24, no. 2, pp. 188–193, 2012.

[147] H. G. Wang *et al.*, "Biofunctionalization of titanium surface with multilayer films modified by heparin-VEGF-fibronectin complex to improve endothelial cell proliferation and blood compatibility," *J. Biomed. Mater. Res. - Part A*, vol. 101 A, no. 2, pp. 413–420, 2013.

[148] H. Xu, K. T. Nguyen, E. S. Brilakis, J. Yang, E. Fuh, and S. Banerjee, "Enhanced endothelialization of a new stent polymer through surface enhancement and incorporation of growth factor-delivering microparticles," *J. Cardiovasc. Transl. Res.*, vol. 5, no. 4, pp. 519–527, 2012.

[149] R. K. Jain, "Tumor angiogenesis and accessibility: Role of vascular endothelial growth factor," *Semin. Oncol.*, vol. 29, no. 6Q, pp. 3–9, 2003.

[150] B. Randone *et al.*, "Dual Role of VEGF in Pretreated Experimental ePTFE Arterial Grafts," *J. Surg. Res.*, vol. 127, no. 2, pp. 70–79, 2005.

[151] B. H. Walpoth *et al.*, "Enhanced intimal thickening of expanded polytetrafluoroethylene grafts coated with fibrin or fibrin-releasing vascular endothelial growth factor in the pig carotid artery interposition model," *J. Thorac. Cardiovasc. Surg.*, vol. 133, no. 5, pp. 1163–1170, 2007.

[152] P. De La Puente, B. Muz, F. Azab, and A. K. Azab, "Cell trafficking of endothelial progenitor cells in tumor progression," *Clin. Cancer Res.*, vol. 19, no. 13, pp. 3360–3368, 2013.

[153] Q. L. Li *et al.*, "Oriented immobilization of anti-CD34 antibody on titanium surface for self-endothelialization induction," *J. Biomed. Mater. Res. - Part A*, vol. 94, no. 4, pp. 1283–1293, 2010.

[154] F. Yang *et al.*, "Combination coating of chitosan and anti-CD34 antibody applied on sirolimus-eluting stents can promote endothelialization while reducing neointimal formation," *BMC Cardiovasc. Disord.*, vol. 12, no. 1, p. 96, 2012.

[155] M. Yin, Y. Yuan, C. Liu, and J. Wang, "Combinatorial coating of adhesive polypeptide and anti-CD34 antibody for improved endothelial cell adhesion and proliferation," *J. Mater. Sci. Mater. Med.*, vol. 20, no. 7, pp. 1513–1523, 2009.

[156] P. Damman *et al.*, "Duration of dual antiplatelet therapy and outcomes after coronary

stenting with the genous TM bio-engineered R Stent TMin patients from the e-HEALING Registry," *Catheter. Cardiovasc. Interv.*, vol. 79, no. 2, pp. 243–252, 2012.

[157] M. A. M. Beijk *et al.*, "Genous^{TM} endothelial progenitor cell capturing stent vs. the Taxus Liberté stent in patients with de novo coronary lesions with a high-risk of coronary restenosis: A randomized, single-centre, pilot study," *Eur. Heart J.*, vol. 31, no. 9, pp. 1055–1064, 2010.

[158] J. Chen, Q. Li, J. Li, and M. F. Maitz, "The effect of anti-CD34 antibody orientation control on endothelial progenitor cell capturing cardiovascular devices," *J. Bioact. Compat. Polym.*, vol. 31, no. 6, pp. 583–599, 2016.

[159] J. Aoki *et al.*, "Endothelial progenitor cell capture by stents coated with antibody against CD34: The HEALING-FIM (Healthy Endothelial Accelerated Lining Inhibits Neointimal Growth-First in Man) registry," *J. Am. Coll. Cardiol.*, vol. 45, no. 10, pp. 1574–1579, 2005.

[160] M. Co *et al.*, "Use of endothelial progenitor cell capture stent (Genous Bio-Engineered R Stent) during primary percutaneous coronary intervention in acute myocardial infarction: Intermediate- to long-term clinical follow-up," *Am. Heart J.*, vol. 155, no. 1, pp. 128–132, 2008.

[161] E. Ribeiro *et al.*, "Clinical results after coronary stenting with the Genous^{TM} Bio-engineered R stent^{TM}: 12-month outcomes of the e-HEALING (Healthy Endothelial Accelerated Lining Inhibits Neointimal Growth) worldwide registry," *EuroIntervention*, vol. 6, no. 7, pp. 819–825, 2011.

[162] J. Li, D. Li, F. Gong, S. Jiang, H. Yu, and Y. An, "Anti-CD133 antibody immobilized on the surface of stents enhances endothelialization," *Biomed Res. Int.*, vol. 2014, 2014.

[163] A. Sedaghat, J. M. Sinning, K. Paul, G. Kirfel, G. Nickenig, and N. Werner, "First in vitro and in vivo results of an anti-human CD133-antibody coated coronary stent in the porcine model," *Clin. Res. Cardiol.*, vol. 102, no. 6, pp. 413–425, 2013.

[164] H. Su *et al.*, "The effect of anti-CD133/fucoidan bio-coatings on hemocompatibility and EPC capture," *J. Biomater. Sci. Polym. Ed.*, vol. 28, no. 17, pp. 2066–2081, 2017.

[165] B. D. Markway, M. T. Hinds, U. M. Marzec, S. R. Hanson, D. W. Courtman, and O. J. T. McCarty, "Capture of Flowing Endothelial Cells Using Surface-Immobilized Anti-Kinase Insert Domain Receptor Antibody," *Tissue Eng. Part C Methods*, vol. 14, no. 2, pp. 97–105, 2008.

[166] S. Liebler, F. Grunert, J. Thompson, M. Wedel, and B. Schlosshauer, "Towards a biofunctionalized vascular prosthesis: immune cell trapping via a growth factor receptor," *J. Tissue Eng. Regen. Med.*, vol. 11, no. 10, pp. 2699–2709, 2017.

[167] S. K. Murthy, T. Kniazeva, J. E. Mayer, V. L. Sales, and B. D. Plouffe, "Development of microfluidics as endothelial progenitor cell capture technology for

cardiovascular tissue engineering and diagnostic medicine," *FASEB J.*, vol. 23, no. 10, pp. 3309–3314, 2009.

[168] T. Matsuda, M. Kuwana, T. Aomizu, M. Yamagishi, H. Ohtake, and G. Watanabe, "Surface design for in situ capture of endothelial progenitor cells: VEGF-bound surface architecture and behaviors of cultured mononuclear cells," *J. Biomed. Mater. Res. Part B Appl. Biomater.*, vol. 101B, no. 1, pp. 50–60, Jan. 2013.

[169] D. Kawahara and T. Matsuda, "Hydrodynamic shear-stress-dependent retention of endothelial and endothelial progenitor cells adhered to vascular endothelial growth factor-fixed surfaces," *J. Biomed. Mater. Res. - Part B Appl. Biomater.*, vol. 100 B, no. 5, pp. 1218–1228, 2012.

[170] J. H. Dirks and W. Federle, "Mechanisms of fluid production in smooth adhesive pads of insects," *J. R. Soc. Interface*, vol. 8, no. 60, pp. 952–960, 2011.

[171] L. Gaume, P. Perret, E. Gorb, S. Gorb, J. J. Labat, and N. Rowe, "How do plant waxes cause flies to slide? Experimental tests of wax-based trapping mechanisms in three pitfall carnivorous plants," *Arthropod Struct. Dev.*, vol. 33, no. 1, pp. 103–111, 2004.

[172] H. F. Bohn and W. Federle, "Insect aquaplaning: Nepenthes pitcher plants capture prey with the peristome, a fully wettable water-lubricated anisotropic surface," *Proc. Natl. Acad. Sci.*, vol. 101, no. 39, pp. 14138–14143, 2004.

[173] D. Jan-Henning, C. C. J., and F. Walter, "Insect tricks: two-phasic foot pad secretion prevents slipping," *J. R. Soc. Interface*, vol. 7, no. 45, pp. 587–593, 2010.

[174] D. C. Leslie *et al.*, "A bioinspired omniphobic surface coating on medical devices prevents thrombosis and biofouling.," *Nat. Biotechnol.*, vol. 32, no. 11, pp. 1134–40, 2014.

[175] J. Chen *et al.*, "An immobilized liquid interface prevents device associated bacterial infection in vivo," *Biomaterials*, vol. 113, pp. 80–92, Jan. 2017.

[176] X. Huang, J. D. Chrisman, and N. S. Zacharia, "Omniphobic slippery coatings based on lubricant-infused porous polyelectrolyte multilayers," *ACS Macro Lett.*, vol. 2, no. 9, pp. 826–829, 2013.

[177] M. J. Kratochvil, M. A. Welsh, U. Manna, B. J. Ortiz, H. E. Blackwell, and D. M. Lynn, "Slippery Liquid-Infused Porous Surfaces that Prevent Bacterial Surface Fouling and Inhibit Virulence Phenotypes in Surrounding Planktonic Cells," *ACS Infect. Dis.*, vol. 2, no. 7, pp. 509–517, 2016.

[178] M. Badv, I. H. Jaffer, J. I. Weitz, and T. F. Didar, "An omniphobic lubricant-infused coating produced by chemical vapor deposition of hydrophobic organosilanes attenuates clotting on catheter surfaces," *Sci. Rep.*, vol. 7, no. 1, p. 11639, 2017.

[179] T.-S. Wong *et al.*, "Bioinspired self-repairing slippery surfaces with pressure-stable omniphobicity.," *Nature*, vol. 477, no. 7365, pp. 443–7, 2011.

[180] A. K. Epstein, T.-S. Wong, R. a Belisle, E. M. Boggs, and J. Aizenberg, "Liquid-

infused structured surfaces with exceptional anti-biofouling performance," *Proc. Natl. Acad. Sci. U. S. A.*, vol. 109, no. 33, pp. 13182–13187, 2012.

[181] I. Sotiri, J. C. Overton, A. Waterhouse, and C. Howell, "Immobilized liquid layers: a new approach to anti-adhesion surface for medical applications.," *Exp. Biol. Med.*, vol. in press, no. 9, pp. 1–10, 2016.

[182] M. Badv, S. M. Imani, J. I. Weitz, and T. F. Didar, "Lubricant-Infused Surfaces with Built-In Functional Biomolecules Exhibit Simultaneous Repellency and Tunable Cell Adhesion," *ACS Nano*, vol. 12, no. 11, pp. 10890–10902, Nov. 2018.

[183] J. Li *et al.*, "Hydrophobic liquid-infused porous polymer surfaces for antibacterial applications," *ACS Appl. Mater. Interfaces*, vol. 5, no. 14, pp. 6704–6711, 2013.

[184] S. Zouaghi *et al.*, "Antifouling Biomimetic Liquid-Infused Stainless Steel: Application to Dairy Industrial Processing," *ACS Appl. Mater. Interfaces*, vol. 9, no. 31, pp. 26565–26573, 2017.

[185] A. Hosseini *et al.*, "Conductive Electrochemically Active Lubricant-Infused Nanostructured Surfaces Attenuate Coagulation and Enable Friction-Less Droplet Manipulation," *Adv. Mater. Interfaces*, vol. 5, no. 18, p. 1800617, Sep. 2018.

[186] P. Wang, Z. Lu, and D. Zhang, "Slippery liquid-infused porous surfaces fabricated on aluminum as a barrier to corrosion induced by sulfate reducing bacteria," *Corros. Sci.*, vol. 93, pp. 159–166, 2015.

[187] P. Wang, D. Zhang, Z. Lu, and S. Sun, "Fabrication of Slippery Lubricant-Infused Porous Surface for Inhibition of Microbially Influenced Corrosion," *ACS Appl. Mater. Interfaces*, vol. 8, no. 2, pp. 1120–1127, 2016.

[188] M. Villegas, Z. Cetinic, A. Shakeri, and T. F. Didar, "Fabricating smooth PDMS microfluidic channels from low-resolution 3D printed molds using an omniphobic lubricant-infused coating," *Anal. Chim. Acta*, vol. 1000, pp. 248–255, 2018.

[189] F. Zhang *et al.*, "Chemical vapor deposition of three aminosilanes on silicon dioxide: Surface characterization, stability, effects of silane concentration, and cyanine dye adsorption," *Langmuir*, vol. 26, no. 18, pp. 14648–14654, 2010.

[190] K. Manabe, K. H. Kyung, and S. Shiratori, "Biocompatible slippery fluid-infused films composed of chitosan and alginate via layer-by-layer self-assembly and their antithrombogenicity," *ACS Appl. Mater. Interfaces*, vol. 7, no. 8, pp. 4763–4771, 2015.

[191] U. Manna and D. M. Lynn, "Fabrication of liquid-infused surfaces using reactive polymer multilayers: Principles for manipulating the behaviors and mobilities of aqueous fluids on slippery liquid interfaces," *Adv. Mater.*, vol. 27, no. 19, pp. 3007–3012, 2015.

[192] S. Sunny, N. Vogel, C. Howell, T. L. Vu, and J. Aizenberg, "Lubricant-Infused Nanoparticulate Coatings Assembled by Layer-by-Layer Deposition," *Adv. Funct. Mater.*, vol. 24, no. 42, pp. 6658–6667, 2014.

[193] S. Yuan, S. Luan, S. Yan, H. Shi, and J. Yin, "Facile Fabrication of Lubricant-Infused Wrinkling Surface for Preventing Thrombus Formation and Infection," *ACS Appl. Mater. Interfaces*, vol. 7, no. 34, pp. 19466–19473, 2015.

[194] Q. Wei *et al.*, "Supramolecular polymers as surface coatings: Rapid fabrication of healable superhydrophobic and slippery surfaces," *Adv. Mater.*, vol. 26, no. 43, pp. 7358–7364, 2014.

[195] C. Howell *et al.*, "Stability of surface-immobilized lubricant interfaces under flow," *Chem. Mater.*, vol. 27, no. 5, pp. 1792–1800, 2015.

[196] P. Kim, T. S. Wong, J. Alvarenga, M. J. Kreder, W. E. Adorno-Martinez, and J. Aizenberg, "Liquid-infused nanostructured surfaces with extreme anti-ice and anti-frost performance," *ACS Nano*, vol. 6, no. 8, pp. 6569–6577, 2012.

[197] N. Maccallum *et al.*, "Liquid-Infused Silicone As a Biofouling-Free Medical Material," *ACS Biomater. Sci. Eng.*, vol. 1, no. 1, pp. 43–51, 2015.

[198] C. Howell *et al.*, "Self-replenishing vascularized fouling-release surfaces," *ACS Appl. Mater. Interfaces*, vol. 6, no. 15, pp. 13299–13307, 2014.

[199] P. Lo *et al.*, "Transparent antifouling material for improved operative field visibility in endoscopy," *Proc. Natl. Acad. Sci.*, vol. 113, no. 42, pp. 11676–11681, 2016.

[200] A. B. Tesler, P. Kim, S. Kolle, C. Howell, O. Ahanotu, and J. Aizenberg, "Extremely durable biofouling-resistant metallic surfaces based on electrodeposited nanoporous tungstite films on steel," *Nat. Commun.*, vol. 6, pp. 1–10, 2015.

[201] J. A. Wilimas *et al.*, "Management of occlusion and thrombosis associated with long-term indwelling central venous catheters," *Lancet*, vol. 374, no. 9684, pp. 159–169, 2009.

[202] D. Press, "Role of duration of catheterization and length of hospital stay on the rate of catheter-related hospital-acquired urinary tract infections," *Res. Reports Urol.*, pp. 41–47, 2015.

[203] N. S. K. Gunda, M. Singh, L. Norman, K. Kaur, and S. K. Mitra, "Optimization and characterization of biomolecule immobilization on silicon substrates using (3-aminopropyl)triethoxysilane (APTES) and glutaraldehyde linker," *Appl. Surf. Sci.*, vol. 305, pp. 522–530, 2014.

[204] T. F. Didar, K. Bowey, G. Almazan, and M. Tabrizian, "A miniaturized multipurpose platform for rapid, label-free, and simultaneous separation, patterning, and in vitro culture of primary and rare cells," *Adv. Healthc. Mater.*, vol. 3, no. 2, pp. 253–260, 2014.

[205] B. D. Ratner, "The catastrophe revisited: Blood compatibility in the 21st Century," *Biomaterials*, vol. 28, no. 34, pp. 5144–5147, 2007.

[206] A. Y. Y. Lee and P. W. Kamphuisen, "Epidemiology and prevention of catheter-related thrombosis in patients with cancer," *J. Thromb. Haemost.*, vol. 10, no. 8, pp. 1491–1499, 2012.

[207] E. A. Vogler and C. A. Siedlecki, "Contact activation of blood-plasma coagulation," *Biomaterials*, vol. 30, no. 10, pp. 1857–1869, 2009.

[208] C. J. Wilson, R. E. Clegg, D. I. Leavesley, and M. J. Pearcy, "Mediation of Biomaterial–Cell Interactions by Adsorbed Proteins : A Review," *Tissue Eng.*, vol. 11, no. 1, 2005.

[209] N. Weber, H. P. Wendel, and G. Ziemer, "Hemocompatibility of heparin-coated surfaces and the role of selective plasma protein adsorption," *Biomaterials*, vol. 23, no. 2, pp. 429–439, 2002.

[210] C. Mao *et al.*, "Various approaches to modify biomaterial surfaces for improving hemocompatibility," *Adv. Colloid Interface Sci.*, vol. 110, no. 1–2, pp. 5–17, 2004.

[211] L. D. Unsworth, Z. Tun, H. Sheardown, and J. L. Brash, "Chemisorption of thiolated poly(ethylene oxide) to gold: Surface chain densities measured by ellipsometry and neutron reflectometry," *J. Colloid Interface Sci.*, vol. 281, no. 1, pp. 112–121, 2005.

[212] L. D. Unsworth, H. Sheardown, and J. L. Brash, "Polyethylene oxide surfaces of variable chain density by chemisorption of PEO-thiol on gold: Adsorption of proteins from plasma studied by radiolabelling and immunoblotting," *Biomaterials*, vol. 26, no. 30, pp. 5927–5933, 2005.

[213] J. H. Lee, H. B. Lee, and J. D. Andrade, "Blood compatibility of polyethylene oxide surfaces," *Prog. Polym. Sci.*, vol. 20, no. 6, pp. 1043–1079, 1995.

[214] M. Shen, L. Martinson, M. S. Wagner, D. G. Castner, B. D. Ratner, and T. a Horbett, "PEO-like plasma polymerized tetraglyme surface interactions with leukocytes and proteins: in vitro and in vivo studies.," *J. Biomater. Sci. Polym. Ed.*, vol. 13, no. 4, pp. 367–90, 2002.

[215] H. Chen, Z. Zhang, Y. Chen, M. A. Brook, and H. Sheardown, "Protein repellant silicone surfaces by covalent immobilization of poly(ethylene oxide)," *Biomaterials*, vol. 26, no. 15, pp. 2391–2399, 2005.

[216] Z. Jin, W. Feng, S. Zhu, H. Sheardown, and J. L. Brash, "Protein-resistant polyurethane via surface-initiated atom transfer radical polymerization of oligo(ethylene glycol) methacrylate," *J. Biomed. Mater. Res. - Part A*, vol. 91, no. 4, pp. 1189–1201, 2009.

[217] J. Yuan, J. Zhang, X. Zang, J. Shen, and S. Lin, "Improvement of blood compatibility on cellulose membrane surface by grafting betaines," *Colloids Surfaces B Biointerfaces*, vol. 30, no. 1–2, pp. 147–155, 2003.

[218] H. Suhara *et al.*, "Efficacy of a new coating material, PMEA, for cardiopulmonary bypass circuits in a porcine model," *Ann. Thorac. Surg.*, vol. 71, no. 5, pp. 1603–1608, 2001.

[219] K. Kottke-Marchant, J. M. Anderson, Y. Umemura, and R. E. Marchant, "Effect of albumin coating on the in vitro blood compatibility of Dacron?? arterial prostheses," *Biomaterials*, vol. 10, no. 3, pp. 147–155, 1989.

[220] I. K. Kang, B. K. Kwon, J. H. Lee, and H. B. Lee, "Immobilization of proteins on poly(methyl methacrylate) films," *Biomaterials*, vol. 14, no. 10, pp. 787–792, 1993.

[221] Y. Marois *et al.*, "An albumin-coated polyester arterial graft: In vivo assessment of biocompatibility and healing characteristics," *Biomaterials*, vol. 17, no. 1, pp. 3–14, 1996.

[222] P. Borgdorff, R. H. Van den Berg, M. A. Vis, G. C. Van den Bos, and G. J. Tangelder, "Pump-induced platelet aggregation in albumin-coated extracorporeal systems," *J. Thorac. Cardiovasc. Surg.*, vol. 118, no. 5, pp. 946–952, 1999.

[223] H. Al-Khaffaf and D. Charlesworth, "Albumin-coated vascular prostheses: A five-year follow-up," *J. Vasc. Surg.*, vol. 23, no. 4, pp. 686–690, 1996.

[224] R. G. Guidoin *et al.*, "Blood compatibility of silicone rubber chemically coated with cross-linked albumin.," *Biomater. Med. Devices. Artif. Organs*, vol. 4, no. 2, pp. 205–24, 1976.

[225] J. A. Gladysz and M. Jurisch, "Structural, Physical, and Chemical Properties of Fluorous Compounds," in *Fluorous Chemistry*, I. T. Horváth, Ed. Berlin, Heidelberg: Springer Berlin Heidelberg, 2012, pp. 1–23.

[226] J. M. Harris and R. B. Chess, "Effect of pegylation on pharmaceuticals.," *Nat. Rev. Drug Discov.*, vol. 2, no. 3, pp. 214–221, 2003.

[227] F. Zhang *et al.*, "Chemical vapor deposition of three aminosilanes on silicon dioxide: Surface characterization, stability, effects of silane concentration, and cyanine dye adsorption," *Langmuir*, vol. 26, no. 18, pp. 14648–14654, 2010.

[228] Z. Z. Liu, Q. Wang, X. Liu, and J. Q. Bao, "Effects of amino-terminated self-assembled monolayers on nucleation and growth of chemical vapor-deposited copper films," *Thin Solid Films*, vol. 517, no. 2, pp. 635–640, 2008.

[229] N. R. James, J. Philip, and A. Jayakrishnan, "Polyurethanes with radiopaque properties," *Biomaterials*, vol. 27, no. 2, pp. 160–166, 2006.

[230] S. Oyola-Reynoso, Z. Wang, J. Chen, S. Çınar, B. Chang, and M. Thuo, "Revisiting the Challenges in Fabricating Uniform Coatings with Polyfunctional Molecules on High Surface Energy Materials," *Coatings*, vol. 5, no. 4, pp. 1002–1018, 2015.

[231] T. A. Berg, J. A. Galdonik, and A. inventors; Boston Scientific Scimed, "Guide catheter having selected flexural modulus segments. Minnesota, US patent 7674411. September 10, 2010," patent 7674411, 2010.

[232] J. W. Yau *et al.*, "Selective depletion of factor XI or factor XII with antisense oligonucleotides attenuates catheter thrombosis in rabbits," *Blood*, vol. 123, no. 13, pp. 2102–2107, 2014.

[233] D. G. Castner and B. D. Ratner, "Biomedical surface science: Foundations to frontiers," *Surf. Sci.*, vol. 500, no. 1–3, pp. 28–60, 2002.

[234] F. Rusmini, Z. Zhong, and J. Feijen, "Protein immobilization strategies for protein biochips," *Biomacromolecules*, vol. 8, no. 6, pp. 1775–1789, 2007.

[235] J. E. Gautrot, W. T. S. Huck, M. Welch, and M. Ramstedt, "Protein-resistant NTA-functionalized polymer brushes for selective and stable immobilization of histidine-tagged proteins," *ACS Appl. Mater. Interfaces*, vol. 2, no. 1, pp. 193–202, 2010.

[236] G. Camci-Unal, H. Aubin, A. F. Ahari, H. Bae, J. W. Nichol, and A. Khademhosseini, "Surface-modified hyaluronic acid hydrogels to capture endothelial progenitor cells," *Soft Matter*, vol. 6, no. 20, p. 5120, 2010.

[237] A. Rosengren, E. Pavlovic, S. Oscarsson, A. Krajewski, A. Ravaglioli, and A. Piancastelli, "Plasma protein adsorption pattern on characterized ceramic biomaterials," *Biomaterials*, vol. 23, pp. 1237–1247, 2002.

[238] Y. Liu and J. Yu, "Oriented immobilization of proteins on solid supports for use in biosensors and biochips: a review," *Microchim. Acta*, vol. 183, no. 1, pp. 1–19, 2016.

[239] T. F. Didar, A. M. Foudeh, and M. Tabrizian, "Patterning multiplex protein microarrays in a single microfluidic channel," *Anal. Chem.*, vol. 84, no. 2, pp. 1012–1018, 2012.

[240] M. Qin *et al.*, "Two methods for glass surface modification and their application in protein immobilization," *Colloids Surfaces B Biointerfaces*, vol. 60, no. 2, pp. 243–249, 2007.

[241] G. Cheng, G. Li, H. Xue, S. Chen, J. D. Bryers, and S. Jiang, "Zwitterionic carboxybetaine polymer surfaces and their resistance to long-term biofilm formation," *Biomaterials*, vol. 30, no. 28, pp. 5234–5240, 2009.

[242] G. Cheng, Z. Zhang, S. Chen, J. D. Bryers, and S. Jiang, "Inhibition of bacterial adhesion and biofilm formation on zwitterionic surfaces," *Biomaterials*, vol. 28, no. 29, pp. 4192–4199, Oct. 2007.

[243] A. S. Anderson *et al.*, "Functional PEG-modified thin films for biological detection," *Langmuir*, vol. 24, no. 5, pp. 2240–2247, 2008.

[244] K. D. Park *et al.*, "Bacterial adhesion on PEG modified polyurethan surfaces," *Biomaterials*, vol. 19, pp. 851–859, 1998.

[245] I. Banerjee, R. C. Pangule, and R. S. Kane, "Antifouling coatings: Recent developments in the design of surfaces that prevent fouling by proteins, bacteria, and marine organisms," *Adv. Mater.*, vol. 23, no. 6, pp. 690–718, 2011.

[246] Z. Z. Sheng *et al.*, "Bioinspired approaches for medical devices," *Chinese Chem. Lett.*, vol. 28, no. 6, pp. 1131–1134, 2017.

[247] S. Mazumder, J. O. Falkinham, A. M. Dietrich, and I. K. Puri, "Role of hydrophobicity in bacterial adherence to carbon nanostructures and biofilm formation," *Biofouling*, vol. 26, no. 3, pp. 333–339, 2010.

[248] N. Vogel, R. a Belisle, B. Hatton, T.-S. Wong, and J. Aizenberg, "Transparency and damage tolerance of patternable omniphobic lubricated surfaces based on inverse colloidal monolayers.," *Nat. Commun.*, vol. 4, p. 2167, 2013.

[249] P. Wang, D. Zhang, S. Sun, T. Li, and Y. Sun, "Fabrication of slippery lubricant-

infused porous surface with high underwater transparency for the control of marine biofouling," *ACS Appl. Mater. Interfaces*, vol. 9, no. 1, pp. 972–982, 2017.

[250] C. Y. K. Lung and J. P. Matinlinna, "Aspects of silane coupling agents and surface conditioning in dentistry: An overview," *Dent. Mater.*, vol. 28, no. 5, pp. 467–477, 2012.

[251] T. F. Didar *et al.*, "Improved treatment of systemic blood infections using antibiotics with extracorporeal opsonin hemoadsorption," *Biomaterials*, vol. 67, pp. 382–392, 2015.

[252] A. Shakeri, N. Sun, M. Badv, and T. F. Didar, "Generating 2-dimensional concentration gradients of biomolecules using a simple microfluidic design," *Biomicrofluidics*, vol. 11, no. 4, p. 044111, Jul. 2017.

[253] H. Yousefi, M. M. Ali, H. M. Su, C. D. M. Filipe, and T. F. Didar, "Sentinel Wraps: Real-Time Monitoring of Food Contamination by Printing DNAzyme Probes on Food Packaging," *ACS Nano*, vol. 12, no. 4, pp. 3287–3294, 2018.

[254] J. Kim, J. Cho, P. M. Seidler, N. E. Kurland, and V. K. Yadavalli, "Investigations of chemical modifications of amino-terminated organic films on silicon substrates and controlled protein immobilization," *Langmuir*, vol. 26, no. 4, pp. 2599–2608, 2010.

[255] D. J. Kim, J. M. Lee, J. G. Park, and B. G. Chung, "A self-assembled monolayer-based micropatterned array for controlling cell adhesion and protein adsorption," *Biotechnol. Bioeng.*, vol. 108, no. 5, pp. 1194–1202, 2011.

[256] P. Filippini *et al.*, "Modulation of osteosarcoma cell growth and differentiation by silane-modified surfaces," *J. Biomed. Mater. Res.*, vol. 55, no. 3, pp. 338–349, 2001.

[257] K. Awsiuk *et al.*, "Spectroscopic and microscopic characterization of biosensor surfaces with protein/amino-organosilane/silicon structure," *Colloids Surfaces B Biointerfaces*, vol. 90, no. 1, pp. 159–168, 2012.

[258] K. Awsiuk *et al.*, "Protein adsorption and covalent bonding to silicon nitride surfaces modified with organo-silanes: Comparison using AFM, angle-resolved XPS and multivariate ToF-SIMS analysis," *Colloids Surfaces B Biointerfaces*, vol. 110, pp. 217–224, 2013.

[259] L. S. Jang and H. J. Liu, "Fabrication of protein chips based on 3-aminopropyltriethoxysilane as a monolayer," *Biomed. Microdevices*, vol. 11, no. 2, pp. 331–338, 2009.

[260] Z. H. Wang and G. Jin, "Covalent immobilization of proteins for the biosensor based on imaging ellipsometry," *J. Immunol. Methods*, vol. 285, no. 2, pp. 237–243, 2004.

[261] T. F. Didar and M. Tabrizian, "Generating multiplex gradients of biomolecules for controlling cellular adhesion in parallel microfluidic channels," *Lab Chip*, vol. 12, no. 21, pp. 4363–4371, 2012.

[262] A. Shakeri, D. Yip, M. Badv, S. M. Imani, M. Sanjari, and T. F. Didar, "Self-cleaning ceramic tiles produced via stable coating of TiO2Nanoparticles," *Materials*

(Basel)., vol. 11, no. 6, 2018.

[263] S. P. Pujari, L. Scheres, A. T. M. Marcelis, and H. Zuilhof, "Covalent surface modification of oxide surfaces," *Angew. Chemie - Int. Ed.*, vol. 53, no. 25, pp. 6322–6356, 2014.

[264] A. R. Yadav, R. Sriram, J. A. Carter, and B. L. Miller, "Comparative study of solution-phase and vapor-phase deposition of aminosilanes on silicon dioxide surfaces," *Mater. Sci. Eng. C*, vol. 35, no. 1, pp. 283–290, 2014.

[265] R. R. Ravindranath, A. Romaschin, and M. Thompson, "In vitro and in vivo cell-capture strategies using cardiac stent technology - A review," *Clin. Biochem.*, vol. 49, no. 1, pp. 186–191, 2016.

[266] W. A. Zoghbi *et al.*, "Sustainable development goals and the future of cardiovascular health: A statement from the global cardiovascular disease taskforce," *J. Am. Coll. Cardiol.*, vol. 64, no. 13, pp. 1385–1387, 2014.

[267] H. F. Guo *et al.*, "A simply prepared small-diameter artificial blood vessel that promotes in situ endothelialization," *Acta Biomater.*, vol. 54, pp. 107–116, 2017.

[268] K. S. Lavery, C. Rhodes, A. Mcgraw, and M. J. Eppihimer, "Anti-thrombotic technologies for medical devices," *Adv. Drug Deliv. Rev.*, vol. 112, pp. 2–11, 2017.

[269] J. A. Gladysz and M. Jurisch, "Structural, physical, and chemical properties of fluorous compounds," in *Topics in Current Chemistry*, vol. 308, Springer, Berlin, Heidelberg, 2011, pp. 1–24.

[270] C. Haensch, S. Hoeppener, and U. S. Schubert, "Chemical modification of self-assembled silane based monolayers by surface reactions," *Chem. Soc. Rev.*, vol. 39, no. 6, p. 2323, 2010.

[271] A. Gang, G. Gabernet, L. D. Renner, L. Baraban, and G. Cuniberti, "A simple two-step silane-based (bio-) receptor molecule immobilization without additional binding site passivation," *RSC Adv.*, vol. 5, no. 45, pp. 35631–35634, 2015.

[272] W. He, P. Liu, J. Zhang, and X. Yao, "Emerging Applications of Bioinspired Slippery Surfaces in Biomedical Fields," *Chem. - A Eur. J.*, vol. 24, no. 56, pp. 14864–14877, 2018.

[273] C. Howell, A. Grinthal, S. Sunny, M. Aizenberg, and J. Aizenberg, "Designing Liquid-Infused Surfaces for Medical Applications: A Review," *Adv. Mater.*, vol. 30, no. 50, pp. 1–26, 2018.

[274] H. H. Chien, K. J. Ma, C. H. Kuo, and S. W. Huang, "Effects of plasma power and reaction gases on the surface properties of ePTFE materials during a plasma modification process," *Surf. Coatings Technol.*, vol. 228, no. SUPPL.1, pp. S477–S481, 2013.

[275] P. Zilla, D. Bezuidenhout, and P. Human, "Prosthetic vascular grafts: Wrong models, wrong questions and no healing," *Biomaterials*, vol. 28, no. 34, pp. 5009–5027, 2007.

Appendix: *Other publications, patents and conference presentations*

Journal Publications:

Imani, S. M.; **Badv, M.**; Shakeri, A.; Yousefi H.; Yip D.; Fine C.; Didar T.; "Micropatterned Biofunctional Lubricant-Infused Surfaces Promote Selective Localized Cell Adhesion and Patterning"; Accepted, Lab on a chip; Manuscript ID: LC-ART-06-2019-000608.

De France, K.; **Badv, M.**; Dorogin, J.; Siebers, E.; Babi, M.; Moran-Mirabal, J.; Lawlor, M.; Cranston, E.; Hoare, T., Tissue Response and Biodistribution of Injectable Cellulose Nanocrystal Composite Hydrogels. **ACS Biomater. Sci. Eng. 2019**, *5* (5), 2235–2246.

R. Wu, S. Xing, **Badv, M.**; Didar, T. F; Lu, Y,"Step-wise assessment and optimization of sample handling recovery yield for nanoproteomic analysis of 1000 mammalian cells" - **Anal. Chem. 2019.** acs.analchem.9b02092.

A. Hosseini, M. Villegas, J. Yang, **M. Badv**, J. I. Weitz, L. Soleymani, T. F. Didar, "Conductive Electrochemically Active Lubricant-Infused Nanostructured Surfaces Attenuate Coagulation and Enable Friction-Less Droplet Manipulation," Adv. Mater. Interfaces, vol. 5, no. 18, p. 1800617, Sep. 2018.

A. Shakeri, D. Yip, **M. Badv**, S. M. Imani, M. Sanjari, and T. F. Didar, "Self-cleaning ceramic tiles produced via stable coating of TiO_2 Nanoparticles," Materials (Basel)., vol. 11, no. 6, 2018.

A. Shakeri, N. Sun, **M. Badv**, and T. F. Didar, "Generating 2-dimensional concentration gradients of biomolecules using a simple microfluidic design," Biomicrofluidics, vol. 11, no. 4, p. 044111, Jul. 2017.

E. Bakaic, N. M. B. Smeets, **M. Badv**, M. Dodd, O. Barrigar, E. Siebers, M. Lawlor, H. Sheardown, T. Hoare, "Injectable and Degradable Poly (Oligoethylene glycol methacrylate) Hydrogels with Tunable Charge Densities as Adhesive Peptide-Free Cell Scaffolds," ACS Biomater. Sci. Eng., vol. 4, no. 11, pp. 3713–3725, Nov. 2018.

K. J. De France, **M. Badv**, J. Dorogin, E. Siebers, V. Panchal, M. Babi, J. Moran-Mirabal, M. Lawlor, E. D. Cranston, T. Hoare, "Tissue Response and Biodistribution of Injectable Cellulose Nanocrystal Composite Hydrogels," ACS Biomater. Sci. Eng., vol. 5, no. 5, p. 2235-2246, May 2019.

Conference Presentations:

Micro- and Nanotechnologies for Medicine Workshop, Los Angeles, USA (2019), **M. Badv**, T. F. Didar, Biofunctional Lubricant-Infused Surfaces for Medical Implants. Poster Presentation.

Society for Biomaterials (SFB), Seattle, USA. (2019), **M. Badv**, F. Sayed F, J. Faugeroux, D. Behr-Roussel, M. Rottman, T. F. Didar, Lubricant-Infused Urinary Catheters Prevent Bacterial Colonization In A Rat Model. Poster Presentation.

IDWeek, Washington, USA. (2018), **M. Badv**, F. Sayed F, J. Faugeroux, D. Behr-Roussel, M. Rottman, T. F. Didar, Perfluorocarbon omniphobic treatment prevents bacterial colonization of urinary catheter in a rat model. Poster Presentation.

Biannual meeting of the Surface Science Division of the CSC and CAP, Montreal, Canada (2017), **M. Badv,** I. H. Jaffer, J. I. Weitz, T. F. Didar, Comparison of vapour phase and liquid phase deposition of fluorosilanes for producing omniphobic lubricant-infused coatings on medical catheters. Poster Presentation.

Canadian Society for Pharmaceutical Sciences (CSPS)/ Canadian Chapter of the Controlled Release Society (CC-CRS) joint conference, Vancouver, Canada (2016), **M. Badv**, O. Salem, Y. Wan, T. Hoare, Poly (oligoethylene glycol methacrylate)-block-poly (D, L-lactide)-based nanoparticles as versatile hydrophobic drug delivery vehicles. Poster Presentation.

Patents:

Fluorinated biofunctional surfaces with "built-in" functional groups that promote targeted binding and prevent non- specific adhesion; patent date filed Jan 9, 2018, no. 62/615,218; Inventors, Didar, T.F., **Badv, M.**, Cetinic, Z.

Process for producing silanized bio-species and one step, rapid top down selective surface immobilization; patent date filed Jan 9, 2018, no. 62/615,205; Inventors, Didar, T.F., **Badv, M.**, Cetinic, Z.

A brush amphiphilic block copolymer enabling fabrication of self-assembled nanoparticles, patent date filed July 11, 2016, no. 62/360,615; Inventors, Hoare, T., Sadowski, L., **Badv, M.**, Luo, H.